**PONTIFÍCIA UNIVERSIDADE CATÓLICA DO PARANÁ**

CLAUDIA MORISHITA

# ON THE ASSESSMENT OF POTENTIAL MOISTURE RISKS IN RESIDENTIAL BUILDINGS ACROSS BRAZIL

**CURITIBA**
**Dezembro – 2020**

**PONTIFÍCIA UNIVERSIDADE CATÓLICA DO PARANÁ**

CLAUDIA MORISHITA

# ON THE ASSESSMENT OF POTENTIAL MOISTURE RISKS IN RESIDENTIAL BUILDINGS ACROSS BRAZIL

Tese apresentada como requisito parcial à obtenção do grau de Doutor em Engenharia Mecânica, Curso de Pós-Graduação em Engenharia Mecânica, Escola Politécnica, Pontifícia Universidade Católica do Paraná.

**Orientador: Prof. Nathan Mendes, Ph. D**
**Coorientador: Julien Berger, Ph. D**

**CURITIBA**
**Dezembro - 2020**

Dados da Catalogação na Publicação
Pontifícia Universidade Católica do Paraná
Sistema Integrado de Bibliotecas – SIBI/PUCPR
Biblioteca Central
Pamela Travassos de Freitas – CRB 9/1960

M861a 2020

Morishita, Claudia
On the assessment of potential moisture risks in residential buildings across Brazil / Claudia Morishita; orientador: Nathan Mendes; coorientador: Julien Berger. – 2020.
99 f. : il. ; 30 cm

Tese (doutorado) – Pontifícia Universidade Católica do Paraná, Curitiba, 2020
Inclui bibliografia

1. Engenharia mecânica. 2. Avaliação de riscos. 3. Edifícios de Apartamentos – Brasil. 4. Umidade. I. Mendes, Nathan. II. Berger, Julien. III. Pontifícia Universidade Católica do Paraná. Pós-Graduação em Engenharia de Produção e Sistemas. IV. Título.

CDD 20. ed. – 620.1

PUCPR

Pontifícia Universidade Católica do Paraná – PUCPR
Polytechnic School
Mechanical Engineering Graduate Program - PPGEM

# DOCUMENT OF APPROVAL

## Claudia Morishita

## On the Assessment of Potential Moisture Risks in Residential Buildings Across Brazil

Doctoral thesis approved as a partial requirement for obtaining the doctoral degree at the Mechanical Engineering Graduate Program of the Polytechnic School of Pontifícia Universidade Católica do Paraná, by the following committee members:

Documento assinado digitalmente
Roberto Lamberts
Data: 30/11/2020 19:05:47 -0300
CPF: 294.003.840-68

**Prof. Dr. Roberto Lamberts**
Universidade Federal de Santa Catarina, UFSC, Thesis Reporter

**Prof. Dr. Monika Wolosyn**
Université Savoie Mont Blanc, France

**Prof. Dr. Lucila Chebel Labaki**
Universidade Estadual de Campinas, UNICAMP

**Prof. Dr. Eduardo Grala da Cunha**
Universidade Federal de Pelotas, UFPel

**Eng. Pedro de Freitas Gois** (invited member)
Tecomat Engenharia

President: **Prof. Dr. Nathan Mendes**
Pontifícia Universidade Católica do Paraná, PUCPR, Thesis Advisor

Curitiba, Brazil, November 30th, 2020

Rua: Imaculada Conceição, 1155 – Prado Velho – CEP: 80215-901 – Curitiba-Paraná-Brasil
Telefone: +55 41 3271-1385 E-mail: ppgem@pucpr.br

LIST of ACRONYMS

| Nomenclature | | |
|---|---|---|
| $h_v$ | vapour convective transfer coefficient | [s/m] |
| $WDR$ | wind-driven rain deposition | [kg/m$^2$·h] |
| $P_v$ | vapour pressure | [Pa] |
| $t_M$ | consecutive duration of $MGR \geq 1$ in the 5$^{th}$ simulated year | [h] |
| $I$ | Index | |
| $L$ | Latent heat transfer rate | [W] |
| $M_L$ | Moisture load | [kg/h] |
| $M$ | maximum Mould Growth Risk | [-] |
| $N$ | normalized Index | |
| $R$ | thermal resistance | [(m²·K)/W] |
| $T$ | temperature | [K] |
| $c$ | specific heat | [kJ/(kg·K)] |
| $i$ | cardinal directions | [-] |
| $t$ | time instant | |
| $\lambda$ | thermal conductivity | [W/(m·K)] |
| $\rho$ | material specific mass | [kg·m$^{-3}$] |
| $\varphi$ | relative humidity | [-] |
| Superscript | | |
| $ext$ | external | |
| $eq$ | equivalent | |
| Subscript | | |
| $air - rain$ | vapour pressure added by the effect of wind-driven rain | |
| $iso$ | Isopleth curve | |
| Acronyms | | |
| CFD | Computational Fluid Dynamics | |
| CTF | Conduction Transfer Function | |
| $FD$ | Facade Deterioration Risk Index | |
| GIS | Geographic Information System | |
| HAM | Heat, Air and Moisture | |
| MGR | Mould Growth Risk | |
| $MI$ | Mould Growth Risk Indicator | |
| TMY | Typical Meteorological Year | |
| $VP$ | Vapour Pressure Indicator | |

# LIST OF FIGURES

# LIST OF TABLES

# TABLE OF CONTENTS

# CHAPTER 1. INTRODUCTION

The excessive moisture in building materials may lead to functional damage (corrosion, stain, decay), thermal discomfort, material deterioration, higher energy consumption, increase power demand, and lead to microorganism's growth, that affects the indoor air quality and causing may cause health problems in its occupants (MENDES, WINKELMANN*, et al.*, 2003; KÜNZEL *et al.*, 2005; BERGER *et al.*, 2015). Moisture transport is a combination of water vapour and liquid displacement, occurring due to different reasons such as capillary migration, diffusion and advection through the porous structures and cracks (SANTOS and MENDES, 2009b; ZHANG and YOSHINO, 2010). The main factors affecting moisture level are outdoor vapour pressure, wind-driven rain, indoor vapour production, air change rate, adsorption and desorption phenomena, leakages and presence of cracks (HOLM, KÜNZEL and SEDLBAUER, 2003; ABADIE and MENDES, 2008). In hot and humid climates, such as most of many cities in Brazil, moisture problems in buildings may be difficult to be handled due to the high outdoor humidity level (NIU, ZHANG and ZUO, 2002; JIN, ZHANG and ZHANG, 2017; YOU *et al.*, 2017).

Besides the climatic humidity load, indoor moisture in residential buildings is generated mainly by human respiration and skin transpiration and household activities such as bathing, cooking and washing (YIK, SAT and NIU, 2004; WOLOSZYN and RODE, 2008b; GEVING and HOLME, 2012). Due to its impact in the building sector and the fact the human being spends a large part of their time inside a built environment, moisture-related issues are extensively studied across different countries. Many studies are found in cold climate countries, where moisture has high impact in building performance, damaging insulation materials and causing indoor environmental issues in the highly sealed constructions (STOPP *et al.*, 2001; MOON, RYU and KIM, 2014; LEE *et al.*, 2016; IBRAHIM *et al.*, 2019).

In Brazil, some of the research is related to mathematical modelling to perform whole-building hygrothermal prediction (MENDES, PHILIPPI and LAMBERTS, 2001), software development (MENDES, OLIVEIRA and SANTOS, 2003; SANTOS and MENDES, 2003), moisture-related characterization of materials (FREITAS DUTRA *et al.*, 2019), and 2-D and 3-D moisture transfer models (BERGER *et al.*,

2019; MELLO, MOURA and MENDES, 2019). There are also studies in a case of study approach concerning building pathology due to moisture as will be further detailed in Chapter 2, but there is a lack of studies in an overall approach. With respect to building standards, the three main existing ones regard the thermal performance (ABNT, 2005), building performance (ABNT, 2013), and energy efficiency (INMETRO, 2010; 2012). However, there is no moisture related standard neither moisture related requirements in the existing ones.

Regarding building performance standards in other South America countries, which have some climatic and social-economic similarities with Brazil (GALLIPOLITI *et al.*, 2012; NETTO and CZAJKOWSKI, 2016), there are moisture-related requirements in the Peruvian and Argentine ones. In Peru, the standard Thermal and luminous comfort with energy efficiency (EM, 2014), provides a calculation method to obtain the internal surface temperature of walls, floors, and roofs, to evaluate the condensation risk according to the dew point in the psychrometric chart. In Argentina, the IRAM standards entitled as "Thermal insulation of buildings: Verification of hygrothermal conditions" refer to the verification of condensation risk of superficial and interstitial water vapour in singular points (IRAM, 2000b) and at the internal layers of external walls, floors, and roofs (IRAM, 2000a). Similarly to the Peruvian standard, it provides a method to obtain the interior surface temperature to assess, by consulting the dew point in the psychrometric chart, the condensation risk. The adoption of the IRAM group of standards related to the thermal performance of buildings is voluntary but mandatory in the cities of Buenos Ayres and Rosario. However, it is presumed that there is no formalized inspection by part of the authorities, being difficult to achieve its effective implementation; it is not fulfilled, or it does so partially (NETTO and CZAJKOWSKI, 2016).

In both Peruvian and Argentinian standards, the calculation method is stationary and there is no simulation method. The interior surface temperature is obtained by the surface resistance combined with design values of internal and external air temperature and relative humidity, according to the bioclimatic zone.

Also, both standards warn that these calculation methods intend to reduce the condensation risk under standard conditions, but cannot ensure to avoid the condensation risk in critical points such as thermal bridges. Other countries such as Uruguay, Paraguay, Colombia, Venezuela, and Bolivia, apparently do not have specific regulation regarding the thermal performance of buildings, besides some more specific standards such as ISO ones. In Chile, as in Brazil, there is no moisture-related requirement in the building thermal regulation (OGUC, 2000).

A study conducted in Australia has analysed the impact of building regulation requirements on moisture problems in residential buildings (NATH, DEWSBURY and DOUWES, 2020), showing that the focus on energy-efficient and carbon-efficient homes has increased the insulation levels of walls as well as the airtightness. Furthermore, energy efficiency compliance does not consider whether the regulatory approved building components may lead or not to moisture accumulation. Their study concluded that, in Australia, the national building regulations may have, unintentionally, led to building construction systems and interior environments that are ideal to condensation and mould growth by not considering moisture-related requirements.

Therefore, considering the Brazilian vast territorial extension and population, it becomes evident the need for additional information related to moisture risk in existing national building standards, which could be adapted to neighbouring countries.

Although the occurrence of moisture disorders in buildings in Brazil is widely known, there is a lack of studies on a general approach, being the topic still underexplored in the country and restricted to a few research groups. Besides, building standards lack in moisture-related requirements, and moisture is not properly taken into account in building thermal performance standards. Despite its importance in building performance, components durability and occupant's health, information regarding the moisture environment and problems associated to moisture storage and accumulation in Brazilian residential buildings on a country scale, either due to climatic conditions or construction methods or internal sources, is hardly available.

## 1.1 OBJECTIVES

Considering the importance of moisture in building performance, in the durability of its components and occupant's health, and the lack of related information in a vast and populous country such as Brazil, the objective of this thesis is to investigate the potential moisture risks in Brazilian residential buildings across the different climates of the country. The hypothesis is that there is moisture risk in Brazilian buildings due to climatic conditions, constructive techniques and cultural habits besides the risk due to the use of low-quality material, failure in the design and construction processes, but the topic is still underestimated and underexplored in the country in a comprehensive manner. The main objective leads to the following questions:

1. What are the potential moisture loads in Brazilian buildings?
2. What is the potential moisture risk for a typical Brazilian popular housing typology across the different climates of the country?

Hence, this work intends to answer these questions.

Firstly, it is conducted a review of characteristics of the country associated with moisture issues, that regard information of the climate, the existing policies and research, and the residential building sector. After, it is conducted a climatic analysis, in which five – being two firstly presented in MORISHITA, BERGER and MENDES (2020) - weather-based indicators are charted in the country map, indicating the areas of the country that receive the highest climatic moisture loads. Next, 1-D whole-building simulations are carried out for a typical Brazilian residential building, considering the main used constructive techniques and usage habits. A mould growth risk (MGR) Index is applied to simulation results as a moisture risk indicator, as mould growths in specific conditions of temperature combined with high humidity level. Also, considering the absence of data related to the indoor humidity environment, it is provided an estimation of the internal moisture load through the latent heat fraction values of the internal gains. The building solar orientation, the material of walls, length of the shower, permeance of painting layers in walls and existence of an exhauster fan in the bathroom are the categorical variables chosen to evaluate their influence on MGR levels.

The analysis approach on both climatic and building scales aim to provide a general panorama of the importance of the climatic conditions and the most used construction methods on the potential moisture risks in Brazilian residential buildings. The goal is not to predict moisture transfer processes through building envelope neither characterize indoor humidity levels, but to present an overview regarding the moisture environment of Brazilian residential dwellings on a country scale, contributing to partly filling the identified gap in research on the topic.

## 1.2 OUTLINE OF THE THESIS

The general context related to the subject of this thesis is provided in the Introduction. Chapter 2 provides information on the characteristics of Brazil that are relevant to the development of the work and comprehension of the results. Chapter 3 gives a brief presentation of the tools employed in the work to carry out the building simulations and to chart the results on the Brazil map. The potential moisture risk at the climatic level is presented in Chapter 4 and on the building scale in Chapter 5. Limitations, assumptions and delimitations of the work are presented in Chapter 6 and discussion, conclusions and needs of further research on the topic are addressed in Chapter 7.

# CHAPTER 2. COUNTRY CHARACTERISTICS ASSOCIATED WITH MOISTURE ISSUES

In this Chapter, it is presented the state-of-the-art concerning country characteristics that supports the development of the thesis. It provides a panorama of the different climates throughout the territory, population distribution, main characteristics of the residential building typologies, and the existing policies related to moisture in the residential building sector. It is also presented some of the research on moisture carried out in Brazil.

Brazil is located in South America and its area of approximately 8.5 million square kilometres is divided into five regions (Fig. 1). About 56% of the 209 million inhabitants live in 5.6% of its 5,570 municipalities (IBGE, 2019a), mainly concentrated in coastal areas as presented in Fig. 2.


Fig. 1. Geographical regions and states

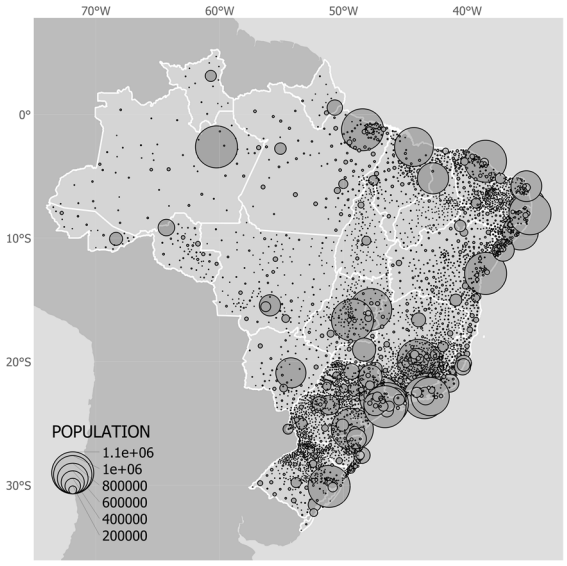


Fig. 2. Population distribution

Fig. 3 exhibits a comparison of land area, population, dwellings, and average monthly income per dwelling between geographic regions. Southeast region corresponds to 11% of the total land area, 42% of the population and 43% of the dwellings. In contrast, the North region encloses 45% of land area and accounts for just 8% of the population and 7% of the dwellings. Northeast with near 28% of the population has the lowest average income per dwelling.

Brazil is a wide and heterogeneous country in terms of climate, distribution of the population and cultural aspects. The population is mostly concentrated in Southern regions, which have higher average incomes; Northern regions are the less occupied and the poorest ones.

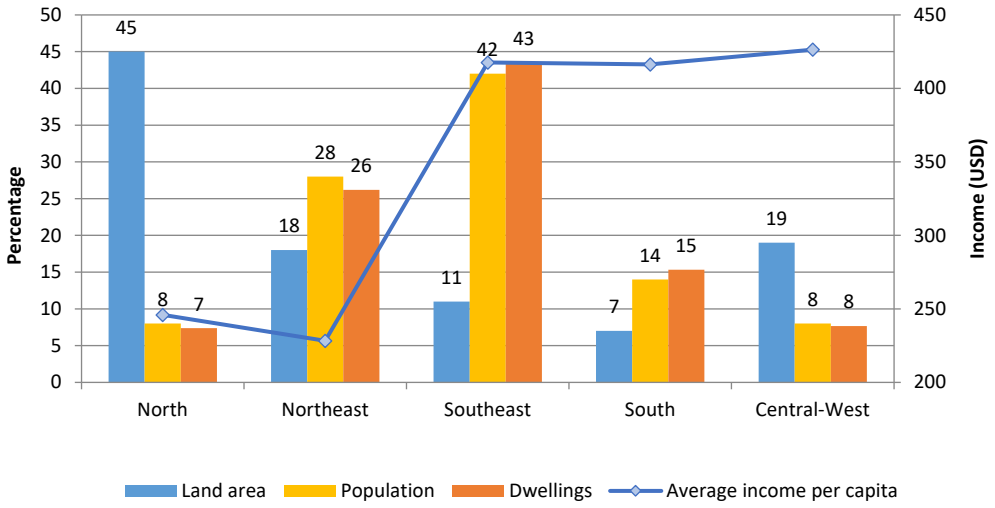


Fig. 3. Percentage of land area, population, dwellings, and average monthly income per dwelling per geographic region of Brazil.
Source: IBGE (2015)

## 2.1 CLIMATIC ASPECTS

As approximately 90% of the territory is located between the Equator Line and the Capricorn Tropic, Brazil has mainly a hot and humid Tropical Climate according to the Köppen classification (Fig. 4) (ALCARDE ALVARES *et al.*, 2013).

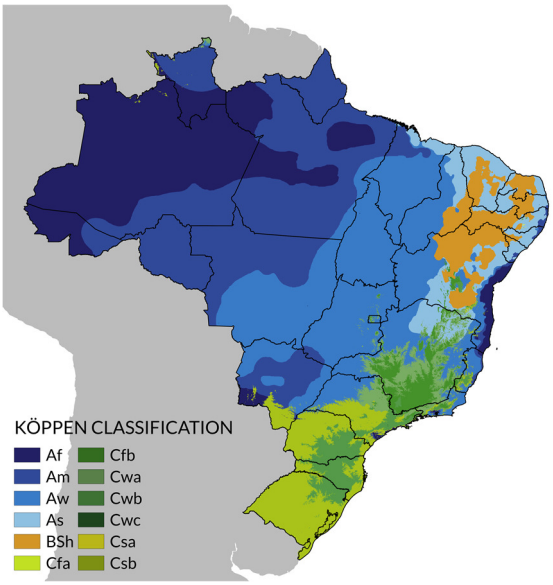


Fig. 4. Climate classification for Brazil according to Köppen criteria

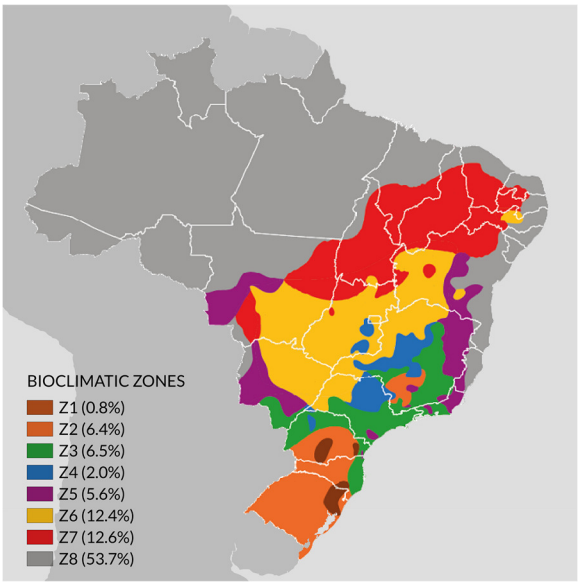


Fig. 5. Bioclimatic Zoning of Brazil

The Köppen classification divides the country into three zones and twelve climate types. The zone 'A' corresponds to the tropical climate and represents 81.4% of the country's territory. Zone 'B', the semi-arid climate, is notably the typical climate of the Northeast region and represents an enclave of scarce rainfall in the Brazilian tropical region. The zone 'C' is the subtropical climate, mostly found in the South Region and covers 13.7% of the territory, but it can also be found in tropical areas with high altitude.

The Bioclimatic Zoning, part of the Thermal Performance of Buildings Standard (ABNT, 2005) (Fig. 5), is a climatic classification widely applied in building research. It classifies the country into eight zones with relatively uniform climatic characteristics, by considering monthly average air temperature and air relative humidity, being the zone 1 the coldest and zone 8 the hottest (Table 1).

Table 1. Annual average minimum and maximum air temperatures of 8 cities for the period of 1981-2010

| Bioclimatic Zone | Koppen climate | City | Location | Min average Temperature [°C] | Max average Temperature [°C] |
|---|---|---|---|---|---|
| 1 | Cfb | Curitiba | 25°25'S \| 49°15'W | 13.4 | 23.5 |
| 2 | Cfb | Teresopolis | 22°24'S \| 42°57'W | 15.6 | 25.0 |
| 3 | Cfb | Sao Paulo | 23°33'S \| 46°38'W | 16.2 | 25.7 |
| 4 | Aw | Brasilia | 15°47'S \| 47°52'W | 16.8 | 26.6 |
| 5 | Aw | Campos | 21°45'S \| 41°19'W | 20.8 | 29.9 |
| 6 | Am | Campo Grande | 20°29'S \| 54°36'W | 18.8 | 29.8 |
| 7 | Aw | Cuiaba | 05°35'S \| 56°05'W | 21.5 | 33.0 |
| 8 | Af | Manaus | 03°06'S \| 60°01'W | 23.5 | 32.0 |

Source: INMET (2012)

These two climatic classifications are the most applied ones in Brazil, but there are others. A comparison of three different methods for climatic zoning with building performance analysis purposes can be found in WALSH, CÓSTOLA and LABAKI (2017) and the need of building performance data to propose climatic zoning for energy efficiency regulation is presented in MAZZAFERRO *et al.* (2020), in which building performance data was used to perform an assessment of seven climatic zoning methods. This study has shown the importance of considering building performance data to improve the quality of climatic zoning for building energy efficiency regulations purposes.

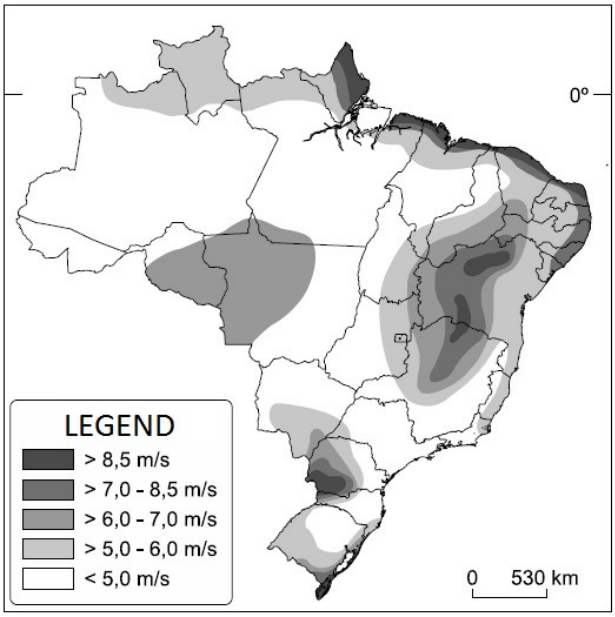


Fig. 6. Average wind speed [m/s]

The action of wind also needs to be mentioned, which combined with high precipitation levels it may lead to WDR occurrence. Fig. 6 illustrates the average wind speeds of the country (CEPEL, 2019). Most of the seacoast has high wind speeds, as well as the semi-arid region and some southern areas.

As part of the Brazilian bioclimatic zoning project, Roriz (2012) developed weather files based on data provided by the National Institute of Meteorology (INMET) (INMET, 2012). The files employ the Typical Meteorological Year (TMY) approach, that discards monthly extreme values and a typical year is obtained by combining months from different years. The result is an average year with hourly data. Due to gaps in the data, the whole year is assembled for only 413 cities (Fig. 7), being many of them from the years 2007 or 2008 onwards.

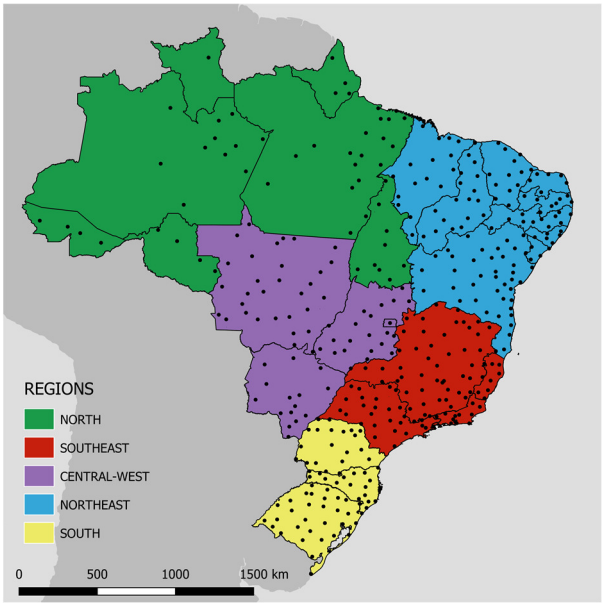


Fig. 7. Geolocation of the 409 cities

All analyses of this work are based on these weather files. The choice of using TMY weather files instead of real measured data is due to the fact the existing official climatic data has a lot of gaps and, for many locations, data is recorded with an 8-hour interval. Furthermore, not all the required variables and periods are publicly available. The employed hourly weather files are a result of the interpolation and statistical analysis of these official climatic data.

## 2.2 RESIDENTIAL BUILDINGS SECTOR CHARACTERISTICS

Even in highly dense urban areas, in Brazil there is still a strong presence of single-storey houses, which represent about 86% of the dwellings (IBGE, 2019a). Despite the climatic and cultural differences between regions, houses have mainly the same construction techniques. About 96.0% of them employ for the envelope masonry with a mortar and painted walls and 62.2% employ clay tile with concrete slab for roofing (SINPHA, 2005). However, there is a trend in the usage of structural walls made of concrete blocks, especially in large apartment complexes of popular housing due to its lower costs with the workforce. Concerning the windows materials, there is no official data available about the type of glass, but double-glazed windows are rarely used, except in a few high standard houses. A study concerning representative Brazilian building typologies for social housing can be found in TRIANA, LAMBERTS and SASSI (2015).

Data from the construction industry relating the type of financing (self, private, or governmental), amount of houses built by construction firms, and the total number of houses (given by official national census) gives a panorama of about 67% to 77% informally built houses (CGEE, 2009). The main characteristic of the informally built house is the direct management of their owner and occupants. They acquire the land, map a building scheme without technical support, provide acquisition of construction material, agency labour (free or informally paid), and build their home. There are programs which offer help to low-income families in their home acquisition process, including for self-building process in order to improve housing quality (KOWALTOWSKI *et al.*, 2005) but this is not the typical scenario. In Brazil, the majority of construction labour lack professional training. Furthermore,

innovative techniques face difficulties to take place, for instance, double-glazed windows, insulation, and vapour barriers. Due to the low demand, these materials are imported, making its price high. These issues– informal construction, lack of professional training and innovative techniques – when combined may lead to this predominance of masonry wall with clay tile roofing usage.

## 2.3 POLICIES REGARDING MOISTURE SAFETY IN BUILDINGS

Despite the high climatic moisture loads, in Brazil, there are no building moisture-related standards (MORISHITA *et al.*, 2020), but related requirements in the energy efficiency regulation, building performance standards and local laws (Table 2).

Table 2. Brazilian residential building standards

| **Residential building standards contents** | | |
|---|---|---|
| NBR 15.220 (2005) | Thermal performance of buildings | Building design requirements by climate zone regarding openings size, openings shading, thermal properties of walls and roofs.<br>Building design passive strategies to improve thermal performance (evaporative cooling, passive solar heating, the thermal inertia of walls, natural ventilation control). |
| RTQ-R (2011) | Labelling for energy efficiency of residential buildings | Building energy efficiency requirements by climate zone for building envelope, house appliances, water heating systems, and air conditioning and ventilation (HVAC) systems. |
| NBR 15.575 (2013) | Performance of residential buildings | Construction procedure requirements for building structure, floors, envelope, roofs and water systems.<br>Building requirements for acoustics, lighting, thermal performance, and durability and maintainability during the operation phase. |
| Local Laws | | Always fulfil state and federal laws; define which standards and codes for design, construction and operation phases the buildings must accomplish. |

To obtain a building permit, the city hall competent body must inspect the building design. The attendance of the standards required by the local law is normally a responsibility of the architect or engineer, but there is no organization to proper control and inspect it.

## 2.4 SOME OF THE RESEARCH ON MOISTURE CARRIED OUT IN BRAZIL

Some research focused on moisture in buildings started in Brazil in the eighties on software application and mathematical modelling (SILVEIRA NETO, 1985; BUENO, PHILIPPI and LAMBERTS, 1994; MENDES, 1997; MENDES, PHILIPPI*, et al.*, 2001; MENDES, WINKELMANN*, et al.*, 2003; MENDES and PHILIPPI, 2004; MENDES and PHILIPPI, 2005), allowing to perform whole-building hygrothermal prediction and software development such as Umidus (MENDES *et al.*, 1999) and Domus (MENDES, OLIVEIRA and SANTOS, 2001; MENDES, OLIVEIRA*, et al.*, 2003; BARBOSA and MENDES, 2008; MENDES *et al.*, 2008;

FREIRE, ABADIE and MENDES, 2009; CASTILLO, MENDES and MOURA, 2018; ROCHA, MENDES and OLIVEIRA, 2018). In 2003, SANTOS and MENDES (2003) presented the software Solum to predict 3-D profiles of temperature and moisture content in soils under buildings and some related research was carried out numerically (SANTOS and MENDES, 2006) and experimentally (AKINYEMI *et al.*, 2007; MENDES, ABADIE and AKINYEMI, 2012). Moisture rising damp related problems are commonly found in Brazilian constructions and it is a great source of concern.

Dos Santos and Mendes (2009a) presented a new model to compute temperature, vapour pressure and air pressure profiles in porous elements which were used to compute 2-D simulation in hollowed porous elements (SANTOS and MENDES, 2009b), thermal bridges (DOS SANTOS, MENDES and PHILIPPI, 2009) and roofs (SANTOS and MENDES, 2013). Mendes *et al.* (2019) present in more details some models developed since the nineties that can be applied for moisture risk assessment.

The Thermal Systems Laboratory (LST) at PUCPR has also performed simulations using the moisture model of EnergyPlus and carried out a study on sensitivity and uncertainty analysis applied to combined heat and moisture models (GOFFART, RABOUILLE and MENDES, 2015). More recently, some 2-D and 3-D research on moisture models were integrated to the whole-building simulation code Domus and has been presented in BERGER *et al.* (2019), and a coupled 1-D and 2-D CFD-HAM model to solve complex heat and moisture transfer through building elements has been presented in MELLO *et al.* (2019).

Regarding moisture-related characterization of porous materials, MENDES (1997) and DUTRA, MENDES and PHILIPPI (2017) presented a method for obtaining the material pore size distribution which can be used to estimate transport coefficients for liquid and vapour phases and FREITAS DUTRA *et al.* (2019) manufactured three innovative clay-based porous materials, which were characterized to allow the phase identification, show sample microstructure and quantify the pore size distribution at different scales. Also, with the aim of better describing the hygroscopic behaviour of bio-based

materials, the modelling of sorption curves considering temperatures and hysteresis influence by comparing four different temperature-dependent models was investigated in PROMIS *et al.* (2019).

The research studies mentioned so far are mainly from the same research group and are focused on mathematical modelling, software development and moisture transfer processes through porous building materials.

During the investigation of existing moisture-related research in Brazil, it is observed there are not many research groups working on the present topic. Many of the studies found are isolated ones from diverse research groups and have mainly a case study approach focused on building pathology due to failure in the construction process. Some examples are given in the following.

Moisture disorders in buildings were analysed by Sobrinho (2008), showing the presence of fungi in the mortar of social houses in the countryside of São Paulo. According to his study, one of the main issues that occur in social houses is rising damp in the mortar due to the lack of waterproofing between the floor slab and the soil.

The influence of driving rain and architectural elements in front of building facades deterioration in a multi-storey residential was assessed by Júnior and Carasek (2014). The study verified that moisture from rain deteriorates facades mostly on parapet walls, windowsill, and drip pans. However, stains occur not only due to facades elements but also by condensation on masonry-based materials at South oriented facades, which can lead to microorganism's growth. Also regarding the driving rain, GIONGO, PADARATZ and LAMBERTS (2011) presented a study of the building exposure to wind-driven rain in the city of Florianopolis by applying a semi-empirical method to climatic data.

RAMALHO *et al.* (2014) inspected in loco ten residential buildings affected by moisture disorders in the countryside of Minas Gerais state to identify the sources of the issues. The observed pathology were stains, efflorescence, tile detachment, fungi growth, and cracks. The identified causes were inadequate waterproofing, leakage of rainwater due to bad execution of rain gutters, poor ventilation, low adhesion of the coating on the substrate, and low quality of materials

PAZ *et al.* (2016) assessed the pathology due to moisture in a residential building in the North region of Brazil, based on bibliography and local inspection. The identified pathology concern detachment of facade cladding, pipe and roofing leakage, cracks in walls, and fungi growth. For each pathology it is suggested a solution, which consists mainly of house repairing such as cleaning, painting, replacing waterproofing, pipe, and cladding. Conclusions indicate that pathology occurs due to failures in the design process, such as pipe sizing, low-quality materials and workforce.

In a more extensive approach, CARVALHO and PINTO (2018) presented a list of pieces of evidence, causes and solutions for different common moisture issues in buildings in Brazil, according to Table 3.

Table 3. Moisture manifestation in buildings

| **Moisture source** | **Evidence** | **Cause** | **Solution** |
|---|---|---|---|
| Accidental | Stains in walls close to pipes | Cracks in pipes, inappropriate design, lack of maintenance | Proper execution of the pipe system<br>Replacement or repair of the damaged pipe |
| Capillarity | Stains and efflorescence in walls close to the floor | Salt crystallisation, high level of the groundwater table, inefficient drainage, fail in waterproofing execution, bad quality mortar | Lowering the groundwater table level for subsequent construction of foundations<br>Correct execution of waterproofing systems<br>Double layered slab |
| Condensation | Stains, fungi, and bacterial microflora inside walls,<br>organic matter decay; wetting zones inside exterior walls | Insufficient thermal insulation of exterior walls, poor ventilation conditions, low temperatures, and high relative humidity | Use thermal inertia of masonry through air circulation<br>Thermal insulation<br>Brushing, immunization and execution of a new finish on the masonry affected by mould |
| Construction | Wetting zones on internal and external walls, efflorescence, and mould | Incidence of rain on the construction site and building materials, acceleration of the construction process, not enough time for the total drying of materials | Correct dosage and trace of mortars and concrete<br>Protection of the construction site against rainwater infiltration during the execution process<br>Increase thermal inertia between the walls through ventilation<br>Increase in the surface temperature of the walls or decrease in the air relative humidity with dehumidifiers |
| Rainfall | Stains and mould in the inner surface of walls exposed to rainfall | Bad quality of mortar, failure in design and execution, double wall (open joints or poorly filled with waterproofing material), rupture of rainwater pipes | Execution of external plaster in masonry next to sidewalks, protecting walls from splashes and standing water<br>Application of silicone-based paints, acrylic or polyurethane varnish on facades<br>Flexible waterproofing systems in roofing slabs and floors (emulsions and cement blankets)<br>Repair of damaged roofing parts<br>Removal of the damp plaster and waterproofing the joints between the materials<br>Protection with waterproof paint |

Source: CARVALHO and PINTO (2018)

The study highlights the lower cost of preventing damages due to moisture in the design and construction processes in comparison with the cost of the process of diagnosis and repairing.

Therefore, some research work in Brazil has been carried out about the moisture in constructions since the ’80s, but still strictly academic or in case study approaches. Despite the academic development

and the high risks of pathology caused by moisture in buildings in such large country with important climatic sources of moisture, there is a lack of assessment of the moisture load in buildings in the country.

## 2.5 DISCUSSION

As presented in Section 2.4, there is moisture-related research being carried out in the country, but there is a lack of a comprehensive study on the country scale. Societal aspects, building standards, construction methods and cultural habits must be discussed as they provide complementary information about the potential moisture risk in conjunction with the climatic characteristics. Standards impose limits and point directions to building's conception and construction; construction methods change the susceptibility of buildings to disorders and cultural habits influence the building's patterns of usage.

The standards and laws have different requirements and are not always respected somehow due to the lack of control. Even for constructions with building permits, these requirements are not always met, as it depends on local laws and supervision. Also, some standards tests require laboratory and equipment that most of the times are located into research laboratories, that may turn its accomplishment more difficult.

Despite being a large country with very different climates, income inequalities and cultural differences, the majority of the houses in Brazil use quite the same construction techniques, the innovative ones face difficulties to take place and labour lack professional training.

There is a cycle between construction methods and standards: the same construction techniques are widely used for years and the standards mainly refer to these types of techniques. Bureaucracy also plays a role in this difficulty in changing construction methods – if it is not standardized it is troublesome be used, especially for large buildings and building complexes that depend on external financing. A positive initiative in this regard is the National Technical Assessment System (SINAT, 2019). It is an initiative to gather the technical and construction chain communities, intending to stimulate

technological innovation and evaluate new products used in the building construction processes and which are not covered by prescriptive technical standards. Another positive initiative is the Brazilian Program of Quality and Productivity in the Habitat (MDR, 2019). To obtain public funding for the *My house, my life*, which is a national program for social housing, constructors must be accredited in the program, with the goal to improve the quality of the habitat and productivity of the construction sector.

Moreover, the large occurrence of informally built houses increases the probability of having a great amount of low-quality buildings and worsens the risk of moisture disorders, as standards rules are not considered, and control or inspection is not always accomplished.

It is possible to find numerous studies concerning building pathology caused by moisture, many from undergraduate students and unpublished in scientific journals, and most of the time it is not possible to track continuity of research on the topic by the authors. The majority of them point low-quality materials, bad execution and design practices as major causes of moisture issues. Also, many of the common references in these studies are from the eighties and nineties (PEREZ, 1985; ALUCCI, FLAUZINO and MILANO, 1988; UEMOTO, 1988; VERÇOZA, 1991), indicating a potential lack of recent research in a broader approach.

This Chapter presented the state-of-the-art related to characteristics of the country which are important for the development of the thesis. The climatic aspects of the country are the primary ones, being the basis employed throughout the whole study. The section about the residential building sector provides a framework of the typical Brazilian dwelling, focus of the building scale analysis of the work. A summary of the main existing building standards points out the shortcoming of policies and requirements related to moisture issues, and some examples of research on the subject conducted in the country highlight a lack of studies concerning the humidity environment of Brazilian buildings on the scale of the country.

# CHAPTER 3. TOOLS

Chapter 2 presented information that is relevant to the development and reading of the study, regarding the climatic aspects, the residential building sector and moisture-related research carried out in Brazil. This chapter provides a brief presentation of tools required to accomplish the expected results, concerning the GIS to chart results in the Brazil map and the employed tool to carry out the 1-D whole-building simulations.

## 3.1 GEOGRAPHIC INFORMATION SYSTEM – GIS

To graphically represent the main results of this work, maps are developed through the open-source geographic information system QGIS (QGIS), a free and open-source GIS tool with a user-friendly interface. It supports vector and multiple raster images layers, allowing to edit, compose and export spatial information and maps. The shapefile (vector file) of Brazil, as well as the geolocation (the centroid of the city polygon) of all cities, are available at the Brazilian Institute of Geography and Statistics - IBGE website (IBGE, 2019b). The results of each location (each Weather file) must be assembled to its geolocation to be charted in the map.

Certain results are plotted using scale-based symbol sizing, in which the size of the symbol varies in size to represent a quantitative variable. For others, full interpolated maps are presented by applying the Inverse Distance Weighted (IDW) method, which is a widely used deterministic model for spatial interpolation (LU and WONG, 2008). Its general idea assumes that the attribute value of any given pair of points is related to each other and that their similarity is inversely related to their distance.

## 3.2 ENERGYPLUS

EnergyPlus is a whole-building energy simulation program employed to model both energy consumption (heating, cooling, ventilation, lighting, and plug and process loads) and water use in buildings. EnergyPlus uses the zone heat balance to model heating, cooling, ventilation and plug loads to predict thermal loads and zone air conditions (WOLOSZYN and RODE, 2008b; TABARES-VELASCO

and GRIFFITH, 2012). It allows the assessment of the interactions between the building envelope, building equipment, and exterior climate. Its development is funded by the United States Department of Energy Building Technologies Office (DOE, 2017b). It is a free, open-source and cross-platform that reads input and with the use of weather data writes output to text files.

EnergyPlus works with two models of heat and moisture transfer algorithms. The Effective Moisture Penetration Depth - EMPD model is a simplified approach to simulate surface moisture adsorption and desorption. Its concept assumes that a thin layer of the internal surface of the wall behaves dynamically and exchanges moisture with the air domain when exposed to cyclic air moisture pulses. The Combined Heat and Moisture Transfer – HAMT model, which algorithm is based on the conservation equations formulated by KÜNZEL (2012), it is a one-dimensional coupled finite element heat and moisture transfer model to simulate the movement and storage of heat and moisture in surfaces, from and to both internal and external environments. Additional information on the Energy Plus models employed in this work is provided in Annex A.

## 3.3 DISCUSSION

This Chapter presented the main specific tools required for the development of the thesis. In both climatic and building analysis, the moisture risk indicators obtained must be charted in the map of Brazil. QGIS, a free tool for editing geospatial data and creating maps, is a suitable one to fulfil the task.

The EnergyPlus is employed to carry out the 1-D whole building simulations to obtain the necessary information to apply the chosen mould growth risk model as a moisture risk indicator on the building approach analysis. As mentioned in Section 2.4, the LST has its own software to perform whole-building hygrothermal prediction *DOMUS* (MENDES *et al.*, 2008). However, by the time when the simulations of this work were carried out, Domus was not scheduled to perform batch simulations due to the use of pixel counting technique that requires a graphical interface. In this sense, as a large number of cases and climatic files had to be used automatically, the simulations of this work were performed using

EnergyPlus, which contains the same model validated for the Wufi program (DOE, 2017a). Next, Chapter 4 presents the moisture risk analysis on the climatic level.

# CHAPTER 4. MOISTURE RISK ON THE CLIMATIC LEVEL

The information presented so far in this work provided the basis for its development. The hypothesis (there is a potential moisture risk in residential Brazilian buildings besides failure in the design and construction processes), problematic (lack of information regarding the humidity environment in Brazilian residential buildings on a country scale), and objective (investigate the potential moisture risks in Brazilian residential buildings across the different climates of the country) were described in the Introduction. Chapter 2 presented the essential background for the development of the thesis, concerning aspects of the climate and the residential building sector, policies regarding moisture safety in buildings, and research conducted on the topic in the country. Chapter 3 presented the main specific tools employed to achieve the expected results of the thesis.

This Chapter 4 presents the climatic analysis of the thesis, intending to estimate the potential moisture load that Brazilian buildings are susceptible to receiving due to climatic conditions. Due to its importance in the building sector, there are many research works regarding weather influence on buildings, which is the focus of this Chapter. Several studies concern the effects of wind-driven rain (WDR), which is an oblique rain with a horizontal velocity vector that occurs when there are rain and wind at the same time (BLOCKEN and CARMELIET, 2004), and is an important source of moisture in building facades. Research on WDR can be distinguished in (i) assessment of WDR load intensity and (ii) assessment of building facades response to WDR. Most of the existing research is focused on the first part (CORNICK and DALGLIESH, 2003; ABUKU *et al.*, 2006; ABADIE and MENDES, 2008; BLOCKEN and CARMELIET, 2008; STRAUBE, 2010; NIK *et al.*, 2015; GE, DEB NATH and CHIU, 2017; ORR *et al.*, 2018) and is still ongoing. The second part focuses mainly on WDR as a boundary condition in studies about heat, air and moisture (HAM) transfer in buildings (KÜNZEL and KIESSL, 1996; ABUKU, MASARU *et al.*, 2009; BLOCKEN and CARMELIET, 2015). Absorption of WDR in buildings envelope can also result in moisture flow towards indoor, increasing the mould growth risk at interior surfaces (KUBILAY *et al.*,

2015), what can affect indoor air quality and occupants' health, by causing allergies and diseases (BERGER *et al.*, 2015).

LISØ *et al.* (2007) present a method for assessing the relative potential of a climate to accelerate frost decay, in which the distributions of rainfall days prior to days with freezing events may provide information about the frost decay risk in building materials. CORNICK and DALGLIESH (2003) establish a moisture index to characterize climates for building envelope design. They propose a method for characterizing climate into zones concerning the risk of damage to building envelopes by comparing wetting and drying indicators. Provisional maps for Canada and the United States are presented.

There are schemes for climate classification across countries, mostly concerning annual rainfall rates, mean air temperature and type of vegetation with agriculture and human habitability purposes (CORNICK and DALGLIESH, 2003). There are also schemes of climate classification concerning building thermal analysis, *e.g.* the Brazilian Bioclimatic Zoning (ABNT, 2005), but the potential climatic moisture load is commonly disregarded despite its importance on building performance.

As shown, it is possible to find numerous studies with different approaches related to the potential climatic moisture risk issues in buildings. However, the majority of them do not consider a country scale approach to achieve a first outline regarding the climatic conditions that may lead to moisture issues in buildings (MORISHITA, MENDES and BERGER, 2016). A weather-based outline may point out the areas of the country more susceptible to risks and provide important information for the establishment of moisture-related standards, guide building constructors for choosing more appropriate moisture safe strategies and indicate the potential for further investigation on the topic.

A comprehensive overview on the scale of the country considering climatic conditions may be an important starting point for potential moisture risks in building analyses. In this Chapter, weather-based indicators are employed for a first outline of the potential moisture risk in buildings considering the main climatic sources of moisture. The present analysis is related to five weather parameters that

are plotted in the country map using Geographic Information System to spatially represent the risk across the country territory.

## 4.1 WEATHER-BASED INDICATORS

To provide an overview of the potential climatic moisture risk on the country scale, five indicators are presented: Vapour Pressure Index ($VP$), Wind-Driven Rain ($WDR$), Mould Growth Risk ($MR$), Air-rain Index ($I_{air-rain}$), and Facade Deterioration Index ($I_{FD}$). The original indicators $I_{air-rain}$ and $I_{FD}$ are based on the combination of vapour pressure with wind-driven rain and were proposed for the first time in MORISHITA *et al.* (2020).

The required climatic parameters for the weather-based indicators are wind speed and direction, rainfall, temperature, and relative humidity. All indicators are hourly based and calculated for a one-year time frame by employing the climatic data presented in Section 2.1.

Table 4 presents the required parameters for the evaluation of the weather-based indicators.

Table 4. Weather-based indicators and related analysed parameters

| | Index | Evaluation requirement | Evaluated Parameters | Parameters Units |
|---|---|---|---|---|
| $I_{air-rain}$ $I_{FD}$ | *VP* | External vapour pressure | Partial vapour pressure | Pa |
| | *WDR* | Wind-driven rain | Annual precipitation | mm/year |
| | | | Wind speed | m/s |
| | | | Wind direction | ° cardinal direction |
| | *MGR* | Isopleth Model | Temperature | K |
| | | | Relative humidity | - |

For the indicators $I_{air-rain}$ and $I_{FD}$ a single value of each indicator $I$ is obtained for each location. For the $I_{air-rain}$, it refers to the maximum calculated value and for the $I_{FD}$ it refers to the integration over the evaluated period.

The indicators are normalized according to

$$N = \frac{I}{\max_t(I)}, \tag{1}$$

where $N$ is one of the normalized weather-based indicators, $I$ is the value of the referred Index and $I_{max}$ is the maximum value of the respective Index, which corresponds to the maximum value of the indicator for the country.

### 4.1.1 Vapour Pressure ($\boldsymbol{VP}$)

The formulation for obtaining the vapour pressure index $VP$ is described below. The external vapour pressure is defined by

$$P_v^{ext} = P_{sat}(T_{ext})\ \varphi\ , \tag{2}$$

given that for temperatures between 263.15 K and 323.15 K the saturation pressure can be calculated as (HENS, 2007):

$$P_{sat} = exp\left(65.8094 - \frac{7066.27}{T_{ext}} - 5.976\ ln(T_{ext})\right), \tag{3}$$

where:

$P_v^{ext}$ is the external vapour pressure [Pa];

$P_{sat}$ is the saturation pressure [Pa];

$\varphi$ is the relative humidity [-];

$T_{ext}$ is the external temperature [K].

The Vapour Pressure index $VP$ is presented through Pa-hours, according to

$$VP = \int_{t_1}^{t_2} \left[\left(P_v^{ext}(t)\right) - \left(P_v^{ext}{}_{ref}\right)\right]\ \mathrm{d}t, \tag{4}$$

where:

$VP$ is the time-integrated vapour pressure [Pa-hours];

$t$ is the time instant;

$P_v^{ext}$ is the external vapour pressure;

$P_v^{ext}{}_{ref}$ is the reference value of vapour pressure for 24°C of temperature and 50% of relative humidity.

### 4.1.2 Wind-Driven Rain ($WDR$)

The wind-driven rain, or driving rain concept, is defined as the amount of rain that passes through a vertical plane in the atmosphere (Fig. 8). It occurs because raindrops are blown sideways at the speed of the wind at a given height above grade (ABUKU, BLOCKEN and ROELS, 2009).

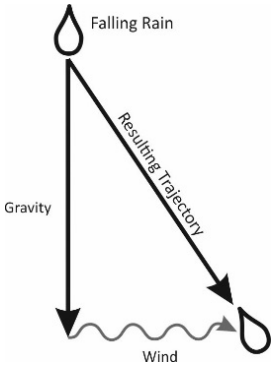

Fig. 8. Driving rain

There are several models for obtaining WDR indices (CORNICK and DALGLIESH, 2003). The annual WDR is the sum of horizontal rainfall and average wind speed, being both calculated over the year. Its great advantage is its easiness of use as these data are commonly available. Its weakness lays on using annual average values what may lead to an underestimation when compared with an hourly-basis calculation. The directional WDR is calculated similarly to the annual WDR but considering wind direction, which can reveal the predominant wind direction during the rainfall event. That is, two different locations can have the same annual WDR index, but the directional WDR approach can reveal which building orientation is receiving more rain load.

In this work, it is applied the hourly-based directional WDR Index proposed by (ASHRAE, 2008), a semi-empirical method to estimate the mass of raindrops that achieve the building walls based on available climatic data. The indicator estimates rain load on walls only because it considers that roof systems are designed and built on such a way there is no water penetration. The indicator is defined by

$$WDR_i = F_E\, F_D\, F_L\, W_s\, cos\, \theta\, R, \tag{5}$$

where:

$WDR_i$ is the driven rain deposition on a vertical wall for the cardinal direction [kg/m$^2$·h];

$F_E$ is the rain exposure factor [-];

$F_D$ is the rain deposition factor [-];

$F_L$ is an empirical constant (0.2) [kg·s/m$^3$·mm];

$W_s$ is the hourly average wind speed [m/s];

$\theta$ is the angle between wind direction and normal to the wall [°] (Fig. 9);

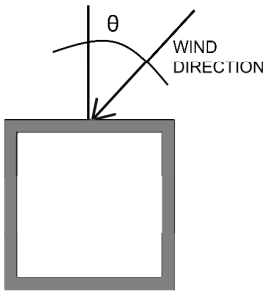


Fig. 9. Definition of wind angle

$R$ is the rainfall intensity [mm/h];

$i$ is the number of cardinal directions [-].

The exposure factor $F_E$ (Table 5) is influenced by the surrounding topography and the height of the building, so that the rain deposition factor $F_D$ (Table 6) is a function of the building shape.

Table 5. Exposure Factor

| Terrain height H [m] | Severe | Medium | Sheltered |
|---|---|---|---|
| H < 10 | 1.3 | 1.0 | 0.7 |
| 11 < H < 15 | 1.3 | 1.1 | 0.8 |
| 16 < H < 20 | 1.4 | 1.2 | 0.9 |
| 21 < H < 30 | 1.5 | 1.3 | 1.1 |
| 31 < H < 40 | 1.5 | 1.4 | 1.2 |
| 41 < H < 50 | 1.5 | 1.5 | 1.3 |
| 51 < H | 1.5 | 1.5 | 1.5 |

Source: (ASHRAE, 2008)

Table 6. Rain Deposition Factor

| | |
|---|---|
| walls below a steep-slope roof | 0.35 |
| walls below a low slope roof | 0.50 |
| walls subject to rain runoff | 1.00 |

Severe exposure includes funnelled wind areas, coastal areas and hilltops. Sheltered exposure includes areas sheltered by trees, valleys and nearby buildings.

The values for rain exposure factor ($F_E$) and rain deposition factor ($F_D$) refer to a low-rise building (< 10m) with walls below a low-slope roof in sheltered surrounding terrain, assuming a common urban one-storey house. The $WDR$ is calculated for the four main cardinal directions and for each direction it is obtained the total year load [kg/m$^2$·year].

### 4.1.3 Mould Growth Risk ($MI$)

To provide an outline regarding the mould growth risk, it is applied the Isopleth model presented by Clarke et al. (ESP-r model) (1999), which is a synthesis over 250 references of the available information about the mould growth characteristics at the time. The isopleth curves are the basis in the development of mould growth, they separate favourable from unfavourable conditions of temperature and relative humidity for its growth (VEREECKEN and ROELS, 2012). There are more up-to-date MGR models such as (SEDLBAUER and KRUS, 2003; JOHANSSON, WADSÖ and SANDIN, 2010; VIITANEN *et al.*, 2011). Nonetheless, isopleth models are suitable for climatic analyses, since it does not depend on determining a type of material and are also of particularly interest for tropical countries due to their high values of temperature and relative humidity. In Clarke's model, the mould species that may affect building materials are divided into six groups considering temperature and relative humidity (Fig. 10). For each one of these species, there is an isopleth curve; when the temperature and the relative humidity exceeds the respective curve, then mould can grow.

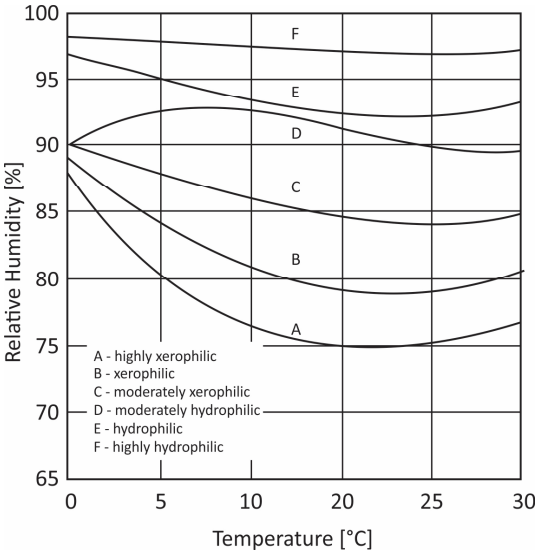


Fig. 10. Limiting growth curves for the 6 mould categories

Nonetheless, Clarke's Isopleth model is based on laboratory stationary experiments and does not consider an interim drying out of the spores. That is, the model does not consider that mould growth can decline under unfavourable conditions and represents the worst-case scenario, because a single exceed of the isopleth line is considered as mould growth. In this work, curve "B" is chosen as the evaluation criterion. It encompasses the fungus species *Aspergillus Versicolor* which may cause allergic reactions and is commonly found in building components (VEREECKEN and ROELS, 2012). Mould growth risk is presented employing MGR-hours, being given by

$$MI = \int_{t_1}^{t_2} \left[ \left( T(t), \varphi(t) \right) > \left( T_{iso}, \varphi_{iso} \right) \right] \, \mathrm{d}t, \tag{6}$$

where:

$MI$ is the mould growth risk index [MGR-hours];

$t$ is the time instant;

$T$ is the temperature [K];

$\varphi$ is the relative humidity [-];

$t_1$ is the lower limit of integration [h];

$t_2$ is the upper limit of integration [h];

$T_{iso}$and $\varphi_{iso}$ are the threshold values of temperature and relative humidity for mould growth of the "B" isopleth curve from Clarke's model.

### 4.1.4 Air-rain ($I_{air-rain}$)

The concept of Sol-Air Temperature is widely used to determine the heat gains through the building envelope. This concept can consider, besides the gains by convection, the solar radiative flux and the infrared exchanges from the sky (ASHRAE, 2013).

Analogously, it is proposed in this work the air-rain Index that considers the external vapour pressure added by the effect of wind-driven rain. This index aims at estimating the maximum potential moisture (liquid and vapour) load that may be deposited on the external surfaces of the building. Therefore, it is calculated for the main cardinal directions (North, South, East and West) as well as the corresponding external vapour pressure (Section 4.1.1) and wind-driven rain (Section 4.1.2). However, there are no restrictions for the evaluation to be carried out for a greater number of directions.

In this work, the combination of the external vapour pressure with WDR is named as equivalent vapour pressure ($P_v^{eq}$) and it is calculated according to Eq. (7)

$$P_{v,i}^{eq}(t) = \left(P_v^{ext} + \frac{WDR_i}{h_v}\right), \quad i = \{1, \dots, n\}, \tag{7}$$

where:

$P_{v,i}^{eq}$ is the equivalent vapour pressure for the cardinal direction [Pa];

$P_v^{ext}$ is the external vapour pressure [Pa] (Eq. (2));

$WDR_i$ is the driven rain deposition on a vertical wall for the cardinal direction [kg/m$^2$·h] (Eq. (5));

$h_v$ is the convective vapour transfer coefficient [s/m];

$i$ is the number of cardinal directions [-].

Finally, the air-rain Index is the maximum value found for $P_{v,i}^{eq}$ between the values calculated for all time instants of the corresponding cardinal direction, according to Eq. (8)

$$I_{air-rain,i}(t) = \max_t \left(P_{v,i}^{eq}(t)\right), \quad (8)$$

where:

$I_{air-rain,i}$ is the air-rain Index for the cardinal direction [Pa];

$P_{v,i}^{eq}$ is the equivalent vapour pressure [Pa];

$i$ is the number of cardinal directions [-];

$t$ is the time instant.

### 4.1.5 Facade Deterioration Risk ($I_{FD}$)

The Facade Deterioration Risk Index $I_{FD}$, also based on the $P_v^{eq}$ concept investigates the moisture load that the building may receive during a certain period. While the $I_{air-rain}$ represents the intensity, the $I_{FD}$ represents the cumulative moisture load and gives its time length for the whole building, consisting of the integration of all values of $P_v^{eq}$ over a time period according to Eq. (9)

$$I_{FD} = \int_{t_1}^{t_2} P_{v,i}^{eq}(t)\,\mathrm{d}t, \quad (9)$$

where:

$I_{FD}$ is the Facade Deterioration Risk Index [Pa-hours];

$P_{v,i}^{eq}$ is the equivalent vapour pressure [Pa];

$t_1$ is the lower limit of integration [h];

$t_2$ is the upper limit of integration [h];

$t_2 - t_1$ is the selected time frame.

## 4.2 RESULTS

### 4.2.1 Vapour Pressure ($\boldsymbol{VP}$)

Fig. 11 presents the Vapour Pressure Index Brazil map.

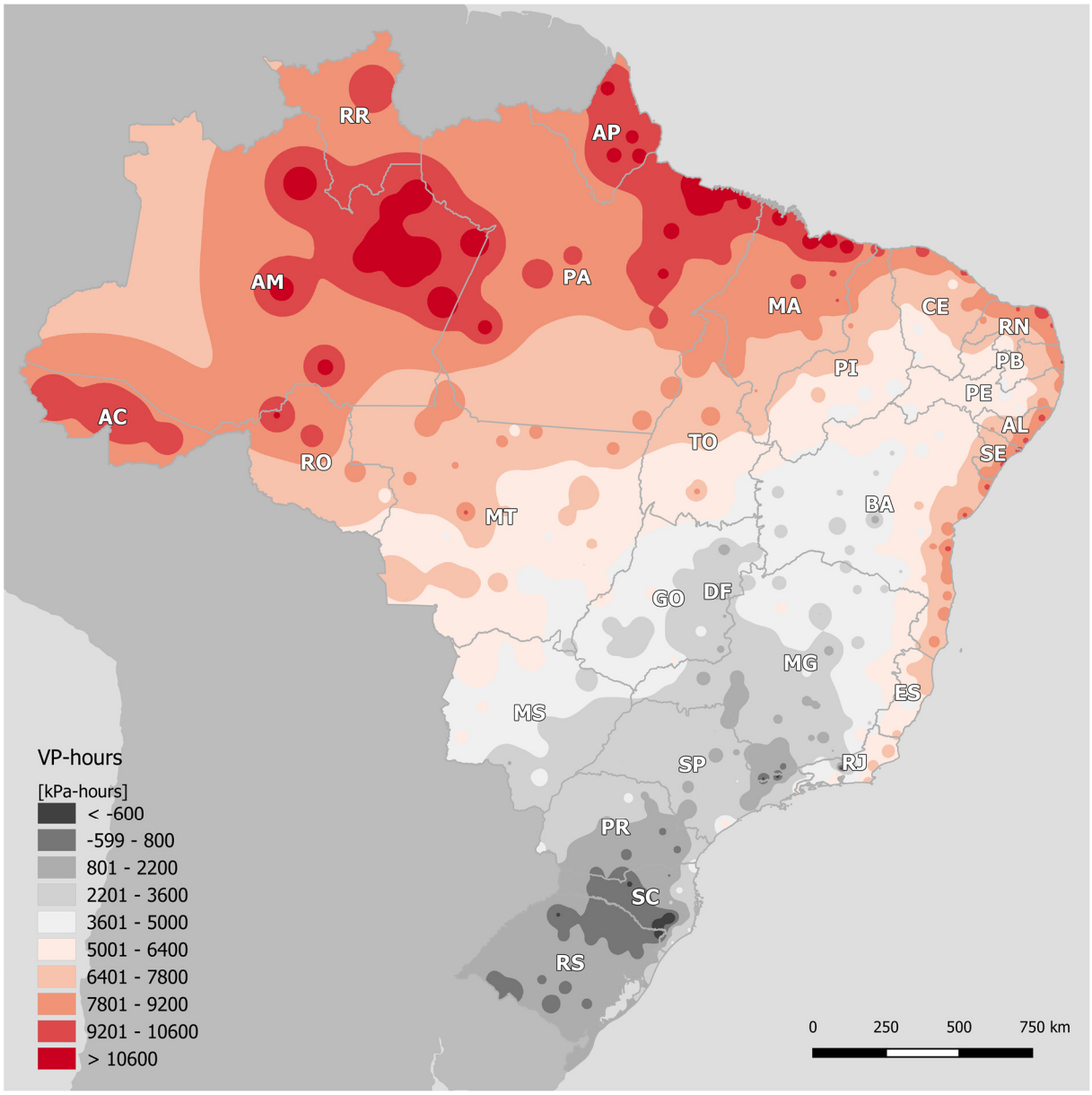


Fig. 11. Vapour Pressure ($VP$) Brazil map

One can see there is a trend of increasing $VP$ values from Southern regions towards Northern regions. High values are also observed in coastal areas from the Northeast region until the RJ state in the Southeast region. High altitude areas in South region between SC and RS states present negative $VP$ values. It is important to mention vapour pressure differences between outdoor and indoor environments play a major role on moisture transport through the porous building envelope and may cause mould growth on internal surfaces, especially in poorly ventilated rooms that receive little sun.

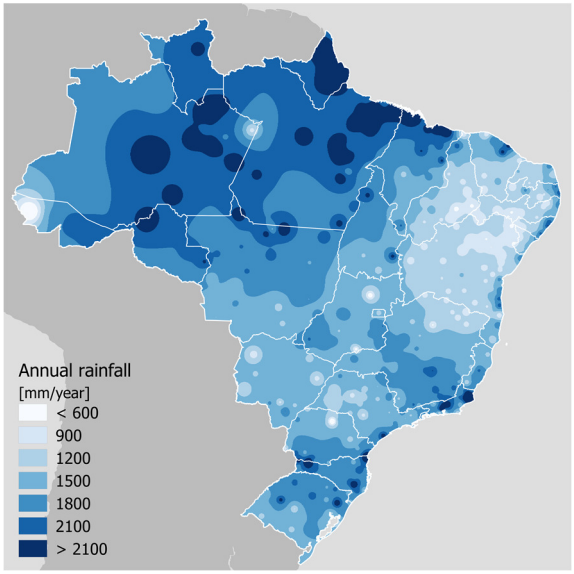


Fig. 12. Annual rainfall

To provide a comparison between rainfall rates and wind-driven rain, Fig. 12 illustrates the annual rainfall for Brazil according to data of the weather files.

The highest rainfall rates are in the North region, where the Amazon forest is located. High rates are also observed along the seacoast and much of the South region.

The lowest rates are observed in a diagonal belt from Central-West towards Northeast, especially in the semi-arid climate area.

Fig. 13 maps illustrate the wind-driven rain ($WDR$) of the four cardinal directions.

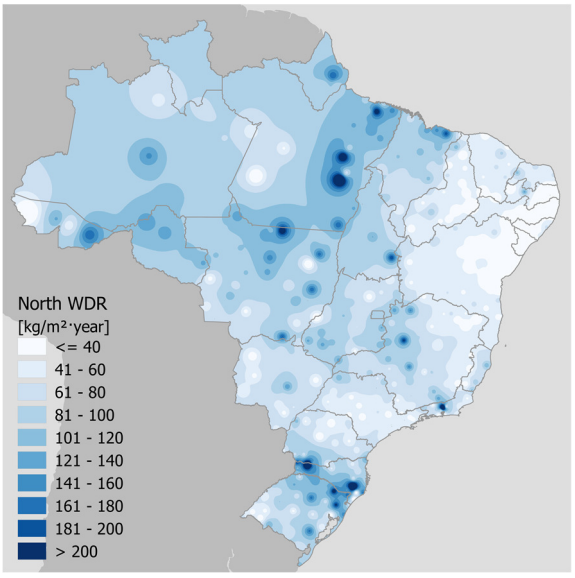


Fig. 13a. $WDR$ for North oriented facades

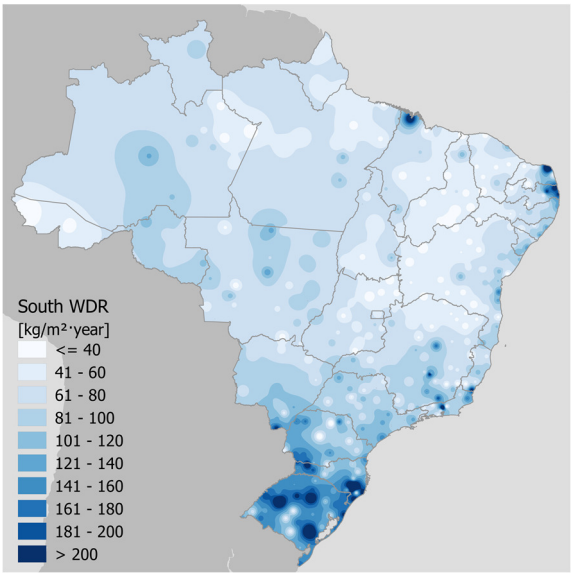


Fig. 13b. $WDR$ for South oriented facades

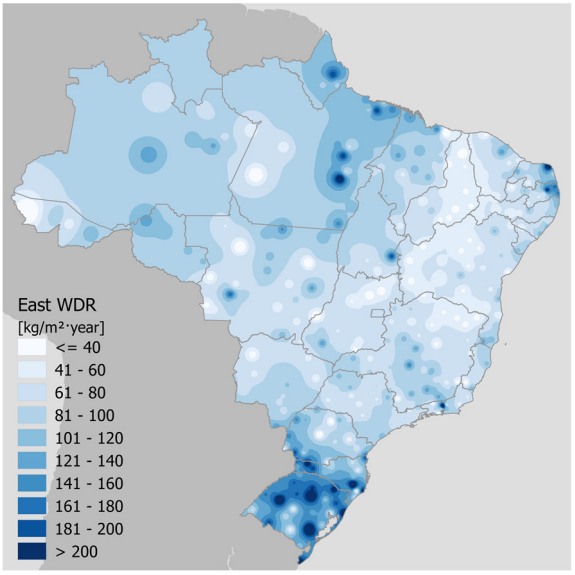


Fig. 13c. $WDR$ for East oriented facades

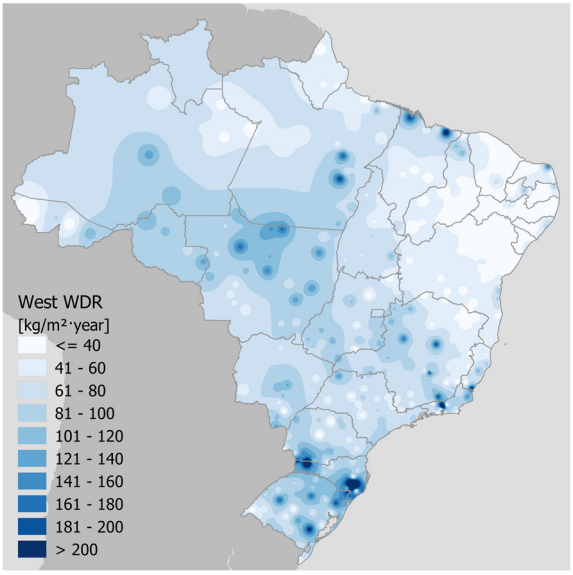


Fig. 13d. $WDR$ for West oriented facades

Unlike the annual rainfall map, in which rainfall rates are in more well-defined regions, the maps in Fig. 13 present more sparse spots of $WDR$ ranges. In South region, high rates are observed in the four cardinal directions and mainly for South oriented facades, which are also the ones that receive the least solar radiation. North $WDR$ map has high values of WDR more uniformly, and West map has the lowest ones. Also, the WDR along the seacoast is less pronounced in comparison with the annual rainfall map.

The results highlight the importance of considering WDR instead of simple rainfall rates for moisture risks in building analyses. WDR indicates which facade orientation is more susceptible of receiving rain load, which is not necessarily correlated to the rainfall rate of the location.

### 4.2.2 Mould Growth Risk ($MI$)

Fig. 14 presents the $MI$ map. The major part of the country presents MGR-hours higher than 50% (4,380 hours) of the year.

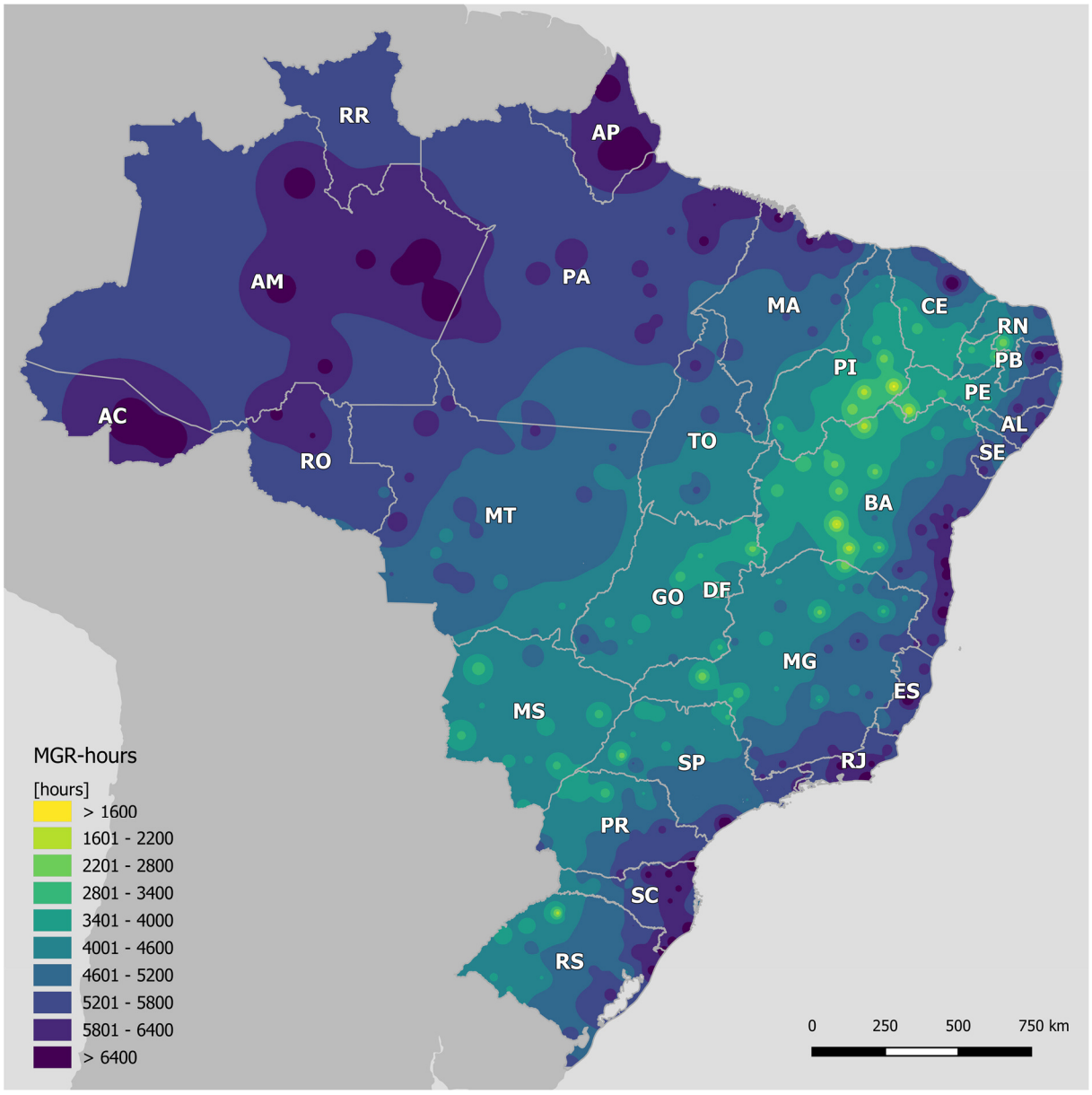


Fig. 14. $MI$ map

As the $MI$ is related to vapour pressure rates, the higher values are observed in the North region and along the seacoast. However, high rates of $MI$ are also observed in southern coastal and mountainous regions, which have low vapour pressure values. The lower values are found in a countryside diagonal belt that starts in the West of RS state towards the Northeast semi-arid area.

Since the MGR also depends on the time exposure, it is also plotted in Fig. 15 map the longest consecutive period of *MI*. When comparing to the population map (Fig. 2), it is possible to notice an overlap of high levels between both MGR-hours and the consecutive period of *MI*, and highly densely populated areas along the seacoast. Some northern areas that present high levels of the $MI$ are lightly

populated ones (AC, AM, PA and AP states) what means that the potential moisture risk can be considered less unsettling in contrast with populous southern and seacoast areas.

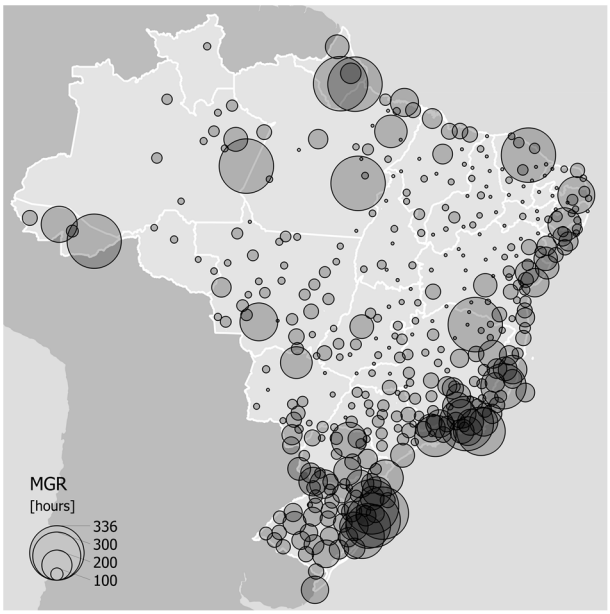


Fig. 15. Consecutive period of *MI*

### 4.2.3 Equivalent vapour pressure ($P_v^{eq}$)

The concept of the equivalent vapour pressure consists of a combination of external vapour pressure with wind-driven rain. For a better understanding of the concept, additional results of these constituting elements are also presented.

Fig. 16 illustrates the maximum values of the external vapour pressure $P_v^{ext}$ and the equivalent vapour pressure $P_v^{eq}$ per city, ordered by $P_v^{eq}$.

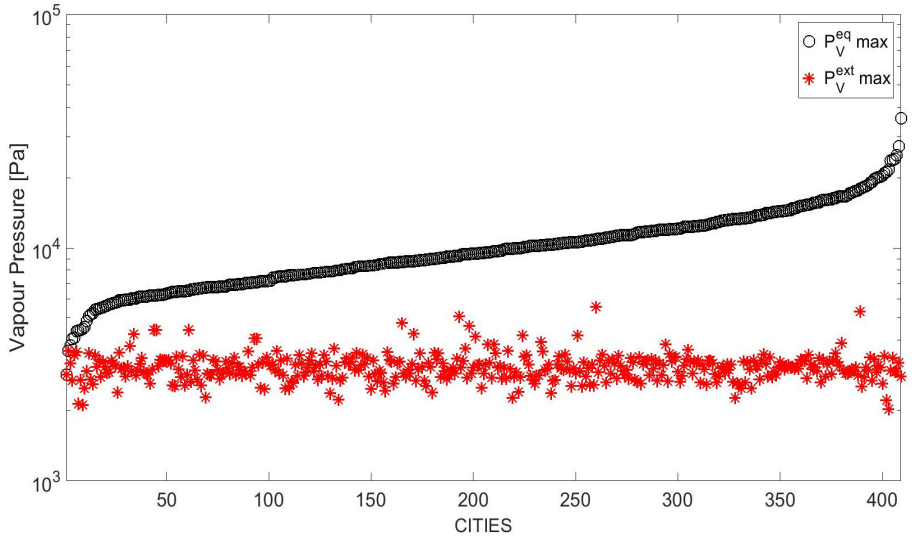


Fig. 16. Comparison of $P_v^{ext}$ and $P_v^{eq}$ magnitudes for the 409 cities

The graphic in Fig. 16 shows that, besides the expected difference in the moisture load, the values of the maximum $P_v^{ext}$ present a variation as high as 3.52x10³ Pa, while for $P_v^{eq}$ this difference raises to 3.31x10$^4$. It highlights the importance of considering the effect of the wind-driven rain when estimating the potential moisture load; $P_v^{eq}$ can achieve much higher and varied values of vapour pressure in comparison with the $P_v^{ext}$. The maximum value obtained for $P_v^{ext}$ is 5.56x10² Pa and for the $P_v^{eq}$ is 3.59x10$^4$ Pa.

To analyse the behaviour of the requirements along the year-period, four cities were chosen. Sao Paulo and Rio de Janeiro (Southeast region), which are the two most populated cities of the country. Sao Joaquim (South region) and Maues (North region) are the cities that obtained, respectively, the lower ($P_v^{eq}$=1.29x10³ Pa) and higher ($P_v^{eq}$=2.96x10³ Pa) mean values of $P_v^{eq}$. Results obtained for these cities are presented in Table 7.

Table 7. Results obtained for four cities

| City | Population [inhabitants] | $N_{FD}$ | $N_{air\text{-}rain\ North}$ | $N_{air\text{-}rain\ East}$ | $N_{air\text{-}rain\ South}$ | $N_{air\text{-}rain\ West}$ | *Mean* $P_v^{eq}$ [Pa] | *Max* $P_v^{eq}$ [Pa] |
|---|---|---|---|---|---|---|---|---|
| Maues | 51,847 | 1.00 | 0.33 | 0.16 | 0.21 | 0.50 | 2.96x10³ | 1.20x10$^4$ |
| Rio de Janeiro | 6,520,266 | 0.74 | 0.15 | 0.26 | 0.35 | 0.22 | 2.19x10³ | 9.51x10³ |
| Sao Joaquim | 24,812 | 0.43 | 0.11 | 0.28 | 0.36 | 0.31 | 1.29x10³ | 9.96x10³ |
| Sao Paulo | 12,106,920 | 0.55 | 0.15 | 0.15 | 0.29 | 0.33 | 1.63x10³ | 7.93x10³ |

Next, Fig. 17 presents monthly values of rainfall and wind-driven rain rates for the four cities.

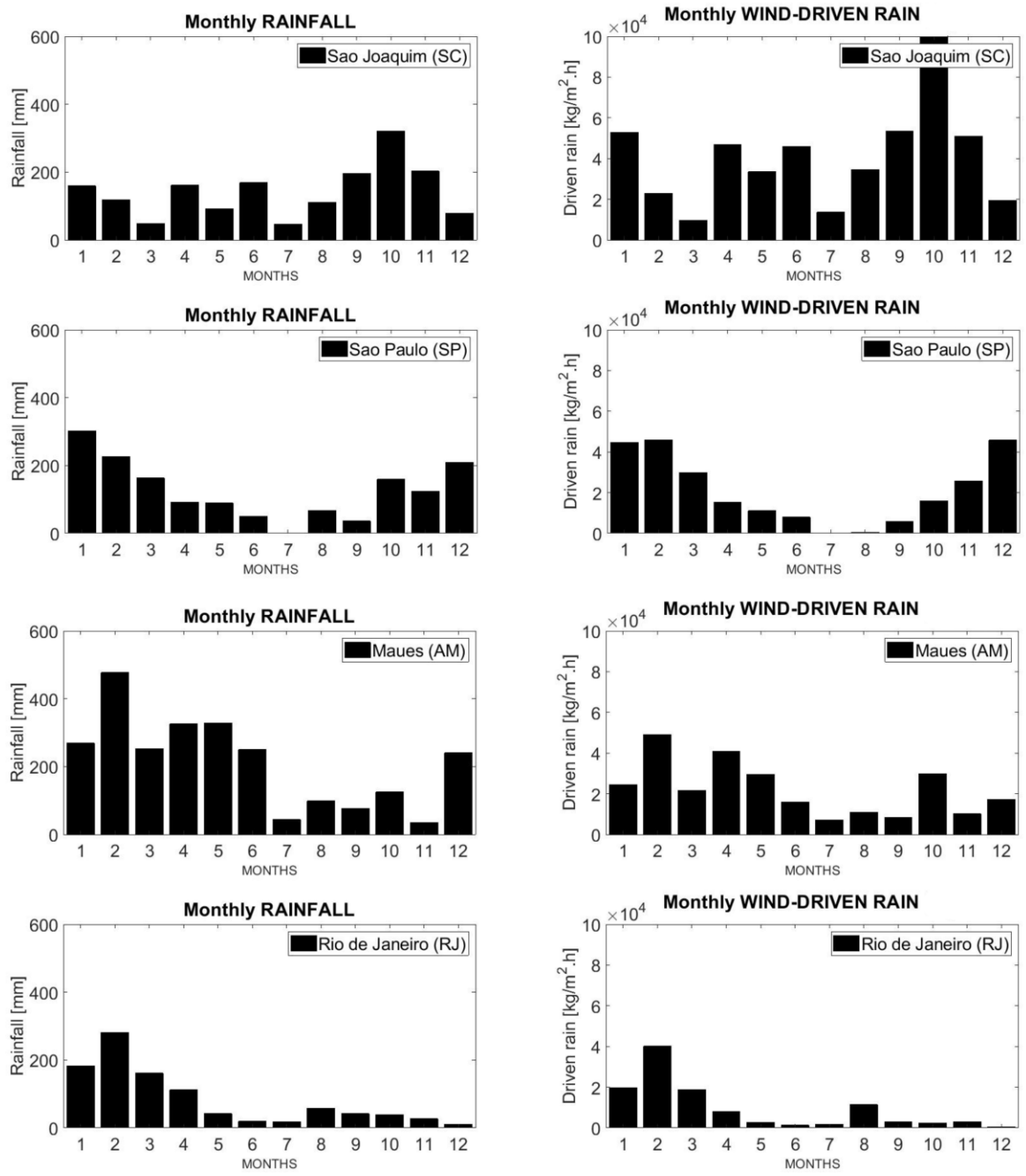


Fig. 17. Comparison of monthly values of rainfall and wind-driven rain rates

The graphics in Fig. 17 show a comparison between the load due to rainfall and the load due to wind-driven rain. Considering simple rainfall rates instead of the combined effect of rain and wind, one can over or underestimate the moisture load. For example, when comparing for January, the cities of Sao Joaquim and Maues, the rainfall rate of Maues (269 mm) is higher than the one for Sao Joaquim (159 mm), but the $WDR$ of Maues (2.44x10$^4$ kg/m$^2$·h) is lower than the one for Sao Joaquim (5.29x10$^4$ kg/m$^2$·h). Therefore, the effect of wind results in a higher moisture load to Sao Joaquim in comparison

to Maues, even though Sao Joaquim has a lower amount of rainfall in mm. Similarly, for Sao Paulo, although October has a higher value of rainfall (159 mm) than November (124 mm), it has a lower value of $WDR$ (1.60x10$^4$ kg/m$^2$·h) compared to the $WDR$ in November (2.57x10$^4$ kg/m$^2$·h).

### 4.2.4 Air-rain ($I_{air-rain}$)

Fig. 18 shows monthly values obtained for $P_v^{ext}$, $P_v^{eq}$ and $I_{air-rain}$.

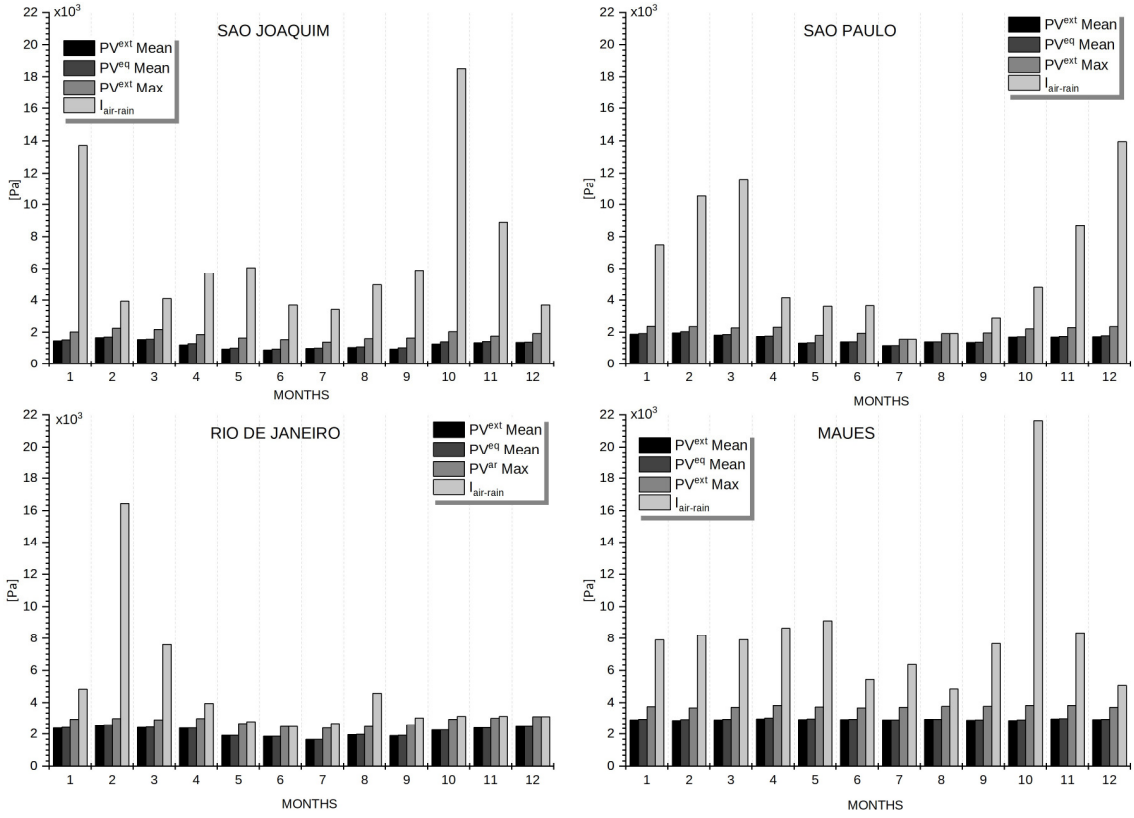


Fig. 18. Monthly mean and maximum values for $P_v^{ext}$, $P_v^{eq}$ and $I_{air-rain}$

When comparing the mean values of external vapour pressure $P_v^{ext}$ and those of equivalent vapour pressure $P_v^{eq}$ there is no significant difference. However, high variation is observed when comparing the maximum values, which is the interest of the $I_{air-rain}$. Considering the $P_v^{eq}$ is directly affected by the WDR, the behaviour of the $I_{air-rain}$ over the year is similar to the $WDR$ (Fig. 17), but some differences can be observed. For example, the peak of $I_{air-rain}$ in October for the city of Maues occurs probably because October has a considerable high rate of WDR, besides it is also the hottest month of the year for that city, drawing attention to the WDR effect when estimating the equivalent vapour pressure.

In the following, Brazil maps are presented with the obtained normalized indicators. Fig. 19 illustrates the maps associated with $N_{air-rain}$ Index for the North, East, South and West facades.

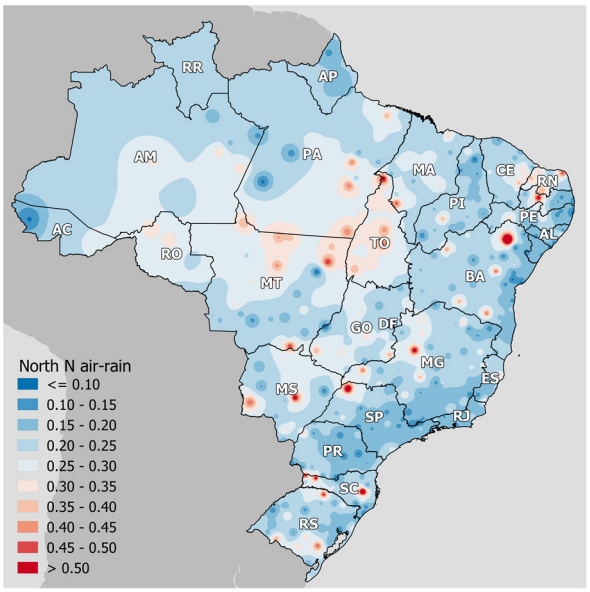


Fig. 19a. $N_{air-rain}$ Index for North oriented facades

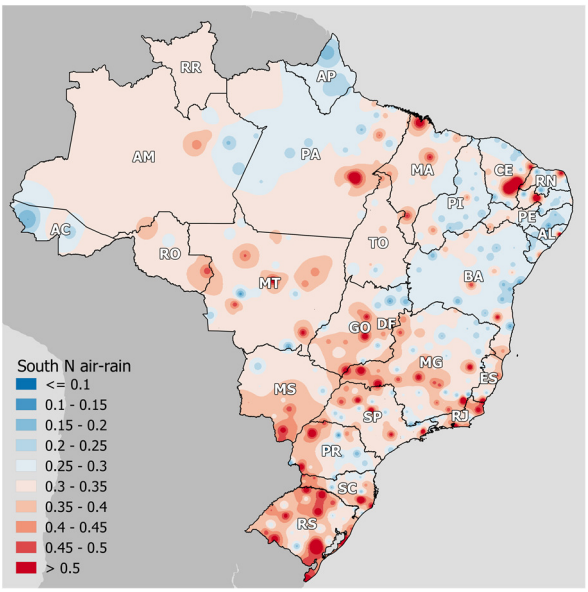


Fig. 19b. $N_{air-rain}$ Index for South oriented facades

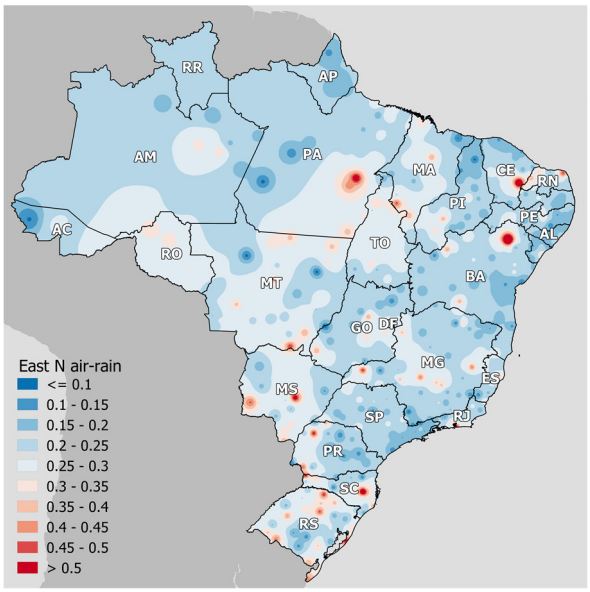


Fig. 19c. $N_{air-rain}$ Index for East oriented facades

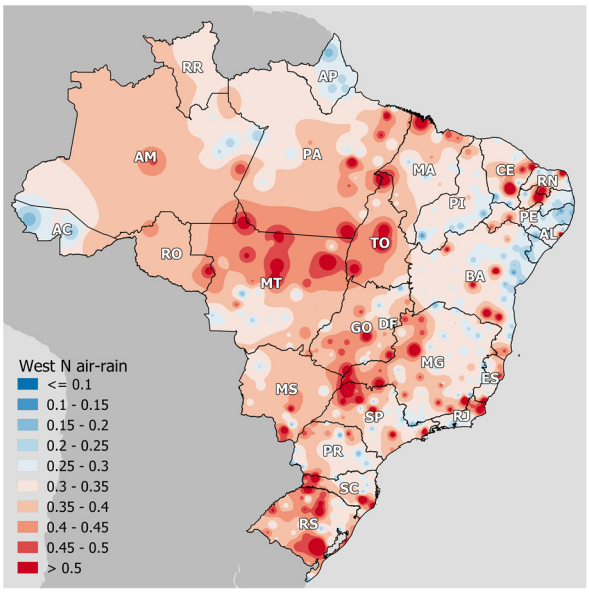


Fig. 19d. $N_{air-rain}$ Index for West oriented facades

Considering the $N_{air-rain}$ Index represents a peak load value and that Brazil is a large country, with very variable rainfall and wind patterns along the seasons, the Fig. 19 maps present some isolated spots. Nonetheless, it is possible to observe some trends on the potential moisture load for the West and South compared to the East and North directions; for the West, there are many spots of values greater than 0.5. North facades, when compared to East facades, present larger areas with Index

values lower than 0.10. However, it presents more occurrence of spots with Index values higher than 0.3. The air-rain Index illustrates how the peak potential moisture load may vary over the regions and cardinal directions.

The West $N_{air-rain}$ map (Fig. 19d) is presented overlapped with the Bioclimatic Zoning map (Fig. 5) in Fig. 20.

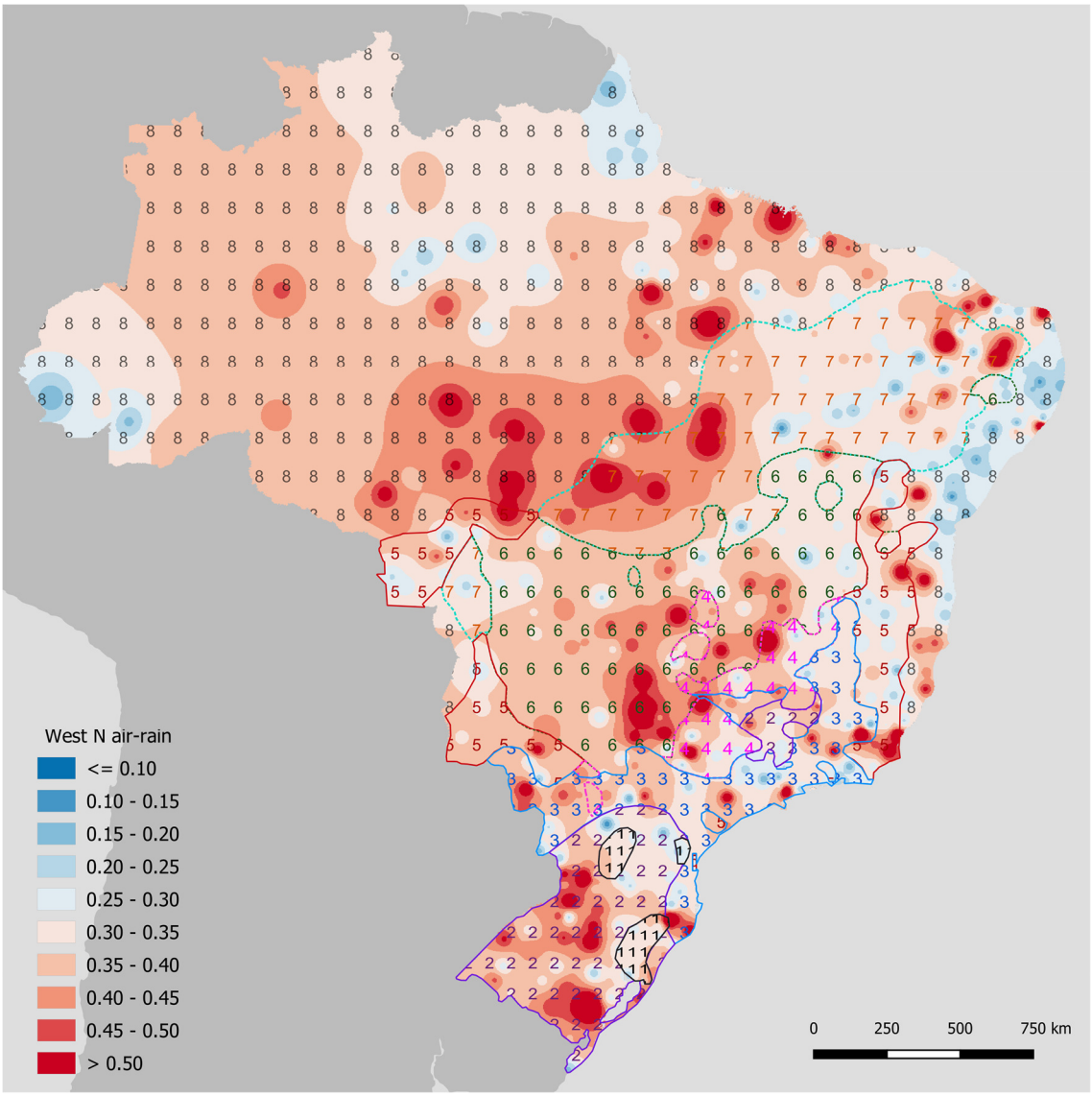


Fig. 20. West $N_{air-rain}$ Index and Bioclimatic Zones

Because the Bioclimatic Zoning is widely applied in building research, the overlapping of the maps in Fig. 20 intends to illustrate the behaviour of the $N_{air-rain}$ across the different Zones. With exception

of Zone 1, which is the coldest and smallest zone (less than 1% of the territory area), the Index vary from low values (0.10-0.15) up to high values (> 0.50) in all other zones.

### 4.2.5 Facade Deterioration risk ($I_{FD}$)

The Facade deterioration Risk Index expresses the cumulative potential moisture load for the evaluated time frame. Fig. 21 shows high monthly values of the Index for the city of Maues during the whole year, approximately the double of the values for Sao Joaquim. The city of Rio de Janeiro has a

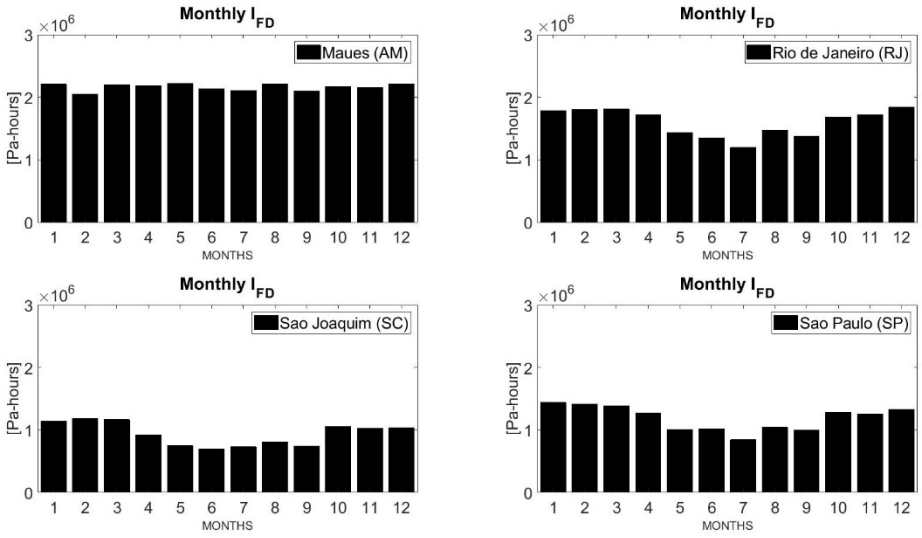


Fig. 21. Monthly values of $I_{FD}$

variation between summer and winter but with high values, close to the Maues ones. It is possible to notice the differences between the intensity load $I_{air-rain}$ and the cumulative load $I_{FD}$ indicators. The values of $I_{air-rain}$ for the city of Maues are much higher than the ones for Rio de Janeiro, but relatively close for the $I_{FD}$. The differences between Maues and Sao Joaquim are very pronounced for $I_{FD}$ but moderate for $I_{air-rain}$. Sao Paulo presents a stable behaviour for both indices. Next, Fig. 22 presents the Brazil map for the normalized Facade Deterioration Risk Index $N_{FD}$.

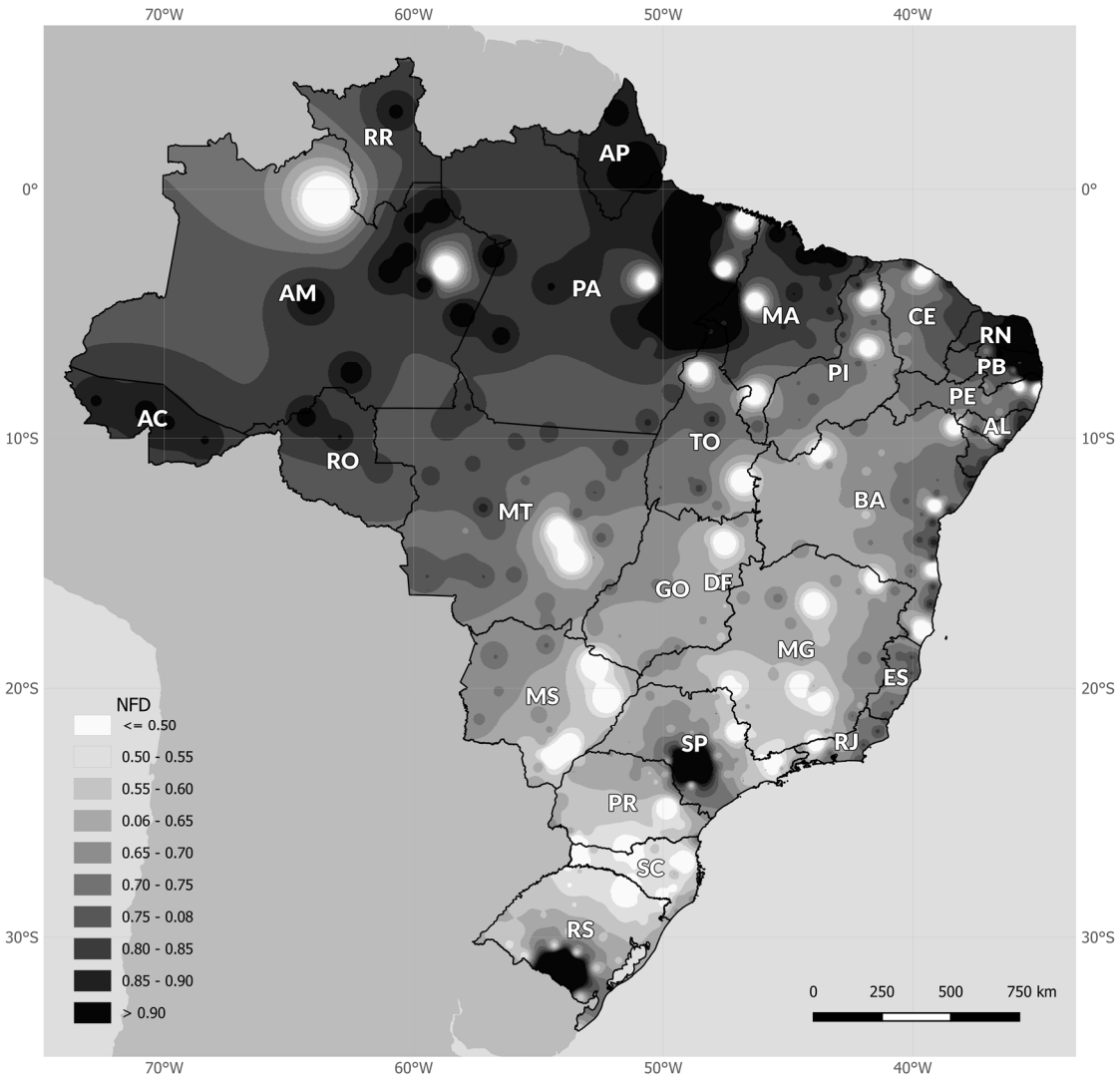


Fig. 22. $N_{FD}$ Index map

Spots of high values of the $N_{FD}$ can be observed in densely populated areas of the Northeast coast and the state of Sao Paulo (SP). In the overall, there is a trend of increasing values of the Index from the Southeast towards Northwest. The observed differences indicate that the $N_{FD}$ may be of interest for estimating the potential moisture load on the assessment of the potential risk of building facade deterioration. Follow, Fig. 23 presents the $N_{FD}$ map overlapped with the Bioclimatic Zoning map (Fig. 5).

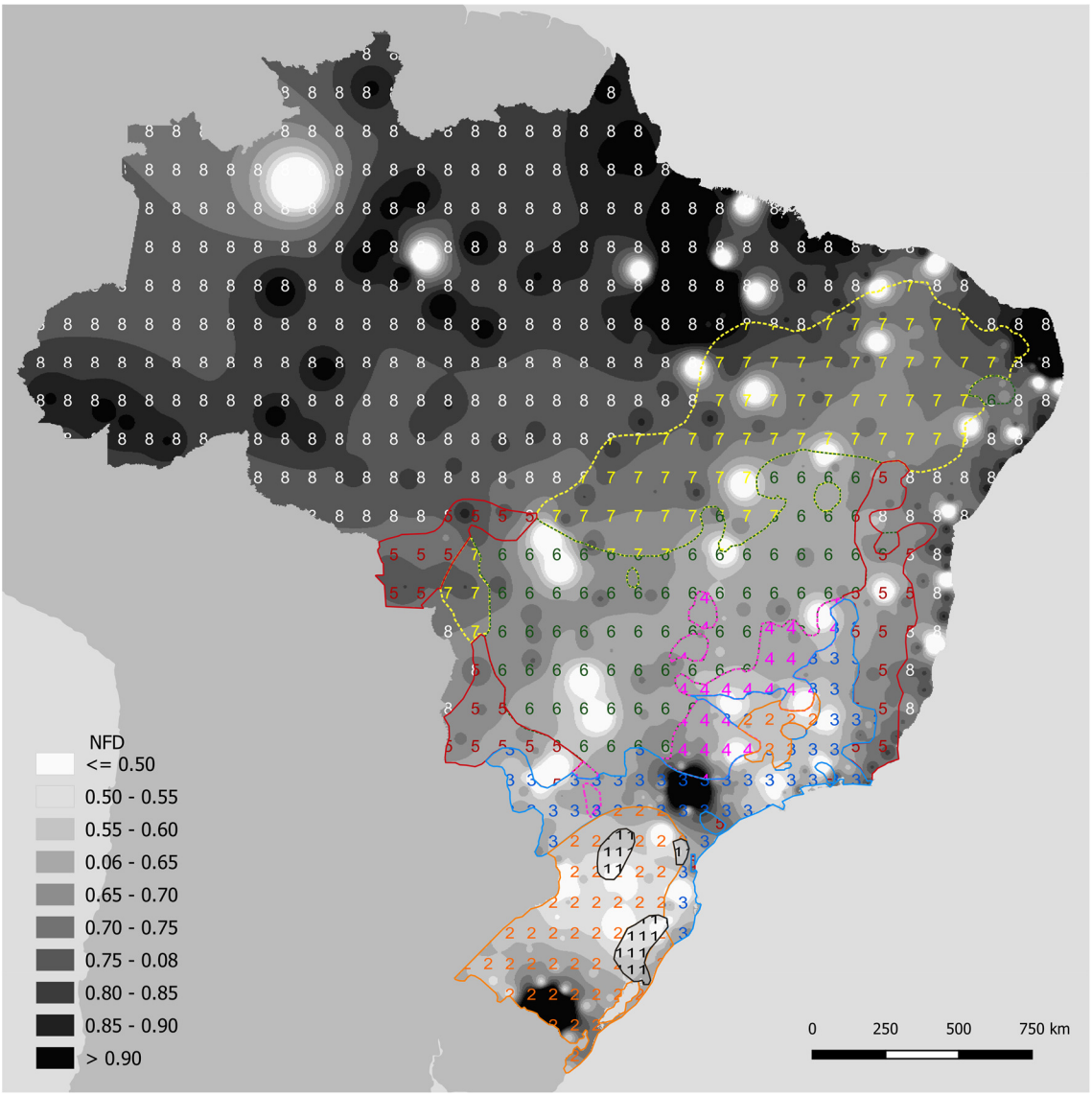


Fig. 23. $N_{FD}$ Index and Bioclimatic Zones

The map in Fig. 23 shows that, for the same bioclimatic zone, the $N_{FD}$ Index may present great variation. In Bioclimatic Zone 8, that corresponds to about 53% of the territory and is the hottest one, it is possible to observe all ranges of the Index. For Zones 2 and 3, which are highly populated, there are spots of low (<= 0.50) and high (> 0.90) $N_{FD}$ values.

## 4.3 CONCLUSIONS

To provide a first overview regarding the climatic potential moisture risk in buildings on the country scale, this Chapter established a method with weather-based indicators. The method focuses only on climatic sources of moisture, not considering materials, building systems nor internal sources of moisture.

A method with weather-based indicators was presented to provide an outline regarding the risks due to weather parameters on the country scale. With GIS software, these indicators can be plotted on maps to easily illustrate the regions of the country under higher climatic moisture loads. The proposed indicators are based on climatic data that are commonly available and intent to be as generic as possible to ease its application for other locations, providing a fast perception of the potential risk even in a country scale.

This climatic analysis has shown that Brazil has important climatic sources of moisture. The plotted maps show an overlap of highly densely populated areas and high climatic moisture risk areas. The overlapped maps of the existing Bioclimatic Zoning with the West $N_{air-rain}$ (Fig. 20) and $N_{FD}$ (Fig. 23) maps show diverse levels of both indicators in the same Zone. As moisture may affect building performance (MENDES, WINKELMANN*, et al.*, 2003; WOLOSZYN and RODE, 2008a; ABADIE and MENDONÇA, 2009), results of the overlapped maps suggest the need for considering moisture-related requirements in standards related to Thermal Performance of Buildings.

This Chapter presented the climatic analysis aiming at estimating the potential moisture load in Brazilian buildings due to climatic conditions. High outdoor vapour pressure values and the combined effect of high rainfall rates with wind action in highly densely populated areas indicate a high climatic potential moisture risk level. In the following, Chapter 5 presents the analysis on the building scale.

# CHAPTER 5. MOISTURE RISK OF A TYPICAL POPULAR BRAZILIAN RESIDENTIAL BUILDING

Regarding the first goal of the present thesis, Chapter 4 revealed the climate as an important potential moisture load. The weather-based indicators plotted in the map of Brazil provide a perspective of the areas of the country that are more susceptible to various climatic moisture sources. Hence, in this Chapter, the climate is also considered with the same weather files database, but as the boundary conditions for 1-D whole-building hygrothermal simulations across Brazil, which additionally to the climate takes into account internal moisture loads and moisture transport/accumulation in a typical popular Brazilian construction.

Despite its occurrence being extensively known, moisture disorders in residential buildings in this country are commonly faced as unavoidable or related to failures during the construction process and research on the topic is still underexplored. Information is hardly available regarding the moisture environment in Brazilian residential dwellings.

Climatic conditions combined with the large occurrence of informal construction, little variation in construction methods and lack of moisture risk assessment requirements in building standards (MORISHITA *et al.*, 2016) lead to the following question: What is the potential moisture risk in Brazilian residential buildings besides construction failure? And, if there is a risk, what is the influence of the conventional construction methods considering the country's types of climate?

Hence, this Chapter aims to provide an overview of the potential moisture risk in residential buildings across Brazil, considering the climatic characteristics and the most common construction techniques used in the country. The goal is not to predict the moisture loads neither to assess the effects of moisture transport on building performance, but to reveal the regions and construction techniques that may be more susceptible to moisture risk.

One-dimensional whole-building model simulations are carried out for a typical Brazilian typology of a residential building for 409 cities in a 5-year time frame. Solar orientation, the material of walls, length of the shower, the painting layer permeance, and the presence of an exhauster fan in the bathroom

are the chosen parameters to be categorically varied. A mould growth risk index is employed as a reference of moisture risk and charted on the country map, supplying a graphical overview of the regions that are more susceptible to potential moisture risks according to the employed parameters.

## 5.1 SIMULATION PROCEDURE

The whole-building 1-D simulations are carried out for 409 cities in a 5-year timeframe using the software EnergyPlus® (V8-7-0), presented in Section 3.2.

To assess the influence of various parameters on the potential moisture risk in buildings, a base case is presented in Section 5.1.1 and the building design parameters chosen to be categorically varied are presented in Section 5.1.3.

### 5.1.1 Base Case building

#### 5.1.1.1 *Building geometry*

The base case building is a one-storey 67 m² single-family house, as a representation of a common Brazilian residential building. It is based on data from the public survey "Home Appliances Information System and Consumer Habits" (SINPHA) (2005) and the Brazilian National Institute of Geography and Statistics (IBGE) (2019a) (Table 8). According to these data, the estimation is about 67 million residents living in the base case building typology, as shown in Table 9.

Table 8. Typical Brazilian dwelling main characteristics.

| Item | Characteristic | Representativeness of total Brazilian dwellings [%] |
|---|---|---|
| Type of single-family building | One storey house | 88 |
| Area | ≈65.0m² | 37 |
| Composition of wall | Masonry with external mortar and painting on both sides | 96 |
| Composition of roof | Clay roofing tile | 45 |
| Composition of ceiling | Concrete slab | 25 |
| Composition of floor | Concrete slab | 64 |
| Composition of the window frame | Iron | 40 |

Sources: SINPHA (2005); IBGE (2019a)

Table 9. Estimation of the population living in the case study typology.

| Dwellings | [1,000 dwellings] | [%] |
|---|---|---|
| Total dwellings Brazil | 65,130.00 | 100 |
| One storey house | 57,499.00 | 88 |
| One storey house with ≅ 65.0 m² area | 21,274.60 | 37 |
| Average residents | [resident/dwelling] | 3.16 |
| Population | [1,000 residents] | [%] |
| Total population Brazil | 206,339.00 | 100 |
| Population living in one storey houses | 181,696.80 | 88 |
| Population living in ≅ 65.0 m² one storey houses | 67,227.80 | 37 |

Sources: SINPHA (2005); IBGE (2019a)

Figs. 24 and 25 illustrate the base case floor plan and geometry, which are based on a model from *Minha casa, Minha vida* (My home, My life) (BRASIL, 2019), a Brazilian public policy for popular housing.

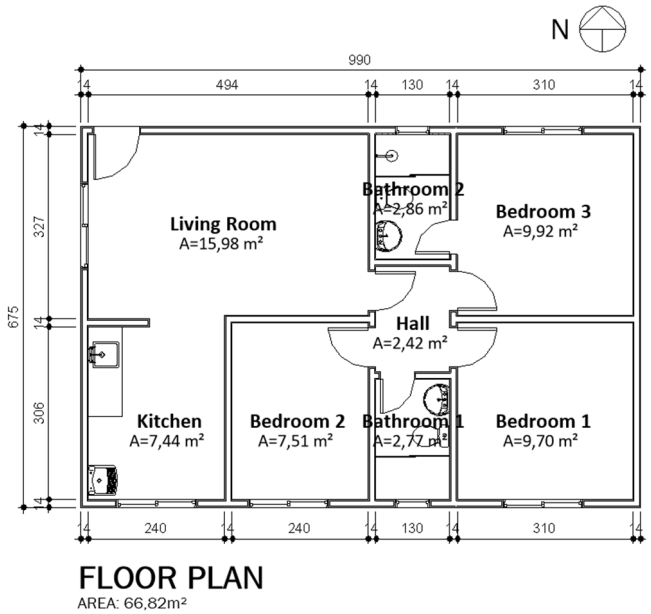


Fig. 24. Case study floor plan

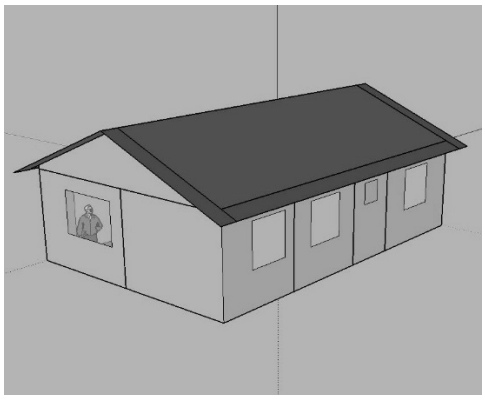

Fig. 25. Case study volumetric sketch

Because of the vapour production from the shower and the south orientation, bathroom 1 can be pointed out as the main critical area. Due to these reasons, the bathroom 1 wall with exterior contact is chosen as the analysis object.

### 5.1.1.2 *Building envelope*

Tables 9 and 10 present the construction details and their thermal properties. Properties for grout and concrete are gathered from the Brazilian standard NBR 15220 (ABNT, 2005), and all the others from the Annex 24 report (KUMARAN, 1996).

Table 10. Construction details

| Construction | Material layers |
|---|---|
| Roof | Roofing clay tile<br>Concrete |
| Ceiling | Concrete |
| Floor | Ceramic tile<br>Concrete |
| Window | Glass clear 4mm |
| Wall | Mortar<br>Clay brick<br>Mortar |
| Wall ceramic | Mortar<br>Clay brick<br>Mortar<br>Ceramic tile |
| Wall grout | Mortar<br>Clay brick<br>Grout |

Table 11. Thermal properties of dry-basis materials

| Material | λ [W/m·K] | ρ [kg/m³] | c [J/kg·K] | Thickness [m] |
|---|---|---|---|---|
| Ceramic tile | 1.05 | 2000 | 920 | 0.005 |
| Clay brick | 0.684 | 1791 | 840 | 0.090 |
| Concrete | 1.75 | 2200 | 1000 | 0.100 |
| Grout | 0.20 | 850 | 850 | 0.025 |
| Mortar | 1.15 | 2000 | 1000 | 0.025 |
| Roofing clay tile | 1.05 | 2000 | 920 | 0.005 |
| Wood | 0.15 | 608 | 1630 | 0.025 |

Due to the lack of measured thermal properties of typical Brazilian building materials and the existing libraries provide properties for the massif material, equivalent properties of the clay hollow brick, which is the envelope's main material, were calculated.

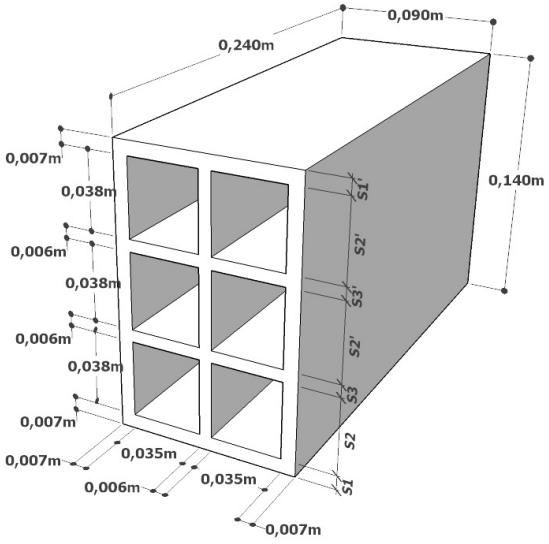


Fig. 26. Clay hollow brick dimensions

Firstly, it is obtained the thermal resistance and the heat capacity of the hollow brick by applying the method proposed by the Brazilian standard NBR 15.220 (ABNT, 2005). Next, the equivalent values of thermal conductivity and thickness are calculated. The hypothesis is to keep the referent properties for thermal inertia, by keeping specific heat and specific mass values and changing the thickness and thermal conductivity of the massif element representing the transport coefficients of the hollow element.

The thermal resistance and heat capacity are calculated per sections, according to Fig. 26. The thermal resistance of the hollow brick is obtained by

$$R_T = \frac{\sum_{i=1}^{n} A_i}{\sum_{i=1}^{n} \frac{A_i}{R_i}}, \tag{10}$$

where:

$R_T$ is the hollow brick total thermal resistance [(m²·K)/W];

$A_i$ is the section area[m²];

$R_i$ is the section thermal resistance [(m²·K)/W];

$n$ is the number of sections [-].

given that the thermal resistance of the section is calculated by

$$R_n = \frac{\delta_n}{\lambda_n}, \tag{11}$$

where:

$R_n$ is the section thermal resistance [(m²·K)/W];

$\delta_n$ is the section thickness [m];

$\lambda_n$ is the section thermal conductivity [W/(m·K)];

$n$ is the number of sections [-].

The heat capacity of the hollow brick is obtained by

$$C_T = \sum_{S=1}^{n} c_S \, \delta_S \, \rho_S, \tag{12}$$

where:

$C_T$ is the heat capacity of the hollow brick [kJ/(m²·K)];

$c_S$ is the section specific heat [kJ/(kg·K)];

$\delta_S$ is the section thickness [m];

$\rho_S$ is the section specific mass [kg·m$^3$];

$n$ is the number of sections.

After the values of thermal resistance and thermal capacity of the hollow brick are obtained, the equivalent thickness (Eq. 4) and equivalent thermal conductivity (Eq. 5) can be calculated.

$$\delta_{eq} = \frac{C_T}{c\rho}, \tag{13}$$

where:

$\delta_{eq}$ is the massif equivalent thickness representing the hollow brick [m];

$C_T$ is the heat capacity of the hollow brick (Eq. 3) [kJ/(m²·K)];

$c$ is the clay specific heat [kJ/(kg·K)];

$\rho$ is the clay specific mass [kg·m$^3$].

$$\lambda_{eq} = \frac{c}{R_T}, \tag{14}$$

where:

$\lambda_{eq}$ is the equivalent thermal conductivity of the material [W/(m·K)];

$\delta_{eq}$ is the equivalent thickness [m];

$R_T$ is the hollow brick total thermal resistance [(m²·K)/W].

The calculated values are presented in Table 12.

Table 12. Properties of the hollow clay brick

| R [(m²·K)/W] | C [kJ/(m²·K)] | δ [m] | λ [W/(m·K)] |
|---|---|---|---|
| 0.267 | 35.169 | 0.023 | 1.496 |

For walls and ceiling of bathroom 1 and bedroom 2, it is employed the Heat and Moisture Transfer (HAMT) heat balance algorithm, which is based on the hygrothermal model proposed by KÜNZEL (1995). For other walls, floors, ceilings and the roof, it is applied the Conduction Transfer Function (CTF) algorithm, which is the basic model of Energy Plus to compute transient heat transfer through multi-layered components (Fig. 27). The material moisture properties of concrete and grout are from the EnergyPlus material library and for clay from the Annex 24 (KUMARAN, 1996). The required moisture properties of the EnergyPlus HAMT model are detailed in Table A.2 and their values in Table A.3 of Annex A.

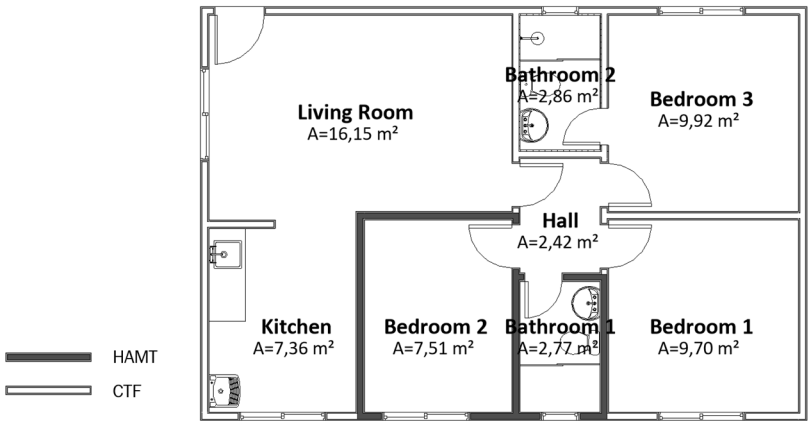


Fig. 27. Heat balance algorithm of the model

Since EnergyPlus does not perform 2-D transfer analyses, the walls were modelled in a relative proportion of the materials. The grout area of the wall is obtained by considering a 30 cm tile and a 0.5 cm width grout as shown in Fig. 28a. The result is an 8 cm stripe, represented by the solid hatch

(Fig. 28b). The wall is divided into two parts in EnergyPlus, one of grout (Fig. 29a) and other of clay tile (Fig. 29b) on the indoor surface.

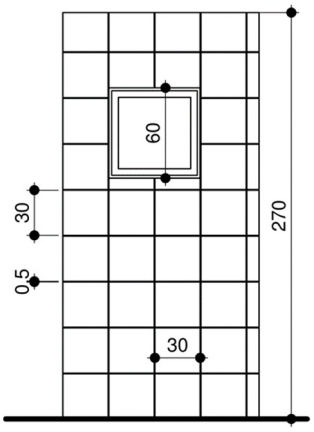


Fig. 28a. Bathroom 1 inside surface

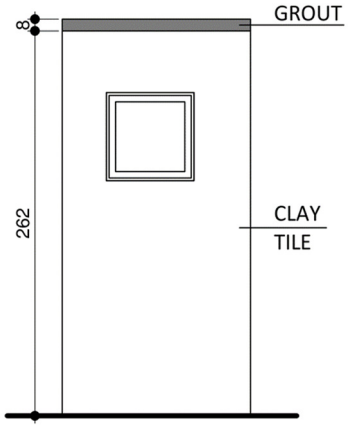


Fig. 28b. Bathroom 1 modelled inside surface

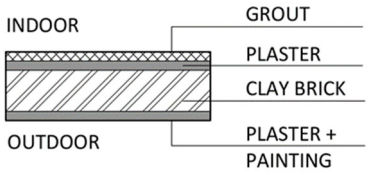


Fig. 29a. Grout part wall

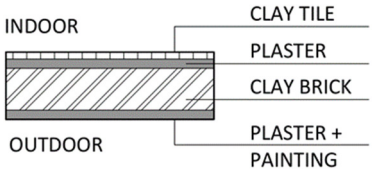


Fig. 29b. Clay tile part wall

### 5.1.2 Internal boundary conditions and heat gains

The model is divided into 8 zones according to Table 13, one of each room. The fixed internal loads (lighting, equipment and metabolic rate), the occupation (Fig. 30) and lighting use (Fig. 31) criteria are based on the Labelling for energy efficiency of residential buildings (RTQ-R, presented in Section 2.1) simulation report (LABEEE, 2011).

Table 13. Zones characteristics and fixed internal loads

| Zone | Area | Ceiling Height | Glazed area | Lighting Power | Equipment Power | Metabolic rate |
|---|---|---|---|---|---|---|
| | [m²] | [m] | [m²] | [W] | [W] | [W/person] |
| Living | 15.81 | 2.7 | 2.16 | 60 | 21 | 110 |
| Kitchen | 7.70 | | 1.44 | 60 | 33 | 110 |
| Hall | 2.42 | | - | 20 | - | - |
| Bedroom 1 | 9.70 | | 1.44 | 40 | - | 80 |
| Bedroom 2 | 7.51 | | 1.44 | 40 | - | 80 |
| Bedroom 3 | 9.92 | | 1.44 | 40 | - | 80 |
| Bathroom 1 | 2.77 | | 0.36 | 20 | - | 110 |
| Bathroom 2 | 2.86 | | 0.36 | 20 | - | 110 |

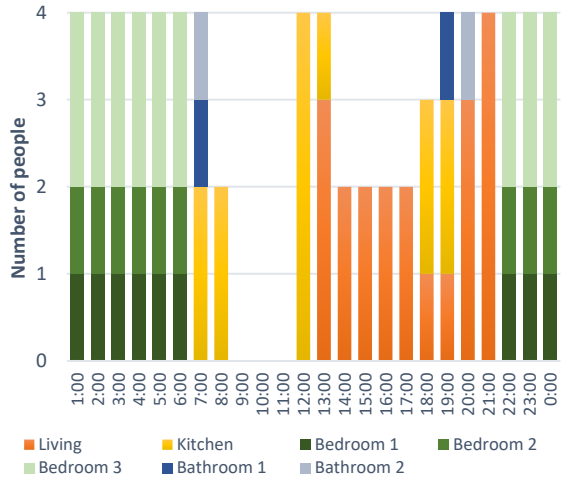


Fig. 30a. Occupation during weekdays

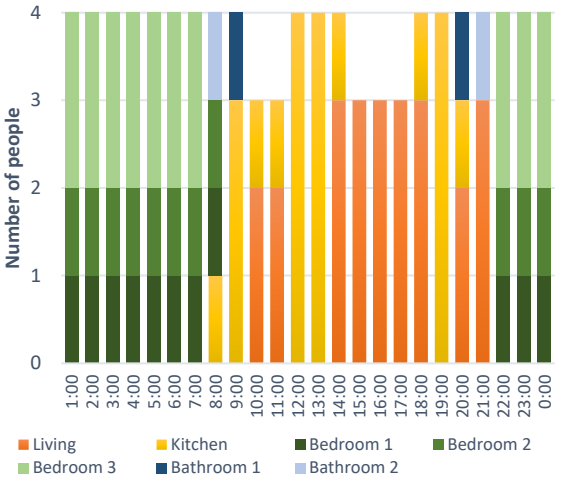


Fig. 30b. Occupation during weekends

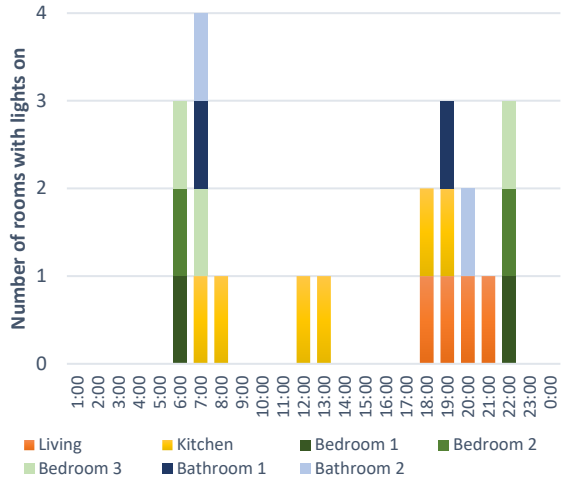


Fig. 31a. Lighting use during weekdays

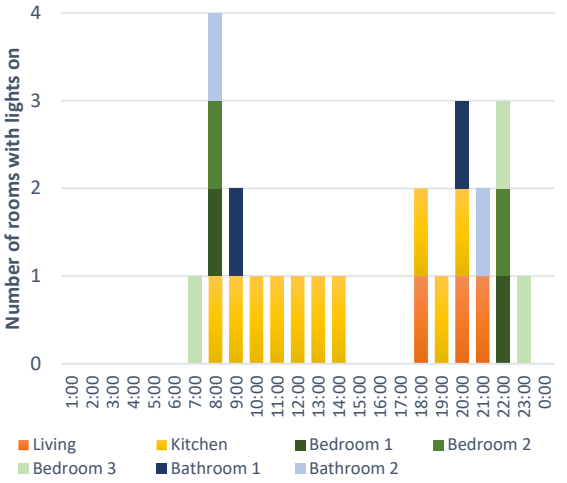


Fig. 31b. Lighting use during weekends

The building is naturally ventilated only, and the operation of the windows is set to open when $T_{indoor} > T_{outdoor}$, controlled by a 24°C setpoint schedule, which is the design value recommended by ASHRAE (2013) for indoor conditions of residential buildings.

During night windows can be only half-opened, considering people generally do not sleep with the entire window opened. Internal doors are closed from 10 p.m. to 7 a.m. and bathrooms doors are also closed during bath period. The external door is always closed.

To consider the vapour produced by showering and by cooking, the *Steam Equipment* object is employed. The moisture production values of 0.45 kg/h for cooking and 2.60 kg/h for showering are obtained from the IEA Annex 14 report (HENS, 1992). It is considered 2 hours of cooking per day on

weekdays and 1 hour on weekends. Length of the shower is 10 minutes (SINPHA, 2005), and both bathrooms are used for shower twice a day, in all days.

### 5.1.3 Parameters variation

To assess the characteristics that may affect the potential moisture risk, some parameters that reflect the Brazilian residential building sector reality are varied as shown in Table 14. Every time one parameter is changed, the others are constant at the base case values, then the variation of moisture risk can be observed for each one.

Table 14. Input parameters variation

| Parameters variation | Variation | Base Case |
|---|---|---|
| Geographic location | 409 cities | - |
| Bathroom solar orientation | North / South / West / East | South |
| Wall material | Clay Brick / Concrete Block | Clay Brick |
| Painting layer in walls | Yes / No | Yes |
| Exhaust fan in the bathroom | Yes / No | No |
| Length of shower | Short / Long | Short |

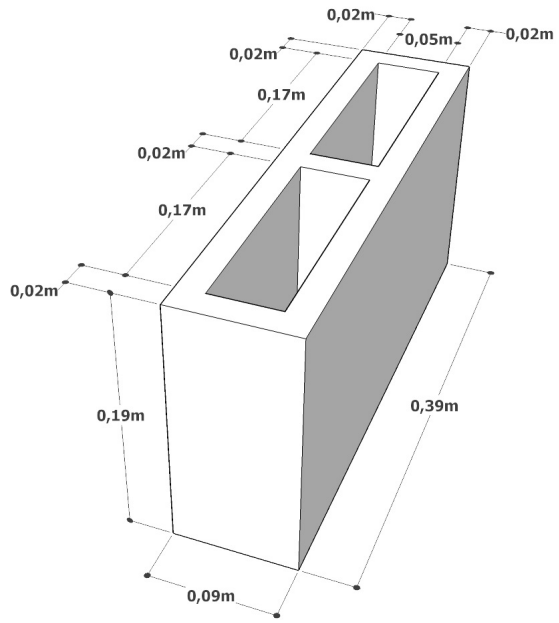


Fig. 32. Concrete block

Although the clay brick is still widely used for residential buildings, there is a trend in the use of concrete blocks, mainly in large residential complexes (MORISHITA *et al.*, 2016). Therefore, the material is chosen to be assessed. The equivalent thickness and thermal conductivity are also calculated for the concrete hollow block (Fig. 32) according to the method presented in Section 5.1.1.2.

Table 15. Properties of the hollow concrete block

| R | C | δ | λ |
|---|---|---|---|
| [(m²·K)/W] | [kJ/(m²·K)] | [m] | [W/(m·K)] |
| 0.184 | 88.882 | 0.040 | 3.439 |

The existence of a painting layer in walls may be of importance for heat and moisture transfer processes. The national survey SINPHA (2005) indicates that painting is not a common practice in all regions of the country, and hence it is chosen as a parameter to be varied. To consider a painting layer in walls, it is employed to HAMT walls the permeance value of $3.13 \times 10^{-10}$ kg/(Pa·s·m²) proposed by ASHRAE (2013).

The use of mechanical ventilation is not a common practice in the country, especially in one-storey dwellings. Yet, the growing amount of multi-storey residential agglomerations have been leading to the increasing use of exhaust fans in the bathrooms due to the lack of external surfaces to allow natural ventilation. The exhaust fan is based on a basic widely used equipment in the country, "Ventokit Classic" (VENTOKIT, 2019), and is set to operate in both bathrooms within the lights schedule (Fig. 31). The EnergyPlus object *Zone Exhaust Fan* is set according to manufacturer specifications and has a total efficiency of 0.7, a pressure rise of 50 Pa and a maximum flow rate of 0,028 m³/s. Length of the shower is 10 (short) and 20 (long) minutes.

## 5.2 SIMULATION POSTPROCESSING

### 5.2.1 Indoor moisture load ($M_L$)

Considering the absence of related data in the country, the internal moisture load production is estimated by considering the latent heat fraction of the internal gains, being given by

$$M_L = \frac{L}{L_v}, \tag{15}$$

where:

$M_L$ is the moisture load (kg/h);

$L$ is the latent heat associated to the internal moisture source (W);

$L_v$ is the latent heat of water vaporization ($2.25 \times 10^6$ J/kg)

The $M_L$ corresponds the mean value of moisture load of the occupied hours and is obtained to the internal loads of occupation, showering, and cooking.

### 5.2.2 Mould Growth Risk model ($MGR$)

The evaluation of moisture-related issues in buildings is often performed considering the surface's temperature and relative humidity reported by numerical solution simulation tools to apply a mould growth risk model, which is the approach of this work. Different models for mould growth prediction can be found in literature, including different approaches and limitations (VEREECKEN and ROELS, 2012; BERGER *et al.*, 2018). The Mould Growth Index employed in this work is the VTT model, based on laboratory studies proposed by VIITANEN and HUKKA (1999). It considers temperature, relative humidity, quality of surface, exposure time and dry periods.

In the first approach, several species of mould were tested on pine and sapwood to determine the influence of temperature, relative humidity, time and type of surface. More recently, the model was adapted to other material types (VIITANEN *et al.*, 2011). This last study reveals that stone-based materials such as concrete and bricks are less sensitive to mould growth than organic ones, but the organic particles accumulated on surfaces may turn them suitable for mould growth.

Since it has no direct connection to the number of living cells of organisms, the correct way to interpret the results is that the mould index stands for the possible activity of the mould fungi on the surface. The description of the mould index is presented in Table 16. To obtain the Mould Index, it must be chosen the sensitivity class of the material (Table 17), the *W* factor (0 for pine and 1 for spruce) and the *SQ* that refers to the surface quality (0 for resawn and 1 for kiln-dried timber).

Table 16. Description of VTT Mould Growth Index.

| Index | Growth Rate | Description |
|---|---|---|
| 0 | No growth | Spores not activated |
| 1 | Small amounts of mould on the surface (microscope) | Initial stages of growth |
| 2 | <10% coverage of mould on the surface (microscope) | |
| 3 | 10-30% coverage mould on the surface (visual) | New spores produced |
| 4 | 30-70% coverage mould on the surface (visual) | Moderate growth |
| 5 | > 70% coverage mould on surface (visual) | Plenty of growth |
| 6 | Very heavy and tight growth | Coverage around 100% |

Source: VIITANEN *et al.* (2011)

Table 17. Mould Growth sensitivity classes and some corresponding materials.

| Sensitivity class | Materials |
|---|---|
| Very sensitive | Pine sapwood |
| Sensitive | Glued wooden boards, PUR with a paper surface, spruce |
| Medium resistant | Concrete, aerated and cellular concrete, glass wool, polyester wool |
| Resistant | PUR polished surface |

Source: VIITANEN *et al.* (2011)

Presently, the initial stage of mould is set as 0, the material is in the sensitive class, the *W* factor is 0 and the *SQ* is 0.5. The mould growth risk Index is calculated for an hourly basis for the 5-year simulated period.

It is obtained, for each evaluated location and within the 5 years, the maximum value of mould growth risk ($M$) and, as mould growth is time-dependent, the consecutive duration, in hours, of $MGR \geq 1$ ($t_M$) of the 5th simulated year.

Some results of $t_M$ are presented in Table 18, which divides the 5th year into 6 uniform ranges of risk classes of 1,460 hours each.

Table 18. Risk classes of $t_M$

| RISK CLASS | $t_M$ [h] | | |
|---|---|---|---|
| NULL | 0 | ≤ P < | 1460 |
| LOW | 1460 | ≤ P < | 2920 |
| MODERATE | 2920 | ≤ P < | 4380 |
| HIGH | 4380 | ≤ P < | 5840 |
| VERY HIGH | 5840 | ≤ P < | 7300 |
| EXTREME | 7300 | ≤ P < | 8760 |

## 5.3 RESULTS

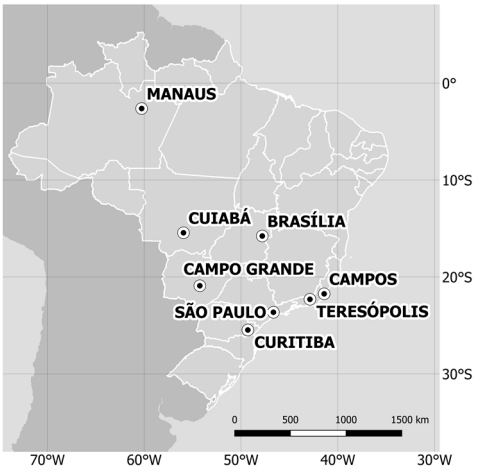


Fig. 33. Location of the 8 cities

To assess the Mould Growth Risk behaviour over time for different walls and climates, a preliminary investigation was performed for 8 cities, one of each Bioclimatic Zone (Table 1, Fig. 33) for 10 years. As shown in the graphics of Fig. 34, the more noticeable values are for the grout wall of bathroom 1 (Fig. 34a).

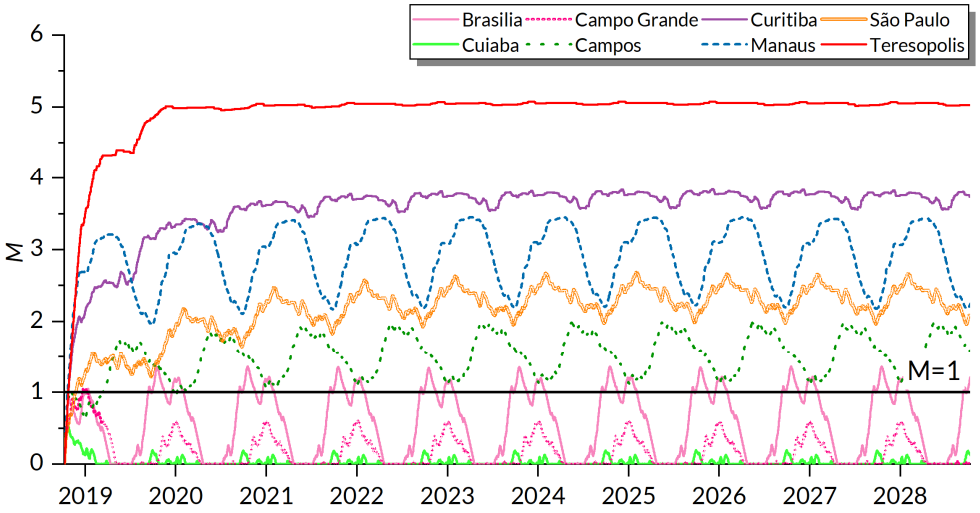


Fig. 34a. Mould Growth Risk of bathroom 1 grout wall for 8 cities

With exception of the Teresopolis city (which is located in a highly humid mountainous region with considerably low temperatures), there is no significant Mould Growth Risk on the bathroom 1 clay tile wall (Fig. 34b) neither on the bedroom 2 wall partition with bathroom 1 (Fig. 34c).

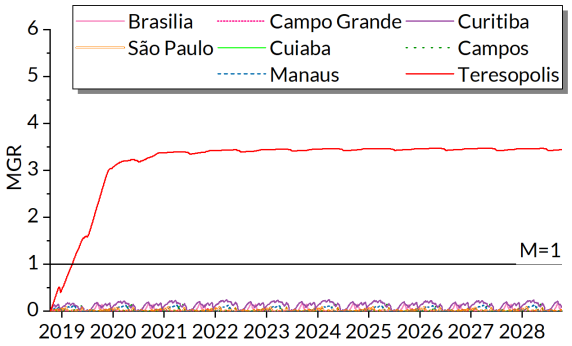


Fig. 34b. Mould Growth Risk of bathroom 1 clay tile wall for 8 cities

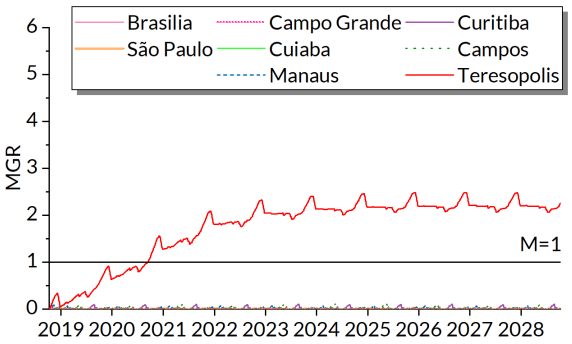


Fig. 34c. Mould Growth Risk of bedroom 2 partition with bathroom's 1 wall for 8 cities

Also, there is a stability trend on growth rates from 4$^{th}$ year onwards. Fig. 34 reinforces the choice of assessing the grout wall of the bathroom for a 5-year time period.

The estimated indoor moisture load of the base case is also obtained to these 8 cities. Table 19 presents, per room, the sum of indoor moisture load from people, shower and cooking.

Table 19. Indoor moisture load

| | **ZB1** | **ZB2** | **ZB3** | **ZB4** | **ZB5** | **ZB6** | **ZB7** | **ZB8** |
|---|---|---|---|---|---|---|---|---|
| Room | Curitiba | Teresopolis | São Paulo | Brasilia | Campos | Campo Grande | Cuiaba | Manaus |
| | | | | moisture load [kg/h] | | | | |
| Living | 0.096 | 0.104 | 0.121 | 0.149 | 0.195 | 0.181 | 0.237 | 0.256 |
| Kitchen | 0.472 | 0.482 | 0.495 | 0.520 | 0.565 | 0.552 | 0.600 | 0.620 |
| Bedroom 1 | 0.007 | 0.009 | 0.011 | 0.012 | 0.028 | 0.023 | 0.040 | 0.050 |
| Bedroom 2 | 0.009 | 0.011 | 0.013 | 0.017 | 0.032 | 0.026 | 0.044 | 0.054 |
| Bedroom 3 | 0.017 | 0.020 | 0.026 | 0.031 | 0.060 | 0.049 | 0.085 | 0.106 |
| Bath 1 | 0.409 | 0.413 | 0.419 | 0.430 | 0.450 | 0.443 | 0.466 | 0.476 |
| Bath 2 | 0.407 | 0.411 | 0.418 | 0.428 | 0.447 | 0.440 | 0.464 | 0.474 |
| TOTAL | 1.417 | 1.450 | 1.503 | 1.588 | 1.777 | 1.715 | 1.936 | 2.036 |

With exception of the city of Campo Grande, there is a growth trend of the moisture load from ZB1, the coldest Zone, towards ZB8, the hottest one. Regardless of showering produces more vapour than cooking, being the reference values of simulation 2.60 kg/h and 0.45 kg/h, respectively (HENS, 1992), the values observed for the Kitchen are higher than the Bath ones due to the activity duration. As mentioned in section 5.1.3, the simulation considers 2 hours of cooking per day, while for showering the duration is 20 minutes per day, for each Bathroom.

The behaviour of the indoor moisture production in a 24-hour period in Winter and Summer solstices for the cities Curitiba (Bioclimatic Zone 1) and Manaus (Bioclimatic Zone 8) is presented in Fig. 35.

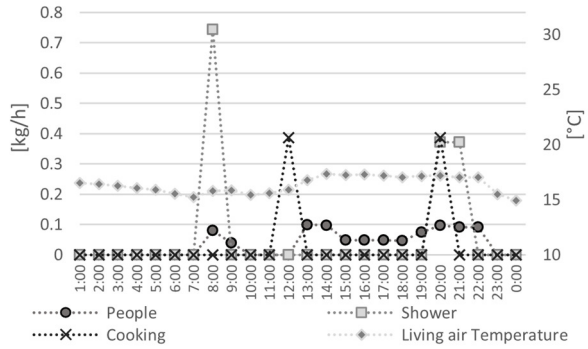


Fig. 35a. Indoor moisture loads for Curitiba (ZB1) on June 21

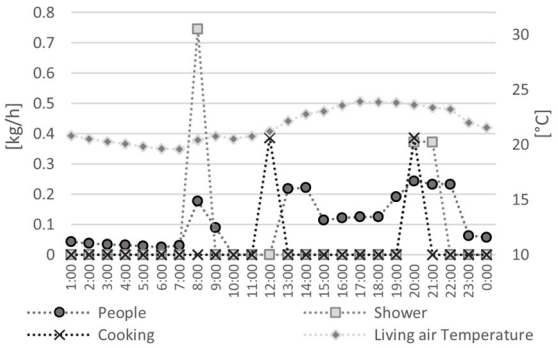


Fig. 35b. Indoor moisture loads for Curitiba (ZB1) on December 21

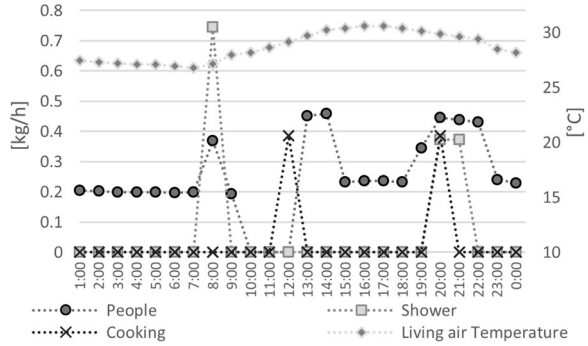


Fig. 35c. Indoor moisture loads for Manaus (ZB8) on June 21

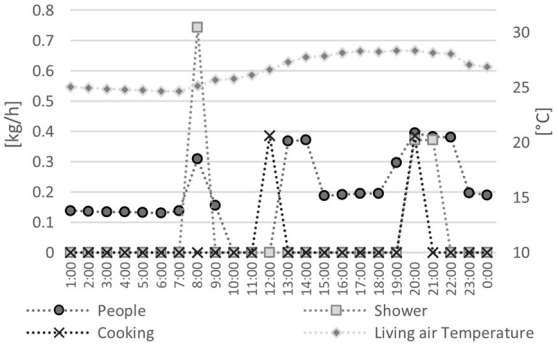


Fig. 35d. Indoor moisture loads for Manaus (ZB8) on December 21

Because the occupation pattern is considered the same for all simulations, the peak values of moisture production are coincident. In Curitiba, for both days the highest contributions in the moisture load are from showering and cooking; in Winter, the load due to occupation and mainly during the sleeping period is extremely low. In Manaus, it can be highlighted the moisture load due to occupation, presenting values similar to the ones produced by cooking and showering. In the morning it is considered that both Bathrooms are used for showering simultaneously, resulting in the peak value. However, in the evening, where showering happens in different moments (20:00 and 21:00), it can be noticed the high contribution from occupation in the moisture load.

Next, results charted in the map of Brazil are presented. The maps of Fig. 36 present a comparison between the base case and the variation cases results. With representation purposes, the base case (black circles) are at times below and at times above of the variation cases (white circles).

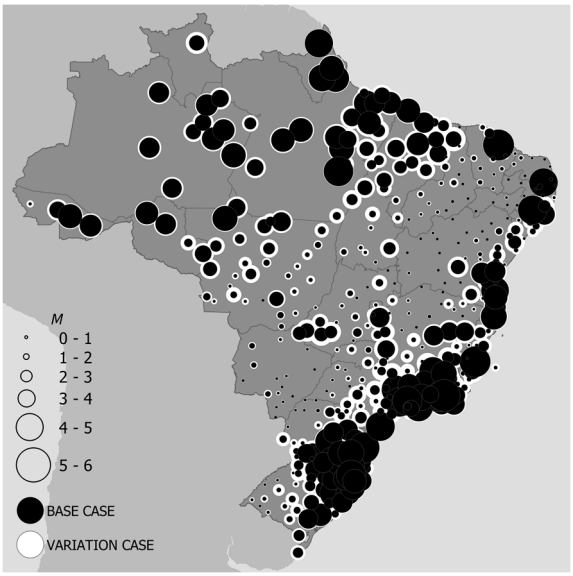


Fig. 36a. Bath long

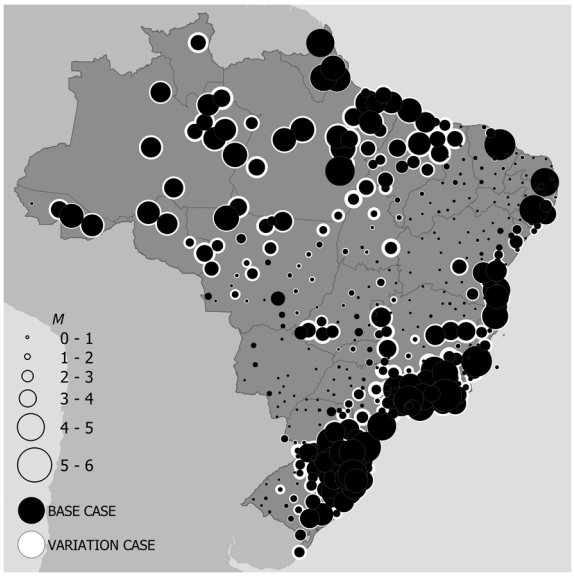


Fig. 36b. Concrete block wall

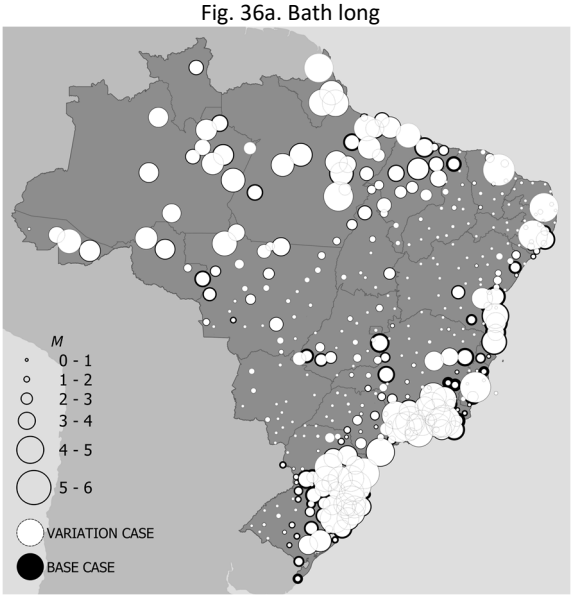


Fig. 36c. North oriented bathroom wall

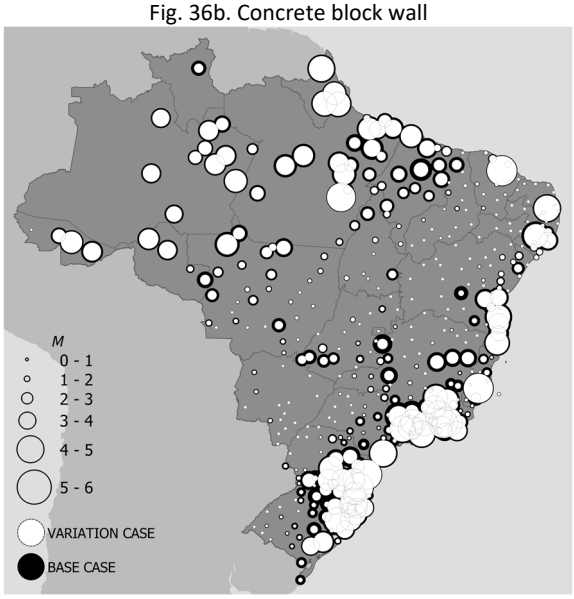


Fig. 36d. No painting layer in walls

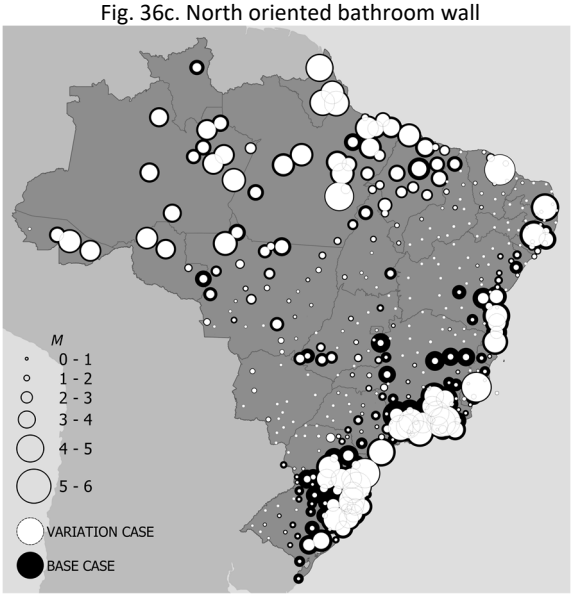


Fig. 36e. Exhauster in bathroom

Overall, there are high values of MGR in southern and coastal regions, which are populated areas (Fig. 2). High levels are also found in the Amazon Forest region what may be less of concern for policy issues since it is a lightly densely populous area. The lower values are found in a diagonal belt from southern west towards northeast areas, where the typical semi-arid climate of the Northeast region, which is an enclave of scarce rainfall in the Brazilian tropical region, is located.

In comparison with the base case, the analysed wall presents a higher $M$ risk when the bath is long (Fig. 36a), and the wall is made of concrete blocks (Fig. 36b). Lower risk is observed when the bathroom wall is North oriented (Fig. 36c), when there is no painting layer (Fig. 36d), and when there is an exhauster fan in the bathroom (Fig. 36e). The results of the East and West oriented walls cases did not present a significant variation of $M$ levels and, therefore, are not presented.

Whereas the bath length and the exhauster fan have shown important influence on MGR levels, two additional maps are presented. The map in Fig. 37a presents the combination of a long bath and the use of exhauster fan and Fig. 37b map assumes the bathroom with an exhauster fan and with no window, which is a trend in new buildings as mentioned in Section 5.1.3.

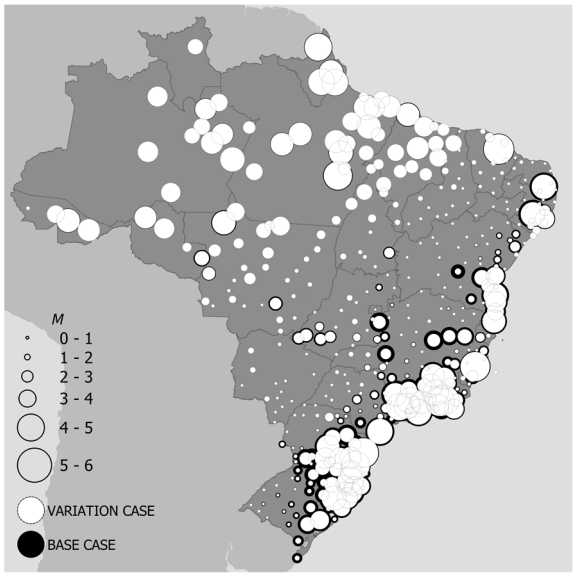


Fig. 37a. Variation Case with long bath and exhauster

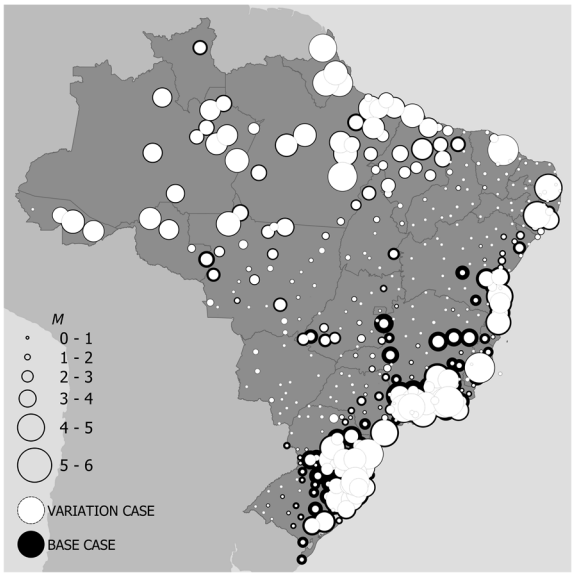


Fig. 37b. Variation Case with exhauster and without window

The Fig. 37a map reveals that for the most of hot and humid northern cities the exhauster can override the effect of a long bath, but it may not be sufficient in southern and coastal areas. The case with

exhauster and without window (Fig. 37b) shows slightly lower MGR levels in comparison with the case with both exhauster and window (Fig. 36e) and similar ones with the bath long and exhauster case (Fig. 37a). These maps reveal that, in Brazil, the effect of the humidity from outdoors can be comparable to that produced by the shower.

Figs. 38 and 39 maps present the $M$ and $t_M$ levels of the cases in which the parameters combination resulted in the highest ($H_M$) and lowest ($L_M$) MGR levels among all the possible combinations. The $H_M$ South oriented case has concrete block walls with a painting layer, long bath, and there is no exhaust fan. The $L_M$ case is North oriented and of clay brick walls without painting layer, short bath, and with exhaust fan. The maps of Fig. 40 expose the difference between these two cases.

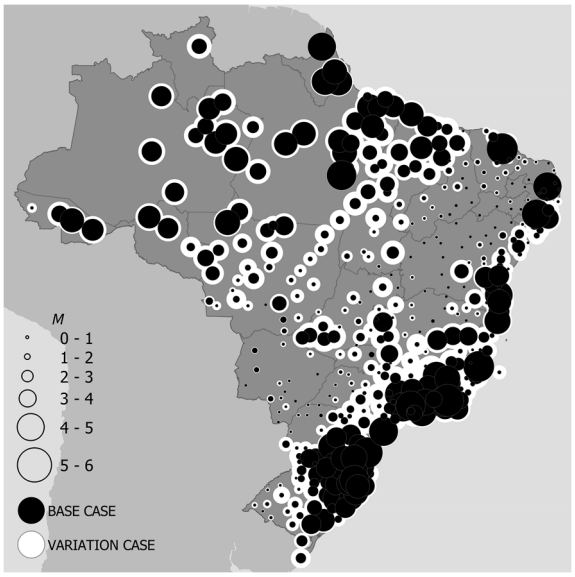


Fig. 38a. $H_M$ $M$ levels

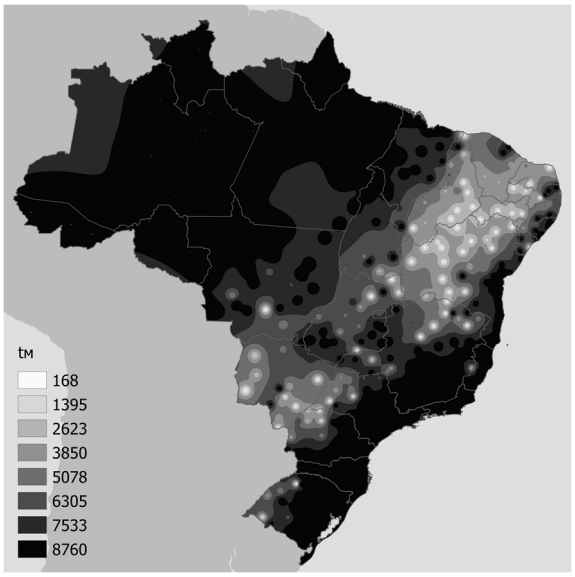


Fig. 38b. $H_M$ $t_M$ [h]

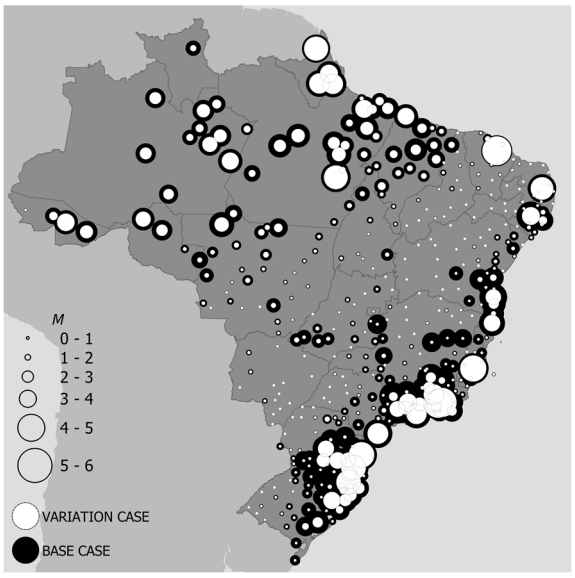


Fig. 39a. $L_M$ $M$ levels

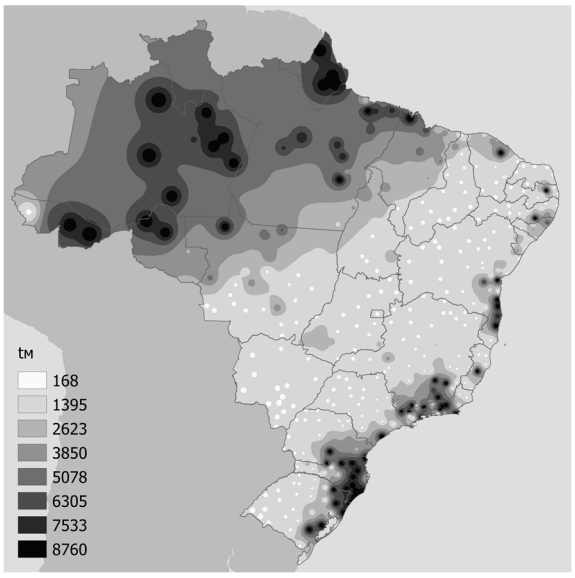


Fig. 39b. $L_M$ $t_M$ [h]


Fig. 40a. $H_M$ - $L_M$ $M$ levels

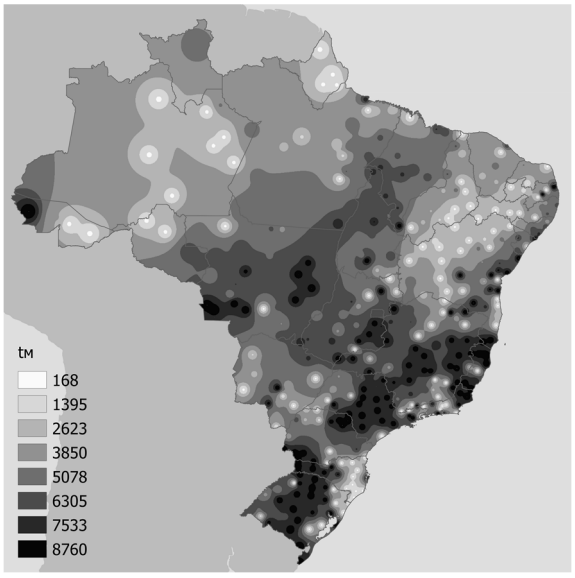


Fig. 40b. $H_M$ - $L_M$ $t_M$ levels [h]

In the map of Fig. 40a we observe a potential of reduction in both $M$ (in the order of 2-4 in the 6-$M$ scale) and $t_M$ (up to 8,760 h in some cities) levels in highly-populated areas of the South and Southeast regions. A less pronounced difference is observed in northern areas, but all over there is a mean of about 3,000 h of $t_M$ reduction across the country.

Following results are based on the $t_M$ ranking of Table 18. Table 20 shows the number of cities, population and $M$ mean level of the Base Case, the $H_{MGR}$ and $L_{MGR}$ for the *Null* and *Extreme* risk classes. These results are acquired from the interpolated maps and comprise all the 5,570 municipalities.

Table 20. Results of Base Case, $H_M$ and $L_M$ per $t_M$ risk class

| Case/$t_M$ Risk class | NULL | | | | EXTREME | | | |
|---|---|---|---|---|---|---|---|---|
| | Number of cities | Population | Population [%] | *M* mean | Number of cities | Population | Population [%] | *M* mean |
| Base Case | 509 | 23,557,500 | 12.35 | 1.10 | 1108 | 78,526,100 | 41.17 | 3.52 |
| $H_M$ | 93 | 4,976,243 | 2.61 | 1.04 | 2886 | 129,324,000 | 67.80 | 3.85 |
| $L_M$ | 3413 | 111,176,800 | 58.60 | 0.85 | 135 | 8,968,560 | 4.70 | 3.06 |

There are no pronounced differences in the mean $M$ levels between the three cases in both $t_M$ risk classes, but very pronounced ones in the number of cities and the estimated population. Considering the Base Case, about 41% of the residents would live in areas where the $t_M$ risk is in the *Extreme* class; when considering the $H_M$ case it rises to 68%, and for the $L_M$ case it decreases to about 5% of the population. In the *Null* class, the $L_M$ case has 2,904 cities and 88 million more residents than the Base case.

The graphics in Figs. 40-42 show, per Bioclimatic Zone, the influence of each evaluated parameter per risk class. The analysed Zones are 1 and 2, which are the coldest ones, Zone 3 which is the most populous one, and Zone 8 which covers more than 50% of the country territory. Zones 1 and 2 are grouped due to the small number of cities.

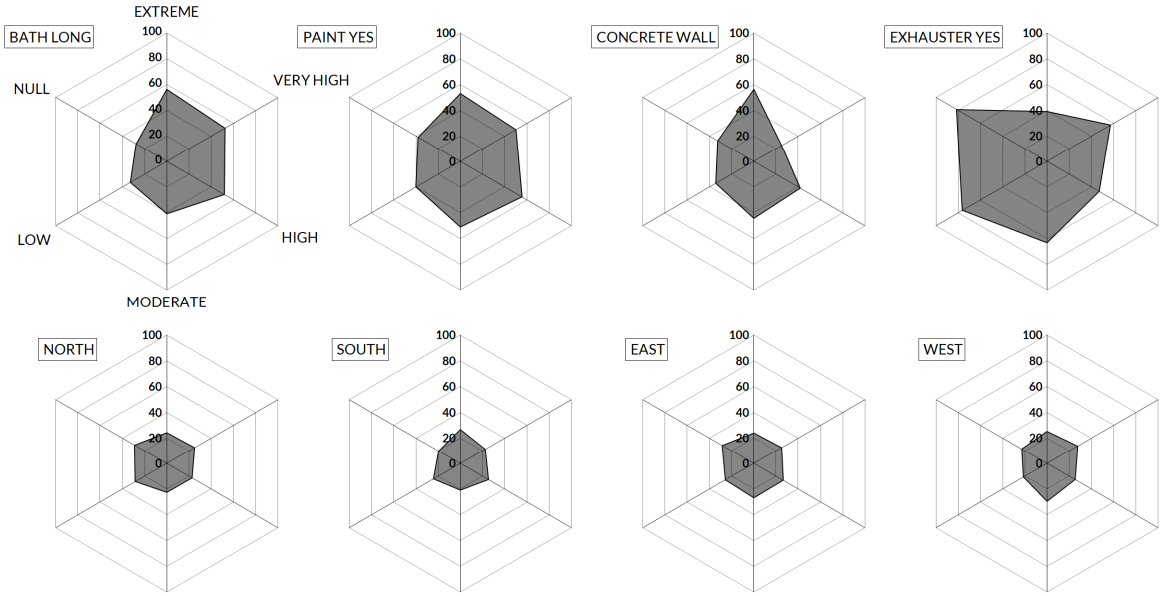


Fig. 41. Parameters influence for Bioclimatic Zones 1 and 2

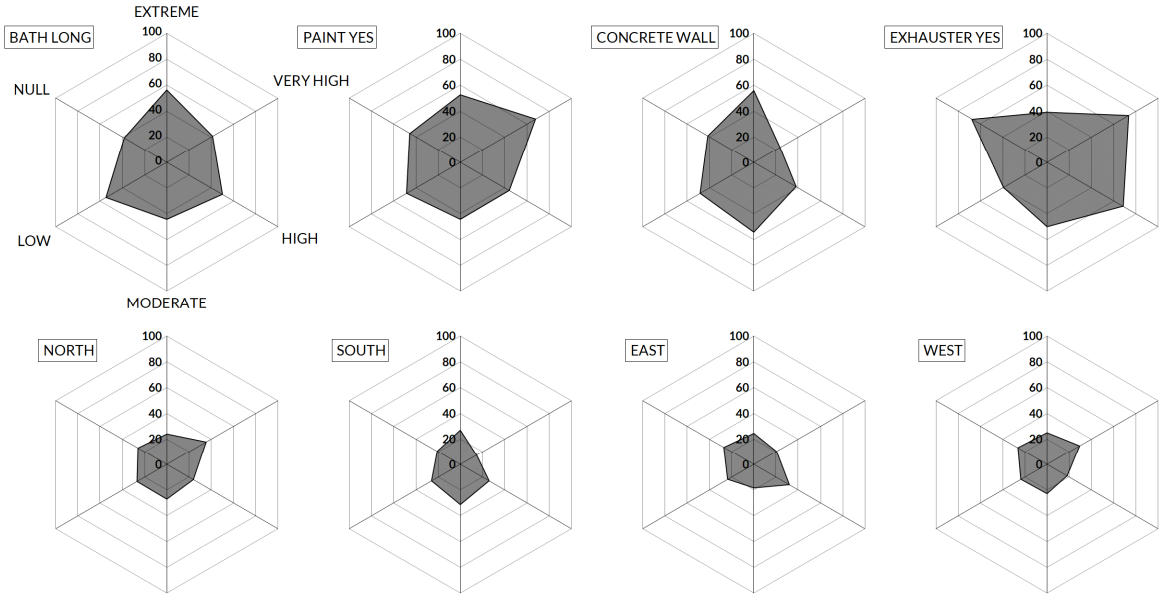


Fig. 42. Parameters influence for Bioclimatic Zone 3

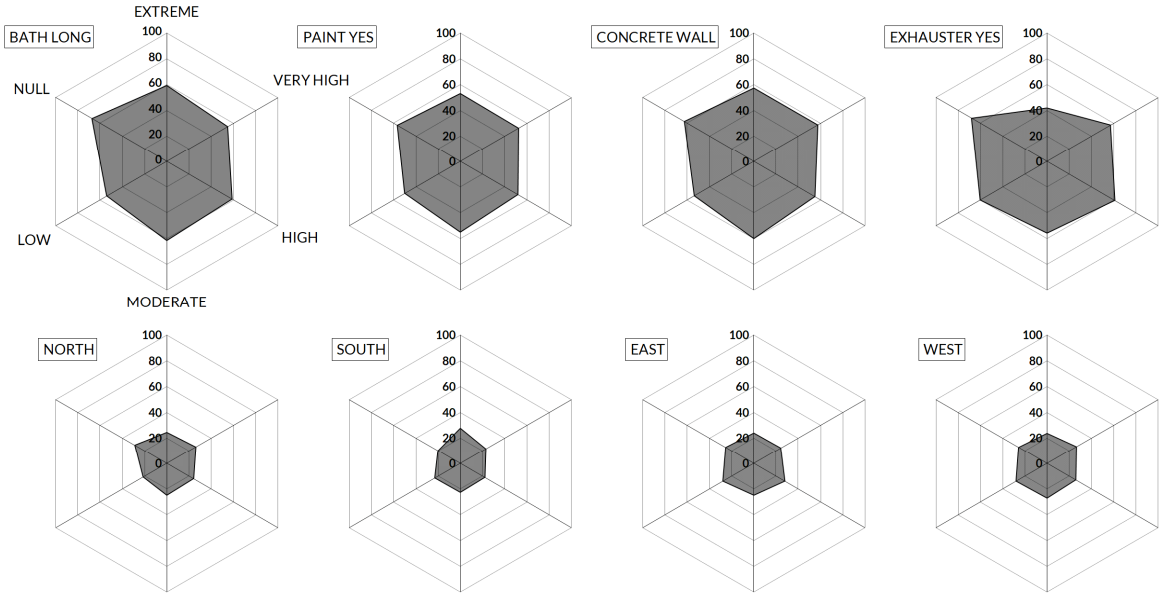


Fig. 43. Parameters influence for Bioclimatic Zone 8

In all Zones, about 60% of the cases in the *Extreme* class have concrete block walls, a long bath and no exhauster. Overall, the painting layer shows a poor inequality between CPMR classes, with exception of the classes *Low* and *Null* in Zones 1 and 2 where 60% of the cases do not have painting layer and the class *Very High* in Zone 3, in which about 70% of the cases have painting layer. Compared to the other Zones, in Zone 8 the varied parameters exert less influence on CPMR levels, except for the exhauster that is existent in about 70% of the *Null* class cases and inexistent in 60% of the *Extreme* class cases.

In hot and humid climates, like the one of Zone 8, the climatic conditions may have more influence in mould growth risk than in mild and temperate climates such as those of Zones 1, 2 and 3, where there is a more notable influence of the varied parameters. Fig. 44 presents the relation between $M$ and $t_M$ of the Base Case with the Bioclimatic Zones and the number of residents. The size of the spheres is associated with the number of residents and the colour with the Bioclimatic Zone. Fig. 45 presents an overlapping of the Bioclimatic Zoning and the Base Case $M$ maps.

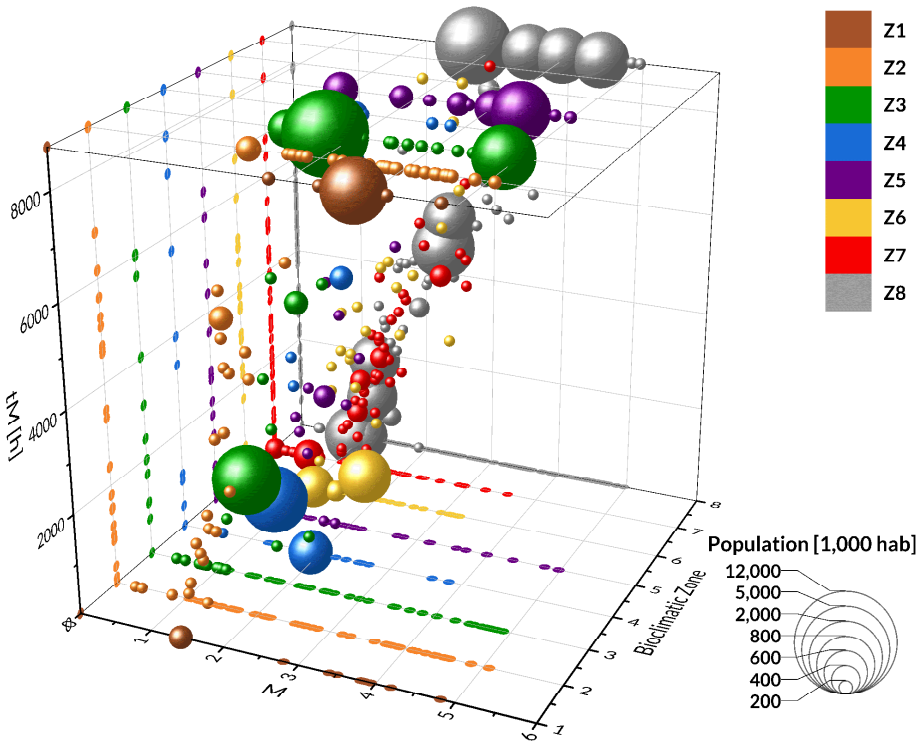


Fig. 44. The relation between the $M$ and $t_M$ of the Base Case with the Bioclimatic Zones and the population

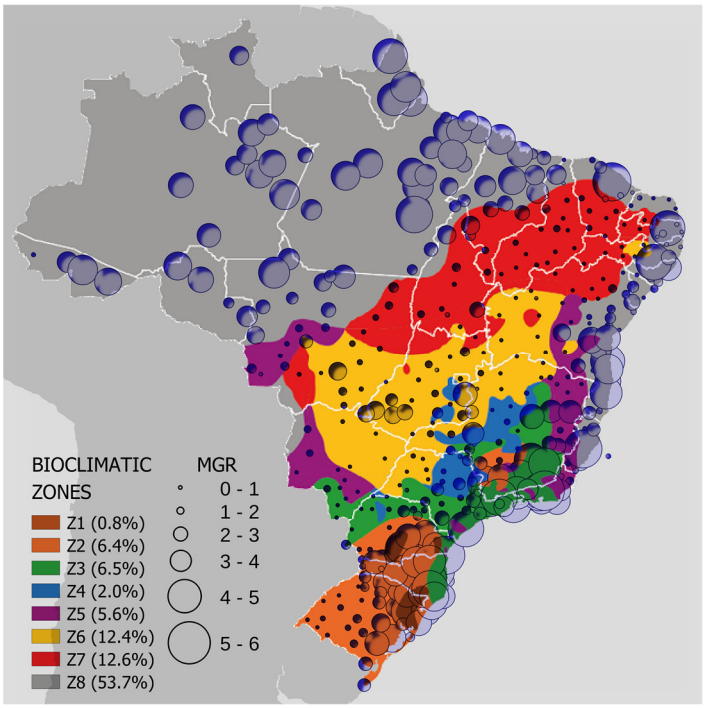


Fig. 45. Base Case $M$ and Bioclimatic Zones

In Fig. 44 it can be seen the concentration of populous cities (sphere size) in the highest level of $t_M$ (8,760 h) with also high $M$ levels (higher than 3), mainly in Zones 3, 5 and 8. The two most populous cities, Sao Paulo and Rio de Janeiro (the biggest green and grey spheres) are in this condition. Cities of Zones 2, 4, 6 and 7 in this condition are less populous ones. High $t_M$ levels are observed in all Zones,

whereas the $M$ values are less pronounced in Zones 4, 6 and 7. High $M$ values are observed in all other Zones, which can be also seen in the map of Fig. 45. Also, there are marked different $M$ levels in the same Zone, and it happens in all Zones. This map highlights that proposing construction methods and design strategies per Bioclimatic Zone without taking the potential moisture risk into account may not be always proper.

## 5.4 CONCLUSIONS

This chapter presented an investigation of the potential moisture risk in Brazilian residential buildings. This investigation was undertaken by applying a mould growth risk index to building simulation results of a common residential typology followed by the charting of the results in the country map. Some moisture-related parameters under the country circumstances were chosen to be varied and therefore assess their influence on the moisture risk. The plotted maps allow an inclusive and visual presentation of the results.

Main drawbacks reveal an important potential moisture risk in residential buildings across Brazil on the building scale. In comparison with the Base Case, the cases that presented a higher level of risk were those with concrete block walls and those with a length of bath long, whereas the cases with exhauster fan in bathroom, North oriented, and without external painting layer presented lower level of risk. As expected, North walls receive more solar radiation and the exhauster fan extracts the humid air from the bathroom and therefore reduce the $M$ levels. However, the painting layer on the external surface of the wall can, in one hand, act as a protection from weather exposure, but in the other hand act as a barrier that may difficult the drying process due to the use of the shower. Both simulated walls follow standards thermal requirements (Section 2.3) but may not be suitable to some regions regarding moisture safety. In hot and humid areas, a basic exhaust fan has shown to be an affordable solution to improve moisture safety, but its efficiency is less pronounced in Southern colder areas. A comparison between cases with an exhauster fan and with and without external openings indicates the humidity from the exterior can be comparable with the humidity produced by the shower.

Having analysed the behaviour of the varied parameters individually, two additional cases were evaluated, those that the parameters combination resulted in the highest ($H_M$) and lowest ($L_M$) MGR levels among all the possible combinations. The comparison between these two cases shows a mean difference of about 3,000 h of $t_M$ across the country. The highest potentials of reducing moisture risk levels are observed in the Southern highly dense areas.

An analysis of the varied parameters according to four Bioclimatic Zones has shown that in Zone 8, which is the hottest one, the climatic conditions may have more influence on the moisture risk than the variation of parameters than in Zones 1, 2 and 3. The $M$ values plotted in the Bioclimatic Zoning map show diverse levels of the indicator in the same Zone, suggesting there is no correlation between the MGR and the Brazilian Bioclimatic Zoning.

On the building simulation analysis, results indicate that the main used construction methods may not be safe by the moisture point of view to all regions of the country. Even the cases that presented the lowest risks have considerable high levels of *MGR* and *CPMR* and mainly in highly densely populous areas. Also, a main concern is the remarkably high potential risk in highly densely populous regions of the country. Nonetheless, when working with building simulation, it is necessary to reflect that building design comprises many criteria such as climate conditions and a large sort of architecture and engineering parameters combinations. Performing numerous simulations requests assuming some simplifications and consequent limitations which were detailed in Chapter 6. But considering the lack of moisture-related information in the Brazilian building stock and moisture-related requirements in building standards, the presented results bring up an important overview of the potential moisture risk in buildings across the country and may help in conducting a more accurate analysis in the topic.

# CHAPTER 6. LIMITATIONS, DELIMITATIONS AND ASSUMPTIONS

In this Chapter, limitations, delimitations, and assumptions are presented. It provides important information to enlighten the boundaries of reliability of this thesis.

## 6.1 LIMITATIONS OF THE STUDY

### 6.1.1 Climatic data

Due to the gaps in the available real measured climatic data, it was chosen to employ the existing weather files, which are the result of the statistical treatment of measured data. However, there are weather files for only about 7% of the Brazilian cities, and which are not well spatially distributed. Most of the weather stations are located in populated areas (along the sea coast), in countryside areas with developed agriculture activities (regions close to the Capricorn Tropic), and the Northeast semi-arid areas with drought monitoring (ALCARDE ALVARES *et al.*, 2013). Despite driving rain is very common in Brazil, it has not been considered in the simulations due to software limitations. Indeed, 1-h based weather files may not provide the most accurate results, in special when considering rain related phenomena.

### 6.1.2 Materials properties

Apparently, no laboratory in Brazil is carrying on measurements to determine moisture-related properties for building materials commonly used in the country. Hence, due to the lack of measurements and libraries, many of the material properties are obtained from similar ones from international sources. Considering the influence of material properties on moisture transfer processes calculation, this limitation brings some uncertainty to this work as shown in (GOFFART *et al.*, 2015).

### 6.1.3 Simulation model - building design, construction techniques and habits of usage

The database from Brazilian Institute of Geography and Statistics - IBGE (IBGE, 2015), which is responsible for the national census and the national survey by household sampling, provides some important information regarding the presence of some equipment in Brazilian dwellings (such as household appliances and electronic devices), built area, type of building (one-storey or multi-storey)

and the number of residents per dwelling. However, there is no information on the building design, occupancy pattern or the habits of usage of equipment. Also, the only information about the construction materials is limited to “durable” and “not durable”. Hence, information about construction materials and patterns of appliances usage is obtained from the database *Information System of Electric Appliances Ownership and Consumption Habits* (SINPHA, 2005) for the year 2005. The survey was conducted by the National Program of Energy Efficiency and coordinated by the Brazilian Ministry of Energy and has constraints. Firstly, it is out-to-date. A new survey was conducted in 2017 but at the time when the base case was defined, the results were not yet available. Besides, when comparing information (built area, number of residents per dwelling, one-storey or multi-storey building, presence of household appliances) which is present in both databases IBGE and SIPNHA, they do not converge. Considering IBGE works with a much larger sampling than SINPHA and its solid reputation on surveys and data statistics, this study gave priority to their database.

## 6.2 DELIMITATIONS OF THE STUDY

### 6.2.1 Climatic data

All analyses are performed based on already existing weather files. Data measuring, statistical treatment, and geoprocessing investigation would extrapolate the limits of the work. On the climatic analysis, it implies that the results refer to a typical average year without extremes. The use of weather files in building simulation means that a real climatic variation along the time frame is not considered, but mainly the building behaviour along the period.

### 6.2.2 Weather-based indicators

Although the study highlights the potentialities of the new indicators, some delimitations can be listed. For instance, it is not considered the drying potential, which is affected by temperature, relative humidity, wind speed, solar radiation, and water availability to be absorbed by the wall (CORNICK and DALGLIESH, 2003). However, the drying potential calculation depends on defining a certain type of surface and therefore brings up a non-desired specificity to a simplified method focused on a country scale. Besides, the $I_{air-rain}$ and $I_{FD}$ indicators have a relative ranking and their thresholds must be

defined by user expertise, based on the results of the calculated parameters. The maximum level of a normalized indicator, represented by the unit, may stand for different values of the respective requirement according to the evaluated location. It is a first attempt at the implementation of the indicators. Accuracy and reliability neither of the input or output data, to validate the usefulness of the indicators, are not measured.

### 6.2.3 1-D simulation

In 1-D multi-zone models, such as the one employed in this thesis, the air temperature and relative humidity are considered uniform in each zone, and the convective heat transfer coefficient is assumed as homogeneous along the surfaces. For moisture risk in buildings assessment, these simplifications may represent a shortcoming, considering that moisture transfer through building materials is not a linear process and also depends on the air velocity, leading to issues occurrence in specific areas of building elements (DOS SANTOS *et al.*, 2009; SANTOS and MENDES, 2014). Moisture risk assessment in buildings may require a detailed analysis of non-uniform boundary conditions, type of materials, granularity, and moisture transfer mechanisms, which may be achieved by 2-D or 3-D models. A precise evaluation may comprise the non-linear heat and mass transfer processes in the solid domain, what may be achieved by a 2-D or 3-D HAM model, and the local convective heat and mass transfer coefficients of the surrounding airflow, which can be achieved by a CFD approach. MELLO *et al.* (2019) presented a coupled HAM-CFD model to assess both the transport of heat and mass through porous media and the impact of the fluid flow over the surface, providing the link between the solid and fluid domains and avoiding limitations such as homogeneous boundary conditions and lack of integration to airflow.

The weakness of these models lies in the fact that they are often applied for short periods due to its computational intensity. In turn, moisture issues are also conditioned to building's long-term time-dependent HAM transfer processes, which are more easily achieved by 1-D HAM models due to their capacity of analysing long periods with low computing resources requirement. The applied simulation program EnergyPlus has a coarse-grained moisture model for the envelope but considering the great

amount of input data files and subsequent computational time, it may be a suitable model at these conditions.

### 6.2.4 Simulation model

To obtain simulation results for a large number of cities, it is defined a base case model which attempts to reflect the reality of residential buildings in Brazil, which is a country with quite different climates, and houses certainly differ in architectural design, materials, equipment, and patterns of usage according to climate, economic situation, and cultural habits. However, to turn possible the batch-simulation of the whole-building for all available weather files in a 5-year time frame, a single base case model with the same geometry, materials, internal loads, and patterns of usage was employed. Also, it was not considered the use of air conditioning, which has a significant presence in some hot regions and high-income classes, and which can affect the internal moisture load. Instead, due to computational effort, it was chosen to analyse the use of an exhaust fan which has more widespread use. In high standard new multi-storey buildings, there is a trend in the use of exhaust fans in bathrooms, even in those naturally ventilated.

## 6.3 ASSUMPTIONS OF THE STUDY

### 6.3.1 Climatic data

It is considered that the employed weather files, which are based on measured climatic data, were developed with appropriate data interpolation and statistics treatment.

### 6.3.2 Interpolation

All maps are accomplished by the Inverse Distance Weighting – IDW, a method for spatial interpolation to predict values of unmeasured locations. It assumes that measured points have a local influence, that is, conditions that are close to one other are more alike than those that are farther. Other interpolation methods available in the GIS software such as the Kriging and the Natural Neighbour Inverse Distance Weighted were tested, but in the scale of the country, no significant difference was

observed. Thus, it was chosen to employ the IDW, which is an easy, well-known and widely applied method for spatial interpolation.

### 6.3.3 1-D Simulation

An assumption related to the 1-D simulation model regards the heat balance algorithm. Some combinations of the heat balance algorithm of the envelope were tested:

a) the whole envelope in HAMT model;

b) the whole envelope in EMPD[1] model;

c) walls and ceilings of Bathroom 1 and Bedroom 2 in HAMT and others in the EMPD model;

d) walls and ceilings of Bathroom 1 and Bedroom 2 in EMPD and others in the CTF model;

e) walls and ceilings of Bathroom 1 and Bedroom 2 in HAMT and others in the CTF model;

Options *a*, *b* and *c* resulted in a very high computational time, inhibiting such numerous simulations. Options *d* and *e* presented some important differences in the values of internal surface temperature and relative humidity. Considering the HAMT model is more accurate in comparison with the EMPD one, even presenting a considerable higher computational time, it is assumed that option *e* was the most cost-effective one.

To assess the EnergyPlus behaviour regarding moisture in the simulation case of this work, some tests were carried out for the cities of Manaus (ZB8) and Caruaru (ZB7). Manaus has a hot and humid while Caruaru a hot and dry climate.

[1] See Section 3.2

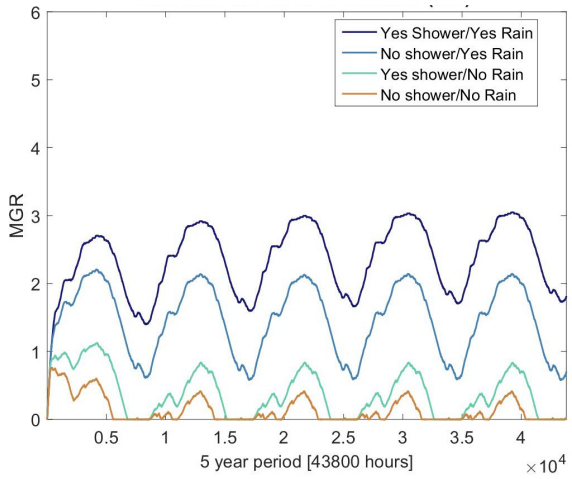


Fig. 46a. Influence of rain and shower on MGR values for the city of Manaus

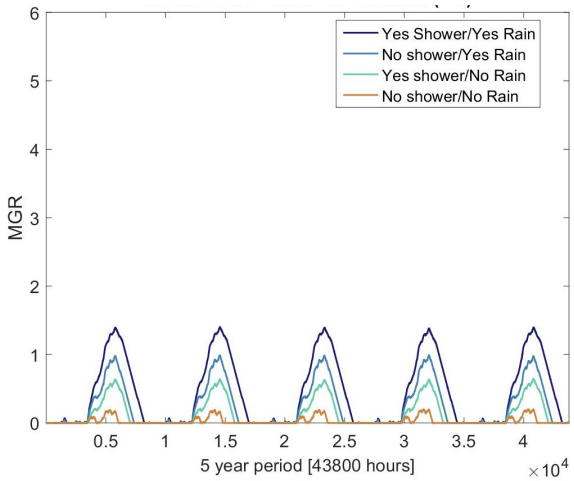


Fig. 46b. Influence of rain and shower on MGR values for the city of Caruaru

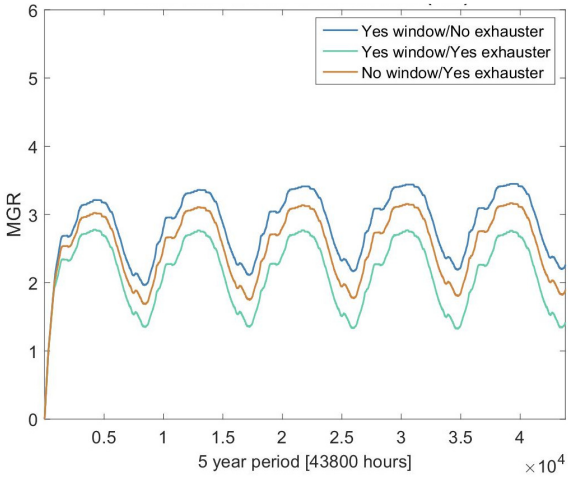


Fig. 47a. Influence of natural ventilation and exhauster on MGR values for the city of Manaus

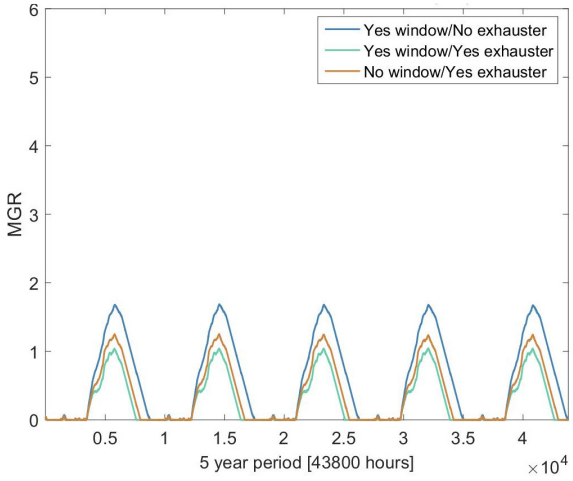


Fig. 47b. Influence of natural ventilation and exhauster on MGR values for the city of Caruaru

Fig. 46 graphics show, for the two cities, a comparison of MGR values considering the existence or not of the shower and rain in all possible combinations. In the *No Rain* cases, all values of rainfall in the weather file were set as zero. The aim was to analyse how an internal surface of the envelope of the simulation model responds to the external humidity from rainfall and the moisture generation from the shower. During this test, it was realized that in EnergyPlus a *Water Equipment* object does not imply in vapour production, its purpose is to compute water consumption. For this reason, it was used the object *Steam Equipment*. To verify its operation, two simulations were performed with rainfall set as zero in the weather file, one with and another without the shower operating.

In the graphics, it is observed that for these cities, the humidity load from rainfall which is transferred towards the internal surface of the wall has a higher impact on the MGR than the humidity produced

by the shower. One possible explanation is the natural ventilation setpoint of 24°C, which implies that in hot cities the window remains open most of the time.

The graphics of Fig. 47 present the impact of the exhauster fan and natural ventilation on MGR values. The objective of this test was to evaluate the response of the simulation model to the external humidity that entries in the bathroom through the window, and to the existence of an exhauster fan. In both cities, it is observed that humidity from outdoors which entries in the bathroom through the window has a more important effect on MGR values than the absence of an exhaust fan.

Seeing the results of these tests, it is assumed, besides the reasons mentioned in Section 6.2.3, that the 1-D model from EnergyPlus may be satisfactory to achieve the objectives of this study.

### 6.3.4 Mould model

As already mentioned, the mould models are applied in this work as indicators of the potential moisture risk, not as a prediction of fungi activity. The Isopleth is an out-of-date model but is applied in the climatic analysis because it does not depend on defining a surface material. Concerning the VTT model, which is widely applied in building research, a recent study (BERGER *et al.*, 2018) indicates some issues on the reliability of its mathematical formulation of the physical model of mould growth. Also, in the VTT model, it is necessary to define the sensitivity of the material and its surface quality. These variables are defined based on reasonableness, which may bring uncertainty, seeing that results are very sensitive to this information. Despite these uncertainties, mould models may be acceptable moisture risk indicators, considering they combine critical conditions of temperature and relative humidity in which mould can grow. Thus, it is assumed that the mould growth models employed in this work are suitable indicators of moisture risk within the objectives of the thesis.

### 6.3.5 Simulation model - building design and habits of usage

Due to the absence of building stock in Brazil, the building geometry and its floor plan are based on a model from *Minha casa, Minha vida* (My home, My life) (BRASIL, 2019), a Brazilian public policy for popular housing. The schedules of rooms occupation, lighting and equipment use are defined based

on the RTQ-R simulation report (LABEEE, 2011) with some adjustments (replacing incandescent bulbs for fluorescent ones and considering that both adults have work outside the home) based in common sense, considering a common Brazilian 4-people family.

### 6.3.6 Parameters variation

The selection of the categorical variables to be varied in building simulation – building solar orientation, the material of walls, length of the shower, permeance of painting layers in walls and existence of an exhauster fan in the bathroom – is based on a common sense that these criteria can be considered as common ones in Brazilian residential buildings reality and that may also impact moisture issues.

### 6.3.7 Risk classes

To allow presenting the influence of the varied parameters on the MGR according to Bioclimatic Zones for a great amount of data, some results are presented according to Risk Classes of $t_M$ (Table 18), which is the consecutive period of $M \geq 1$ in the 5$^{th}$ year of simulation. However, the graphics of the MGR values show different behaviours for different cases and cities in the perspective of a 1-year timeframe. In some circumstances, there is a rapid growth in the very first (1-3) months and a trend towards stability. In others, there is a stable growth in the first six months until the peak in winter and a stable and equivalent decline in the final six months (from winter towards summer). Still, in some cases, there is a stable growth in the first months towards a peak value in winter and a less pronounced decrease from the peak in winter towards summer. These different patterns of evolution of $M$ values along the 1-year period can be observed in Fig. 34a; the values of $t_M$ may present varied behaviours along the year for different cities and simulation cases. Due to this, it was chosen to divide the 1-year timeframe into 6 uniform Risk Classes of 1460 hours each.

# CHAPTER 7. FINAL REMARKS

In the present Chapter, an overview of the main findings and shortcomings of the thesis as well as recommendations for further research are addressed.

This thesis investigated the potential moisture risks in Brazilian residential buildings across the different national climates. The work was based on the hypothesis that there is moisture risk in Brazilian buildings due to climatic conditions, constructive techniques and cultural habits besides the risk due to the use of low-quality material, failure in the design and construction processes, being the topic however, underexplored in the country in a comprehensive manner. The development of the work was based on the questions:

1. What are the potential moisture loads in Brazilian buildings?
2. What is the potential moisture risk for a typical Brazilian popular housing typology across the different climates of the country?

On the climatic analysis, weather-based indicators were presented to provide an outline regarding the risks due to weather conditions on the country scale. The proposed climatic moisture risk indicators Vapour Pressure ($VP$), Wind-Driven Rain ($WDR$), Mould Growth Risk ($MGR$), air-rain Index ($I_{air-rain}$) and Facade Deterioration Risk Index ($I_{FD}$), are based on climatic data that are commonly available, providing a fast perception of the potential risk even on a country scale and applies to other locations.

On the building scale analysis, the investigation was undertaken by performing simulations of a common residential typology, considering the same climatic data employed in the climatic analysis. The indoor moisture load was estimated through the latent heat of the internal gains. Some moisture-related parameters following the country circumstances were chosen to be varied and therefore assess their influence on the moisture risk. A mould growth risk index was applied to simulation results focusing on the indoor surface of the bathroom as a moisture risk indicator.

The results of both scale analyses were plotted in the Brazil map using a Geographic Information System, providing a general panorama of the areas of the country that are more susceptible to moisture load.

One main contribution of the climatic analysis is the introduction of the equivalent vapour pressure $P_v^{eq}$ concept, that aims to estimate the total climatic external vapour pressure by adding the effect of wind-driven rain. The two new presented indicators $I_{air-rain}$ and $I_{FD}$ are based on this concept and estimate, respectively, the intensity and the cumulative potential moisture load that building envelopes are susceptible of receiving.

On the building scale investigation, results indicate that the main used construction methods may not be safe by the moisture point of view to all regions of the country. Also, a main concern is the remarkably high potential risk in highly densely populous regions of the country. Nonetheless, when working with building simulation, it is necessary to reflect that building design comprises many criteria such as climate conditions and a large sort of architecture and engineering parameters combinations. Performing numerous simulations requests assuming some simplifications and consequent limitations which were detailed in Chapter 6. But considering the lack of moisture-related information in the Brazilian building stock and moisture-related requirements in building standards, the presented results bring up an important overview of the potential moisture risk in buildings across the country and may help in conducting a more accurate analysis in the topic.

Summarizing, on the climatic scale, high outdoor vapour pressure values and the combined effect of high rainfall rates with wind action in highly densely populated areas indicate a high climatic potential moisture risk level. On the building scale, even the cases that presented the lowest risks have considerable high levels of Mould Growth Risk ($M$) and consecutive period of Mould Growth Risk ($t_M$) and mainly in high densely populous areas. Both types of simulated walls follow standards thermal requirements but may not be suitable to some regions regarding moisture safety. As the presented maps point great variation of the potential moisture load across the country and moisture disorders

are directly affected by the type of materials, the usage of the same construction techniques is possibly not appropriate for all regions, both by the thermal performance and by the moisture risk point of view. A basic exhaust fan has shown to be an affordable improvement of moisture safety.

The maps indicate that Brazil has important potential moisture risk in highly densely populated areas, both due to climatic conditions and common construction methods and patterns of usage. The overlapped maps of results from both climatic and building scales with the existing Bioclimatic Zoning, which is widely applied in building research, show diverse levels of moisture risk in the same Zone. The Bioclimatic Zoning proposes for each zone strategies such as material thermophysical properties for the envelope, size of openings and need of cooling/heating systems to improve the thermal performance of buildings. Considering the moisture load is of great importance for the thermal performance of buildings and the thermal comfort of its occupants, these maps indicate a potential need for additional information related to moisture risk in existing building standards, but they do not intend to be assertive. To imply a revision in existing standards, extensive study and improvements are required, such as *in loco* data survey and exhaustive simulations comprising large quantity and combination of variation in building envelope materials, internal loads, patterns of usage and geometry.

Given the lack of information regarding moisture risks in Brazilian buildings in a general panorama, the main original contributions of this work can be listed as follow:

- An unprecedented analysis on the scale of the country regarding the potential moisture risk in buildings in Brazil;
- Proposal of weather-based indicators to assess the potential moisture load in buildings due to climatic conditions and which can be applied to other locations;
- General panorama of the potential moisture risk of a typical Brazilian residential building;
- Five moisture-related indicators plotted on the map of Brazil;

- Evidence of the need to develop moisture requirements/guidelines in existing building standards and of great potential for further research on the topic.

Climatic conditions, informally built houses, lack of qualified labour, innovative techniques and a lack of moisture-related standards put the populous country in an attention position concerning moisture disorders in buildings. Due to cultural issues and the great amount of informal construction, moisture disorders are currently faced as something unavoidable, particularly for condensation and mould growth. Therefore, moisture is commonly neglected by building owners in Brazil.

Moisture research in Brazil started in the eighties but is still underexplored and mainly concentrated in universities with a modest application with the building industry. So far there is a lack of studies in the country that assess the influence of moisture on building energy performance, material deterioration and building pathology.

Results of this work indicate a great potentiality of further research on the topic and a need in developing moisture-related requirements in Brazilian building standards. On the climatic approach, one possible improvement is additional evaluation with real measured data and also for other locations. On the building scale, a study considering other building typologies such as semi-detached houses and multi-storey buildings and the use of air conditioning. Also, the evaluation of simulation cases with more specific parameters regarding the different climates and patterns of usage according to regional cultural habits. Another important potential improvement is a detailed investigation on the type of materials, granularity, and moisture transfer mechanisms, which can be achieved by a 2-D or 3-D heat and moisture transfer analysis.

A potential work in the short term could also be a joined analysis with the existing Bioclimatic Zoning, both on the climatic scale and the building scale. Simulations can be performed considering the Bioclimatic Zoning proposals for each zone (thermophysical properties for the envelope, size of openings, need of cooling/heating systems, and passive strategies to improve thermal performance), to assess their impact, per zone, on the moisture risk. This would also promote the accuracy of building

performance assessment by regulation methods as moisture can play an important role also on the heat transfer through porous building envelopes.

**Acknowledgements**

The Brazilian Agencies Conselho Nacional de Desenvolvimento Científico e Tecnológico (CNPq) and Coordenação de Aperfeiçoamento de Pessoal de Nível Superior (CAPES – Finance Code 001) of the Ministry of Education for the financial support of this work, and the International Cooperation Program CAPES/COFECUB (Grant # 774/13 Process 99999.000497/2016-09), in collaboration with the laboratory LOCIE at the Université Savoie Mont-Blanc, France.

**Articles**

MORISHITA, C., MENDES, N. and BERGER, J. Issues about moisture in residential buildings of Brazil. In: CIB World Building Congress, 2016, Tampere, Finland. Tampere University of Technology. p.865-884.

MORISHITA, C., BERGER, J. and MENDES, N. Weather-based indicators for analysis of moisture risks in buildings. Science of The Total Environment, v.709, 2020/03/20/, p.134850. 2020. Available at: http://www.sciencedirect.com/science/article/pii/S0048969719348429.

## REFERENCES

ABADIE, M. O. and MENDES, N. Numerical assessment of turbulence effect on the evaluation of wind-driven rain specific catch ratio. **International Communications in Heat and Mass Transfer**, v.35, n.10, 2008/12/01/, p.1253-1261. 2008. https://doi.org/10.1016/j.icheatmasstransfer.2008.08.013.

ABADIE, M. O. and MENDONÇA, K. C. Moisture performance of building materials: From material characterization to building simulation using the Moisture Buffer Value concept. **Building and Environment**, v.44, n.2, 2009/02/01/, p.388-401. 2009. https://doi.org/10.1016/j.buildenv.2008.03.015.

ABNT - Associação Brasileira de Normas Técnicas. **Desempenho térmico de edificações** NBR 15220, Brazilian Association of Technical Standards, 2005. (in Portuguese).

_____. Edificações habitacionais - Desempenho. NBR 15575: Brazilian Association of Technical Standards 2013.

ABUKU, M., BLOCKEN, B. and ROELS, S. Moisture response of building facades to wind-driven rain: Field measurements compared with numerical simulations. **Journal of Wind Engineering and Industrial Aerodynamics**, v.97, n.5, 2009/08/01/, p.197-207. 2009. https://doi.org/10.1016/j.jweia.2009.06.006.

ABUKU, M., JANSSEN, H., BLOCKEN, B., CARMELIET, J. and ROELS, S. Wind-driven rain load on building enclosures–towards the reliable prediction of absorption and evaporation. **IEA Annex**, v.41. 2006.

ABUKU, M., JANSSEN, H., POESEN, J. and ROELS, S. Impact, absorption and evaporation of raindrops on building facades. **Building and environment**, v.44, n.1, 2009/01/01/, p.113-124. 2009. https://doi.org/10.1016/j.buildenv.2008.02.001.

AKINYEMI, O. D., MENDES, N., JONSSON, M., MEISSNER, J. and DE LINHARES, S. Effects of Psychrometrics Conditions on the Drying of a Porous Soil. **Journal of Building Physics**, v.31, n.1, July 1, 2007, p.73-89. 2007. https://doi.org/10.1177/1744259107079124.

ALCARDE ALVARES, C., LUIZ STAPE, J., CESAR SENTELHAS, P., LEONARDO DE MORAES GONÇALVES, J. and SPAROVEK, G. Köppen's climate classification map for Brazil. **Meteorologische Zeitschrift**, v.22, n.6, p.711-728. 2013. http://dx.doi.org/10.1127/0941-2948/2013/0507.Accessed: 27 feb 2017.

ALUCCI, M., FLAUZINO, W. and MILANO, S. **Bolor em edifícios: causas e recomendações. Tecnologia de Edificações**. IPT–Instituto de pesquisas Tecnológicas do Estado de São Paulo, Coletânea de trabalhos Div. de Edificações do IPT. São Paulo: Pini. 1988. (in Portuguese).

ASHRAE - American Society of Heating, Refrigerating and Air-Conditioning Engineers. **Propose new Standard 160** Criteria for moisture-control design analysis in buildings. Atlanta GA, ASHRAE, 2008. 24 p.

_____ - American Society of Heating, Refrigerating and Air-Conditioning Engineers. **Ashrae Handbook** Fundamentals. Atlanta GA, ASHRAE, 2013.

BARBOSA, R. M. and MENDES, N. Combined simulation of central HVAC systems with a whole-building hygrothermal model. **Energy and Buildings**, v.40, n.3, p.276-288. 2008.

BERGER, J., LE MEUR, H., DUTYKH, D., NGUYEN, D. M. and GRILLET, A.-C. Analysis and improvement of the VTT mold growth model: Application to bamboo fiberboard. **Building and environment**, 2018/03/28/. 2018. https://doi.org/10.1016/j.buildenv.2018.03.031.

BERGER, J., WOLOSZYN, M., GUERNOUTI, S. and BUHE, C. Factors governing the development of moisture disorders for integration into building performance simulation. **Journal of Building Engineering**, v.3, p.1-15. 2015. http://doi.org/10.1016/j.jobe.2015.04.008.

BERGER, J., WOLOSZYN, M., MAZUROSKI, W., MENDES, N. and GUERNOUTI, S. 2D whole-building hygrothermal simulation analysis based on a PGD reduced order model. **Energy and Buildings**, v.112, 1/15/, p.49-61. 2019. http://dx.doi.org/10.1016/j.enbuild.2015.11.023.

BLOCKEN, B. and CARMELIET, J. A review of wind-driven rain research in building science. **Journal of Wind Engineering and Industrial Aerodynamics**, v.92, n.13, p.1079-1130. 2004. http://doi.org/10.1016/j.jweia.2004.06.003.

_____. Guidelines for the required time resolution of meteorological input data for wind-driven rain calculations on buildings. **Journal of Wind Engineering and Industrial Aerodynamics**, v.96, n.5, p.621-639. 2008. http://doi.org/10.1016/j.jweia.2008.02.008.

BLOCKEN, B. and CARMELIET, J. Impact, runoff and drying of wind-driven rain on a window glass surface: Numerical modelling based on experimental validation. **Building and Environment**, v.84, n.C, p.170-180. 2015. https://doi.org/10.1016/j.buildenv.2014.11.006.

BRASIL. **Minha Casa Minha Vida** Ministério das Cidades. Available at: http://www.minhacasaminhavida.gov.br/. (in Portuguese).

BUENO, A. D., PHILIPPI, P. C. and LAMBERTS, R. Influence of water vapour sorption on the thermal behaviour of mortar samples. In: British Masonry Society, 1994. p.52-54.

CARVALHO, Y. M. and PINTO, V. G. Umidade em edificações: conhecer para combater. **ForScience**, v.6, n.3. 2018. (in Portuguese).

CASTILLO, S. R., MENDES, N. and MOURA, L. M. Improvements in Software DOMUS about Atmospheric Radiative Exchange and Long-wave Boundary Conditions. In: 17th Brazilian Congress of Thermal Scineces and Engineering - ENCIT, 2018, Águas de Lindóia, SP: Abcm. p.1-8.

CEPEL - Centro de Pesquisas em Energia Solar e Eólica. **Potencial Eólico de Energia**, Electrical Energy Research Center, 2019. (in Portuguese).

CGEE - Management and Strategic Studies Center. **Relatório Prospectivo Setorial: 2009**. Civil Industry. Brasília: CGEE, 219 p. 2009. (in portuguese).

CLARKE, J., JOHNSTONE, C., KELLY, N., MCLEAN, R., ROWAN, N. and SMITH, J. A technique for the prediction of the conditions leading to mould growth in buildings. **Building and Environment**, v.34, n.4, p.515-521. 1999. http://doi.org/10.1016/S0360-1323(98)00023-7.

CORNICK, S. and DALGLIESH, W. A. A moisture index to characterize climates for building envelope design. **Journal of Thermal Envelope and Building Science**, v.27, n.2, p.151-178. 2003. http://doi.org/10.1177/1097196303036210.

DOE - Department of Energy U.S. **EnergyPlus Documentation**. Engineering Reference. 2017a.

_____. EnergyPlus v.8-7-0 2017b.

DOS SANTOS, G. H., MENDES, N. and PHILIPPI, P. C. A building corner model for hygrothermal performance and mould growth risk analyses. **International Journal of Heat and Mass Transfer**, v.52, n.21–22, 10//, p.4862-4872. 2009. http://dx.doi.org/10.1016/j.ijheatmasstransfer.2009.05.026.

DUTRA, L., MENDES, N. and PHILIPPI, P. C. On the characterization of pore size distribution of building materials. **Journal of Building Physics**, v.41, n.3, p.247-263. 2017. https://doi.org/10.1177/1744259117698515.

EM - NORMAS LEGALES. **Confort Térmico y Lumínico con Eficiencia Energetica**, EM: 110. Lima, 2014. (in Spanish).

FREIRE, R. Z., ABADIE, M. O. and MENDES, N. Integration of Natural Ventilation Models in the Hygrothermal and Energy Simulation Program PowerDomus. In: Proceedings of the 11th International Building Performance Simulation Association Conference, 2009. p.1037-1044.

FREITAS DUTRA, L., FREITAS, M. E., GRILLET, A.-C., MENDES, N. and WOLOSZYN, M. Microstructural Characterization of Porous Clay-Based Ceramic Composites. **Materials (Basel, Switzerland)**, v.12, n.6. 2019. https://doi.org/10.3390/ma12060946.

GALLIPOLITI, V., SOGARI, N., GEA, M. and BUSSO, A. Evaluación del Desempeño Higrotérmico Energético de Una Vivienda Social en la Ciudad de Corrientes. **Avances en Energías Renovables y Medio Ambiente**, v.14, p.17-05.24. 2012.

GE, H., DEB NATH, U. K. and CHIU, V. Field measurements of wind-driven rain on mid-and high-rise buildings in three Canadian regions. **Building and environment**, v.116, n.Supplement C, 2017/05/01/, p.228-245. 2017. http://doi.org/10.1016/j.buildenv.2017.02.016.

GEVING, S. and HOLME, J. Mean and diurnal indoor air humidity loads in residential buildings. **Journal of Building Physics**, v.35, n.4, April 1, 2012, p.392-421. 2012. http://doi.org/10.1177/1744259111423084.

GIONGO, M., PADARATZ, I. J. and LAMBERTS, R. Determinação da exposição à chuva dirigida em Florianópolis, SC: índices de chuva dirigida e métodos semi-empíricos. **Ambiente Construído**, v.11, p.7-23. 2011.

GOFFART, J., RABOUILLE, M. and MENDES, N. Uncertainty and sensitivity analysis applied to hygrothermal simulation of a brick building in a hot and humid climate. **Journal of Building Performance Simulation**, p.1-21. 2015. https://doi.org/10.1080/19401493.2015.1112430.

HENS, H. IEA annex 14: condensation and energy. **Journal of thermal insulation**, v.15, n.3, p.261-273. 1992.

HENS, H. **Building Physics - Heat, Air and Moisture. Fundamentals and Engineering Methods with Examples and Exercises**. Berlin: Ernst & Sohn, 270p. p. 2007.

HERB, W. R., JANKE, B., MOHSENI, O. and STEFAN, H. G. Ground surface temperature simulation for different land covers. **Journal of Hydrology**, v.356, n.3-4, p.327-343. 2008. https://doi.org/10.1016/j.jhydrol.2008.04.020.

HOLM, A., KÜNZEL, H. M. and SEDLBAUER, K. The hygrothermal behaviour of rooms: combining thermal building simulation and hygrothermal envelope calculation. **IBPSA Proceedings Building Simulation Eindhoven**. 2003.

IBGE - Brazilian Institute of Geography and Statistics. National Survey by Household Sampling - Social indicators year 2014. **Pesquisa Nacional por Amostra de Domicílios**. Available at: https://ww2.ibge.gov.br/home/estatistica/populacao/trabalhoerendimento/pnad2015/default.shtm.

_____ - Instituto Brasileiro de Geografia e Estatística. Brazilian Institute of Geography and Statistics. **Brasil - Características da população**. Available at: https://www.ibge.gov.br/estatisticas/sociais/populacao.html.

_____ - Instituto Brasileiro de Geografia e Estatística. Brazilian Institute of Geography and Statistics. **Mapas**. Available at: http://portaldemapas.ibge.gov.br/portal.php#homepage.

IBRAHIM, M., SAYEGH, H., BIANCO, L. and WURTZ, E. Hygrothermal performance of novel internal and external super-insulating systems: In-situ experimental study and 1D/2D numerical modelling. **Applied Thermal Engineering**, v.150, 2019/03/05/, p.1306-1327. 2019. https://doi.org/10.1016/j.applthermaleng.2019.01.054.

INMET - Instituto Nacional de Meteorologia. **(INMET)**. Available at: http://www.inmet.gov.br/portal/.

INMETRO - INSTITUTO NACIONAL DE METROLOGIA, NORMALIZAÇÃO E QUALIDADE INDUSTRIAL. **Portaria INMETRO nº 372 de 17/09/2010**. Requisitos Técnicos da Qualidade para o Nível de Eficiência Energética de Edifícios Comerciais, de Serviços e Públicos. Available at: http://www.inmetro.gov.br/legislacao/rtac/pdf/RTAC001599.pdf. Accessed: dezembro 2010.

_____ - INSTITUTO NACIONAL DE METROLOGIA, NORMALIZAÇÃO E QUALIDADE INDUSTRIAL. **Portaria n° 18, de 16 de janeiro de 2012**. Regulamento Técnico da Qualidade para o Nível de Eficiência Energética de Edificações Residenciais (RTQ-R). Available at: http://www.inmetro.gov.br/legislacao/rtac/pdf/RTAC001788.pdf. Accessed: dezembro 2010. (in portuguese).

IRAM - INSTITUTO ARGENTINO DE NORMALIZACIÓN Y CERTIFICACIÓN. **Aislamiento térmico de edificios: verificación del riesgo de condensación del vapor de agua superficial e intersticial en paños centrales**, Norma IRAM Nº 11625. Buenos Ayres, 2000a. (in Spanish).

_____ - INSTITUTO ARGENTINO DE NORMALIZACIÓN Y CERTIFICACIÓN. **Aislamiento térmico de edificios: verificación riesgo de condensación intersticial y superficial en puntos singulares**, Norma IRAM Nº 11630. Buenos Ayres, 2000b. (in Spanish).

JIN, L., ZHANG, Y. and ZHANG, Z. Human responses to high humidity in elevated temperatures for people in hot-humid climates. **Building and Environment**, v.114, p.257-266. 2017. https://doi.org/10.1016/j.buildenv.2016.12.028.

JOHANSSON, S., WADSÖ, L. and SANDIN, K. Estimation of mould growth levels on rendered façades based on surface relative humidity and surface temperature measurements. **Building and Environment**, v.45, n.5, p.1153-1160. 2010. http://dx.doi.org/10.1016/j.buildenv.2009.10.022.

JÚNIOR, C. M. M. and CARASEK, H. Índices de chuva dirigida direcional e análise do nível de umedecimento em fachadas de edifício multipavimentos em Goiânia, GO. **Ambiente Construído**, v.11, n.3, p.23-37. 2014. http://dx.doi.org/10.1590/S1678-86212011000300003. (in Portuguese).

KOWALTOWSKI, D. C. C. K., PINA, S. A. M. G., RUSCHEL, R. C., LABAKI, L. C., BERTOLLI, S. R., FILHO, F. B. and FÁVERO, É. A house design assistance program for the self-building process of the region of Campinas, Brazil: Evaluation through a case study. **Habitat international**, v.29, n.1, p.95-111. 2005. 10.1016/S0197-3975(03)00065-1.

KUBILAY, A., DEROME, D., BLOCKEN, B. and CARMELIET, J. Wind-driven rain on two parallel wide buildings: Field measurements and CFD simulations. **Journal of Wind Engineering & Industrial Aerodynamics**, v.146, n.C, p.11-28. 2015. https://doi.org/10.1016/j.jweia.2015.07.006.

KUMARAN, M. Iea annex 24 final report, vol. 3, task 3: Material properties. **IEA, Acco Leuven, Leuven**. 1996.

KÜNZEL, H. **Simultaneous heat and moisture transport in building components**. One-and two-dimensional calculation using simple parameters. Verlag Stuttgart: Fraunhofer Institute of Building Physics, 65 p. 1995.

KÜNZEL, H. M., HOLM, A., ZIRKELBACH, D. and KARAGIOZIS, A. N. Simulation of indoor temperature and humidity conditions including hygrothermal interactions with the building envelope. **Solar Energy**, v.78, n.4, 2005/04/01/, p.554-561. 2005. https://doi.org/10.1016/j.solener.2004.03.002.

KÜNZEL, H. M. and KIESSL, K. Calculation of heat and moisture transfer in exposed building components. **International Journal of Heat and Mass Transfer**, v.40, n.1, p.159-167. 1996. https://doi.org/10.1016/S0017-9310(96)00084-1.

LABEEE - Laboratório de Eficiência Energética em Edificações. **Relatório técnico**. Relatório técnico da base de simulações para o RTQ-R. Florianópolis: LabEEE. 2011. (in Portuguese).

LEE, E. S. **Improved Hydronic Loop System Solution Algorithm with a Zone-Coupled Horizontal Ground Heat Exchanger Model for Whole Building Energy Simulation**. Oklahoma State University, 2013

LEE, H.-H., OH, H.-R., LIM, J.-H. and SONG, S.-Y. Evaluation of the Thermal Environment for Condensation and Mold Problem Diagnosis Around Built-in Furniture in Korean Apartment Buildings during Summer and Winter. **Energy Procedia**, v.96, 2016/09/01/, p.601-612. 2016. https://doi.org/10.1016/j.egypro.2016.09.108.

LIDDAMENT, M. W. **Air infiltration calculation techniques: An applications guide**: Air infiltration and ventilation centre Berkshire, UK. 1986.

LISØ, K. R., KVANDE, T., HYGEN, H. O., THUE, J. V. and HARSTVEIT, K. A frost decay exposure index for porous, mineral building materials. **Building and environment**, v.42, n.10, p.3547-3555. 2007. http://doi.org/10.1016/j.buildenv.2006.10.022.

LU, G. Y. and WONG, D. W. An adaptive inverse-distance weighting spatial interpolation technique. **Computers & Geosciences**, v.34, n.9, 2008/09/01/, p.1044-1055. 2008. https://doi.org/10.1016/j.cageo.2007.07.010.

MAZZAFERRO, L., MACHADO, R. M. S., MELO, A. P. and LAMBERTS, R. Do we need building performance data to propose a climatic zoning for building energy efficiency regulations? **Energy and Buildings**, v.225, 2020/10/15/, p.110303. 2020. https://doi.org/10.1016/j.enbuild.2020.110303.

MDR. **Programa Brasileiro da qualidade e produtividade do habitat** PBQP-H, Ministério do Desenvolvimento Regional, 2019. (in Portuguese).

MELLO, L. A., MOURA, L. M. and MENDES, N. A model for assessment of heat and moisture transfer through hollow porous buildings elements. **Case Studies in Thermal Engineering**, v.14, p.100446. 2019. https://doi.org/10.1016/j.csite.2019.100446.

MENDES, N. **Modelos para previsão da transferência de calor e umidade em elementos porosos de edificações**. Federal University of Santa Catarina, Florianópolis, 1997. 225 p.

MENDES, N., ABADIE, M. O. and AKINYEMI, O. D. Numerical and experimental assessment of ground temperature and water content under mild weather conditions. **Special Topics & Reviews in Porous Media**, v.3, n.4, 2012-11-16, p.329-339. 2012. 10.1615/SpecialTopicsRevPorousMedia.v3.i4.40.

MENDES, N., BARBOSA, R. M., FREIRE, R. Z. and OLIVEIRA, R. C. L. F. A simulation environment for performance analysis of HVAC systems. **Building Simulation**, v.1, n.2, p.129-143. 2008. https://doi.org/10.1007/s12273-008-8216-7.

MENDES, N., CHHAY, M., BERGER, J. and DUTYKH, D. **Numerical Methods for Diffusion Phenomena in Building Physics: A Practical Introduction**: Springer International Publishing. 2019.

MENDES, N., OLIVEIRA, R. and SANTOS, G. H. D. DOMUS 2.0: A whole-building hygrothermal simulation program. In: International Conference on Building Performance Simulation (IBPSA), 2003, Netherlands. p.863-870.

MENDES, N., OLIVEIRA, R. C. L. F. and SANTOS, G. H. D. DOMUS 1.0: a Brazilian PC program for building simulation. In: International Conference on Building Performance Simulation, 2001, Rio de Janeiro, Brazil: Ibpsa. p.83-90.

MENDES, N. and PHILIPPI, P. C. Multitridiagonal-Matrix Algorithm for Coupled Heat Transfer in Porous Media: Stability Analysis and Computational Performance. **Journal of Porous Media**, v.7, n.3, 2004-09-01, p.193-211. 2004. 10.1615/JPorMedia.v7.i3.40.

MENDES, N. and PHILIPPI, P. C. A method for predicting heat and moisture transfer through multilayered walls based on temperature and moisture content gradients. **International Journal of Heat and Mass Transfer**, v.48, n.1, 1//, p.37-51. 2005. http://dx.doi.org/10.1016/j.ijheatmasstransfer.2004.08.011.

MENDES, N., PHILIPPI, P. C. and LAMBERTS, R. A new mathematical method to solve highly-coupled equations of heat and mass transfer in porous media. **International Journal of Heat and Mass Transfer**, v.45, n.3, p.509-518. 2001. https://doi.org/10.1016/S0017-9310(01)00172-7.

MENDES, N., RIDLEY, I., LAMBERTS, R., PHILIPPI, P. C. and BUDAG, K. Umidus: a PC program for the prediction of heat and mass transfer in porous building elements. In: International Conference on Building Performance Simulation (IBPSA), 1999, Japan. v. 1. p.277-283.

MENDES, N., WINKELMANN, F. C., LAMBERTS, R. and PHILIPPI, P. C. Moisture effects on conduction loads. **Energy and Buildings**, v.35, p.631-644. 2003. http://doi.org/10.1016/S0378-7788(02)00171-8.

MOON, H. J., RYU, S. H. and KIM, J. T. The effect of moisture transportation on energy efficiency and IAQ in residential buildings. **Energy and Buildings**, v.75, p.439-446. 2014. http://doi.org/10.1016/j.enbuild.2014.02.039.

MORISHITA, C., BERGER, J. and MENDES, N. Weather-based indicators for analysis of moisture risks in buildings. **Science of The Total Environment**, v.709, 2020/03/20/, p.134850. 2020. https://doi.org/10.1016/j.scitotenv.2019.134850.

MORISHITA, C., MENDES, N. and BERGER, J. Issues about moisture in residential buildings of Brazil. In: CIB World Building Congress, 2016, Tampere, Finland. **Tampere University of Technology**. p.865-884.

NATH, S., DEWSBURY, M. and DOUWES, J. Has a singular focus of building regulations created unhealthy homes? **Architectural Science Review**, v.63, n.5, 2020/09/02, p.387-401. 2020. 10.1080/00038628.2019.1703636.

NETTO, G. R. and CZAJKOWSKI, J. D. Comparación entre las normas de desempeño térmico edilício de Argentina y Brasil. **Ambiente Construído**, v.16, p.105-122. 2016. (Spanish).

NIK, V. M., MUNDT-PETERSEN, S. O., KALAGASIDIS, A. S. and DE WILDE, P. Future moisture loads for building facades in Sweden: Climate change and wind-driven rain. **Building and Environment**, v.93, p.362-375. 2015. https://doi.org/10.1016/j.buildenv.2015.07.012.

NIU, J. L., ZHANG, L. Z. and ZUO, H. G. Energy savings potential of chilled-ceiling combined with desiccant cooling in hot and humid climates. **Energy and Buildings**, v.34, n.5, 2002/06/01/, p.487-495. 2002. https://doi.org/10.1016/S0378-7788(01)00132-3.

OGUC - Ordenanza General de Urbanismo y Construcciones. **Reglamentación Térmica**. Chile, 2000. (in Spanish).

ORR, S. A., YOUNG, M., STELFOX, D., CURRAN, J. and VILES, H. Wind-driven rain and future risk to built heritage in the United Kingdom: Novel metrics for characterising rain spells. **Science of The Total Environment**, v.640-641, 2018/11/01/, p.1098-1111. 2018. https://doi.org/10.1016/j.scitotenv.2018.05.354.

OUYANG, K. and HAGHIGHAT, F. A procedure for calculating thermal response factors of multi-layer walls - State space method. **Building and Environment**, v.26, n.2, p.173-177. 1991. https://doi.org/10.1016/0360-1323(91)90024-6.

PAZ, L. A. F., COSTA, L. C., PAULA, M. O., ALMEIDA, W. J. D. D. and FERNANDES, F. Levantamento de patologias causadas por umidade em uma edificação na cidade de Palmas-TO. **Revista Eletrônica em Gestão, Educação e Tecnologia Ambiental**, v.20, n.1, p.174-180. 2016. (in Portuguese).

PEREZ, A. R. Umidade nas edificações: recomendações para a prevenção da penetração de água da chuva pelas fachadas. **Tecnologia de Edificações**, n.2, p.35-42. 1985. (in Portuguese).

PROMIS, G., FREITAS DUTRA, L., DOUZANE, O., TRAN LE, A. D. and LANGLET, T. Temperature-dependent sorption models for mass transfer throughout bio-based building materials. **Construction and Building Materials**, v.197, 2019/02/10/, p.513-525. 2019. https://doi.org/10.1016/j.conbuildmat.2018.11.212.

QGIS - QGIS. **Open Source Geographic Information System**.

RAMALHO, M. B., PRATES, V. D. G., SILVA, K. G., BASTOS, D. M. and OLIVEIRA, N. B. Avaliação das manifestações patológicas da umidade de edificações em cidades do Vale do Jequitinhonha e Mucuri – MG. In: Congresso Brasileiro de Educação em Engenharia (COBENGE), 2014, Brasil. (in Portuguese).

ROCHA, A. P. D. A., MENDES, N. and OLIVEIRA, R. C. Domus method for predicting sunlit areas on interior surfaces. **Ambiente Construído**, v.18, n.3, p.83-95. 2018.

RORIZ, M. **Arquivos Climáticos de Municípios Brasileiros**. Available at: http://www.labeee.ufsc.br/sites/default/files/arquivos_climaticos/correcao_epw_antac.pdf. (in Portuguese).

SANTOS, G. H. D. and MENDES, N. The solum program for predicting temperature profiles in soils: mathematical models and boundary conditions analyses. In: 8th International Conference on Building Performance Simulation, 2003, Eindhoven - Netherlands: Ibpsa. p.1-8.

_____. Simultaneous heat and moisture transfer in soils combined with building simulation. **Energy and Buildings**, v.38, n.4, 4//, p.303-314. 2006. http://dx.doi.org/10.1016/j.enbuild.2005.06.011.

_____. Combined Heat, Air and Moisture (HAM) Transfer Model for Porous Building Materials. **Journal of Building Physics**, v.32, n.3, January 1, 2009, p.203-220. 2009a. https://doi.org/10.1177/1744259108098340.

_____. Heat, air and moisture transfer through hollow porous blocks. **International Journal of Heat and Mass Transfer**, v.52, n.9–10, 4//, p.2390-2398. 2009b. http://dx.doi.org/10.1016/j.ijheatmasstransfer.2008.11.003.

_____. Numerical analysis of passive cooling using a porous sandy roof. **Applied Thermal Engineering**, v.51, n.1–2, 3//, p.25-31. 2013. http://dx.doi.org/10.1016/j.applthermaleng.2012.08.046.

SANTOS, G. H. D. and MENDES, N. Hygrothermal bridge effects on the performance of buildings. **Heat and Mass Transfer**, v.53, p.133-138. 2014.

SEDLBAUER, K. and KRUS, M. A new model for mould prediction and its application in practice. In: 2nd International conference on Building Physics, 2003.

SILVEIRA NETO, A. D. Soluções exatas para o problema de transporte simultâneo de calor e massa em elementos porosos unidimensionais. 1985.

SINAT - National Technical Assessment System. **Sistema Nacional de Avaliações Técnicas**. Available at: http://pbqp-h.mdr.gov.br/projetos_sinat.php.

SINPHA. Information System of Electric Appliances Ownership and Consumption Habits. **Sistema de Informações de Posses de Eletrodomésticos e Hábitos de Consumo**. Available at: http://www.procelinfo.com.br/data/Pages/LUMIS05070313PTBRIE.htm. (in portuguese).

SOBRINHO, M. M. B. Estudo da ocorrência de fungos e da permeabilidade em revestimentos argamassados em habitações de interesse social. In: XII National Meeting of Built Environment Technology 2008, Fortaleza - Brazil. **ANTAC**. São Paulo. v. Dissertation. p.33-42. (in portuguese).

STOPP, H., STRANGELD, P., FECHNER, H. and HÄUPL, P. The hygrothermal performance of external walls with inside insulation. **Thermal Performance of the Exterior Envelopes of Buildings VIII, Clearwater Beach, Florida**. 2001.

STRAUBE, J. Simplified Prediction of Driving Rain on Buildings: ASHRAE 160P and WUFI 4.0. **Building Science Digests**, v.148. 2010.

TABARES-VELASCO, P. C. and GRIFFITH, B. Diagnostic test cases for verifying surface heat transfer algorithms and boundary conditions in building energy simulation programs. **Journal of Building Performance Simulation**, v.5, n.5, 2012/09/01, p.329-346. 2012. https://doi.org/10.1080/19401493.2011.595501.

TRIANA, M. A., LAMBERTS, R. and SASSI, P. Characterisation of representative building typologies for social housing projects in Brazil and its energy performance. **Energy Policy**, v.87, 2015/12/01/, p.524-541. 2015. https://doi.org/10.1016/j.enpol.2015.08.041.

UEMOTO, K. L. **Patologia: Danos causados por eflorescência. Coletânea de trabalhos da Div. de Edificações do IPT**. São Paulo: Pini, 561-64 p. 1988. (in Portuguese).

VENTOKIT. Air renovators. **Renovadores de ar**. Available at: http://www.ventokit.com.br/. (in portuguese).

VERÇOZA, E. J. **Patologia das edificações**. Porto Alegre: Editora Sagra, p172 p. 1991. (in Portuguese).

VEREECKEN, E. and ROELS, S. Review of mould prediction models and their influence on mould risk evaluation. **Building and Environment**, v.51, 5//, p.296-310. 2012. http://dx.doi.org/10.1016/j.buildenv.2011.11.003.

VIITANEN, H. and HUKKA, A. A mathematical model of mould growth on wooden material. **Wood Science and Technology**, v.33, n.6, p.475-485. 1999. https://doi.org/10.1007/s002260050131.

VIITANEN, H., OJANEN, T., PEUHKURI, R., LÄHDESMÄKI, K., VINHA, J. and SALMINEN, K. Classification of material sensitivity - New approach for mould growth modeling. In: **Proceedings 9th Nordic Symposium on Building Physics NSB 2011, Tampere, Finland, 29 May - 2 June 2011** Tampere University of Technology, 2011, p. 867-874.

WALSH, A., CÓSTOLA, D. and LABAKI, L. C. Comparison of three climatic zoning methodologies for building energy efficiency applications. **Energy and buildings**, v.146, p.111-121. 2017. 10.1016/j.enbuild.2017.04.044.

WALTON, G. N. Thermal analysis research program reference manual. **National Bureau of Standards**. 1983.

_____. **AIRNET: a computer program for building airflow network modeling**: National Institute of Standards and Technology Gaithersburg, MD. 1989.

WOLOSZYN, M. and RODE, C. **Annex 41 Whole Building Heat, Air, Moisture response**. Modelling Principles and Common Exercises: International Energy Agency - IEA. 2008a.

_____. Tools for performance simulation of heat, air and moisture conditions of whole buildings. **Building Simulation**, v.1, n.1, p.5-24. 2008b. https://doi.org/10.1007/s12273-008-8106-z.

YIK, F. W. H., SAT, P. S. K. and NIU, J. L. Moisture Generation through Chinese Household Activities. **Indoor and Built Environment**, v.13, n.2, April 1, 2004, p.115-131. 2004. http://doi.org/10.1177/1420326X04040909.

YOU, S., LI, W., YE, T., HU, F. and ZHENG, W. Study on moisture condensation on the interior surface of buildings in high humidity climate. **Building and Environment**, v.125, p.39-48. 2017. https://doi.org/10.1016/j.buildenv.2017.08.041.

ZHANG, H. and YOSHINO, H. Analysis of indoor humidity environment in Chinese residential buildings. **Building and Environment**, v.45, n.10, p.2132-2140. 2010. http://dx.doi.org/10.1016/j.buildenv.2010.03.011.

# A. ANNEX

Table A.1. Simulation tool models description. Source: DOE (2017a)

| | INPUT/MODEL | DESCRIPTION | SOURCE |
|---|---|---|---|
| Simulation tool | EnergyPlus v 8.7.0 | 1-D whole-building simulation tool | DOE (2017b) |
| Initial conditions | Zone and surface temperatures | 23°C | - |
| | Zone humidity ratio | Outdoor humidity | Weather file |
| Surface heat transfer convection algorithm | Inside | Thermal Analysis Research Program (TARP) - variable natural convection based on the temperature difference | WALTON (1983) |
| | Outside | DOE-2 - a combination of the MoWiTT and BLAST detailed convection models | Lawrence Berkeley Laboratory (LBL) DOE2.1E-053 source code |
| Heat balance algorithm | Conduction Transfer Function (CTF) | State space method | OUYANG and HAGHIGHAT (1991) |
| | Combined Heat and Moisture transfer (HAMT) | One-dimensional coupled finite element | KÜNZEL (1995) |
| Ground temperature | Finite difference | 1-D heat transfer finite-difference. Uses weather file ground temperatures to obtain surface boundary conditions. An annual simulation is run on the model during the initialization until the annual ground temperature profile has reached steady periodic behaviour and then ground temperatures are cached for retrieval during the rest of the simulation. It does not consider ground moisture transport. | HERB *et al.* (2008) LEE (2013) |
| Natural ventilation | Air Flow Network Multizone | Simulation of zone pressures due to envelope leakage driven by wind. It calculates multizone airflows due to the wind and surface leakage including adjacent zones and outdoors and allows exhaust fans to be included as part of the airflow network. It consists of three main steps: (i) pressure and airflow calculations, (ii) node temperature and humidity calculations, (iii) sensible and latent heat calculations. Conservation of air mass flow rate at each linkage provides the convergence criterion. | AIRNET (WALTON, 1989) |
| Heat gains | Lights | For fluorescent lights, the electric input is converted 20% to visible radiation, 20% thermal radiation and 60% convective gain | (ASHRAE, 2013) |
| | People | Polynomial function to divide the total metabolic heat gain into sensible and latent portions. | |

Table A.2. Simulation inputs

| INPUT | INPUT ITEM | VALUE | UNIT | DESCRIPTION/SOURCE | ENERGYPLUS OBJECT |
|---|---|---|---|---|---|
| Timestep | | 300 | [s] | EnergyPlus HAMT example file | TimeStep |
| Building environment | | City | - | Towns, city outskirts, centre of large cities | Building |
| Run period | | 5 | [years] | | RunPeriod |
| Ventilation setpoint | | 24 | [°C] | (ASHRAE, 2013) | Schedule:Compact |
| Ground Temperature | Model | Finite difference | - | (DOE, 2017a) | Site:GroundTemperature:Undisturbed |
| | Thermal conductivity | 1 | [W/m·K] | Default values | |
| | Density | 1200 | [kg/m³] | | |
| | Specific heat | 1200 | [J/kg ·K] | | |
| Material CTF | Roughness | Table 10<br>Table 11<br>Table 12<br>Table 15 | [-] | NBR 15220 (ABNT, 2005)<br>Annex 24 (KUMARAN, 1996) | Material |
| | Thickness | | [m] | | |
| | Conductivity | | [W/m·K] | | |
| | Density | | [kg/m³] | | |
| | Specific Heat | | [J/kg ·K] | | |
| Material glazing | Thickness | 0.004 | [m] | EnergyPlus materials library<br>Glass Clear 4mm | WindowMaterial:Glazing |
| | Solar Transmittance | 0.837 | | | |
| | Solar Reflectance | 0.075 | | | |
| | Visible Transmittance | 0.898 | | | |
| | Visible Reflectance | 0.081 | | | |
| | Infrared Transmittance | 0 | | | |
| | Infrared Hemispherical Emissivity | 0.84 | | | |
| | Conductivity | 0.9 | [W/m·K] | | |
| Material HAMT | Porosity | | [m³/m³] | Annex 24 (KUMARAN, 1996)<br>EnergyPlus materials library | MaterialProperty:HeatAndMoistureTransfer |
| | Initial water content ratio | | [kg/kg] | | |
| | Sorption isotherm (humidity fraction, moisture content) | | [-], [kg/m³] | | |
| | Suction | | [kg/m³], [m²/s] | | |
| | Redistribution | | [kg/m³], [m²/s] | | |
| | Diffusion | | [-] | | |
| | Thermal conductivity | | [kg/m³], [W/m·K] | | |
| Wall painting layer | Permeance | $3.13x10^{-10}$ | [kg/(Pa·s·m²)] | ASHRAE (2013) | SurfaceProperties:VaporCoefficients |
| Vapour production | Shower | 2.60 | [kg/h] | Annex 14 (HENS, 1992) | SteamEquipment |
| | Cooking | 0.45 | | | |

| | | | | | | |
|---|---|---|---|---|---|---|
| People | Number of people | | Table 13 | [-] | (LABEEE, 2011) | People |
| | Metabolic rate | | | [W] | | Activity Schedule |
| Lights | Lighting level | | | | | Lights |
| Electric Equipment | Design level | | | | | ElectricEquipment |
| Ventilation Openings | Control mode of openings | | Ventilation setpoint | | The openable window or door is opened if Tzone > Tout and Tzone > Tsetpoint | AirflowNetwork:MultiZone:Surface |
| | Opening factor | Door | 1 | [-] | Effective opening area of openable windows and doors | |
| | | Window | 0.5 | | | |
| | | Bathroom window | 0.3 | | | |
| | Air Mass Flow Coefficient when the opening is closed | | 0.001 | [kg/s·m] | Crack around the perimeter when openings are closed (LIDDAMENT, 1986) | AirflowNetwork:MultiZone:Component:DetailedOpening |
| Ventilation Exhaust Fan | Air Mass Flow Coefficient When the Zone Exhaust Fan is Off | | 0.01 | [kg/s] | | AirflowNetwork:MultiZone:Component:ZoneExhaustFan |
| | Total efficiency | | 0.7 | [-] | | Fan:ZoneExhaust |
| | Pressure rise | | 50 | [Pa] | (VENTOKIT, 2019) | |
| | Maximum flow rate | | 0.028 | [m³/s] | | |

| | | | | | |
|---|---|---|---|---|---|
| Outputs | HAMT Surface Inside Face | Temperature | [°C] | | Output:Variable |
| | | Relative Humidity | [-] | | |

Table A.3. Moisture materials EnergyPlus input data

| FIELD | UNIT | CLAY[1] | MORTAR[1] | GROUT[2] | CONCRETE[2] |
|---|---|---|---|---|---|
| **SETTINGS** | | | | | |
| Porosity | [m³/m³] | 0.313 | 0.327 | 0.650 | 0.760 |
| Initial content water ratio | [kg/kg] | 0.001 | 0.001 | 0.200 | 0.010 |
| **SORPTION ISOTHERM** | | | | | |
| Number of isotherm coordinates | | 10 | 12 | 8 | 10 |
| Relative humidity fraction 1 | [-] | 0.05 | 0.251 | 0.113 | 0.202 |
| Moisture content 1 | [kg/m³] | 0.267563301 | 2.09547 | 0.85 | 19.665 |
| Relative humidity fraction 2 | [-] | 0.1 | 0.254 | 0.328 | 0.2205 |
| Moisture content 2 | [kg/m³] | 1.432198926 | 2.25666 | 2.55 | 22.31 |
| Relative humidity fraction 3 | [-] | 0.2 | 0.445 | 0.432 | 0.449 |
| Moisture content 3 | [kg/m³] | 2.11144679 | 2.79396 | 3.825 | 38.4675 |
| Relative humidity fraction 4 | [-] | 0.4 | 0.451 | 0.576 | 0.454 |
| Moisture content 4 | [kg/m³] | 3.112864168 | 2.97306 | 5.1 | 38.4675 |
| Relative humidity fraction 5 | [-] | 0.6 | 0.648 | 0.786 | 0.6506 |
| Moisture content 5 | [kg/m³] | 3.913805199 | 4.79988 | 8.075 | 54.165 |
| Relative humidity fraction 6 | [-] | 0.7 | 0.652 | 0.843 | 0.655 |
| Moisture content 6 | [kg/m³] | 4.325825203 | 4.04766 | 9.35 | 54.165 |
| Relative humidity fraction 7 | [-] | 0.8 | 0.847 | 0.936 | 0.824 |
| Moisture content 7 | [kg/m³] | 5.040462263 | 5.87448 | 16.15 | 72.565 |
| Relative humidity fraction 8 | [-] | 0.9 | 0.854 | 0.973 | 0.8725 |
| Moisture content 8 | [kg/m³] | 7.31967179 | 5.9103 | 23.375 | 85.1 |
| Relative humidity fraction 9 | [-] | 0.95 | 0.952 | | 0.924 |
| Moisture content 9 | [kg/m³] | 10.27661375 | 8.25651 | | 91.08 |
| Relative humidity fraction 10 | [-] | 1 | 0.956 | | 0.964 |
| Moisture content 10 | [kg/m³] | 16.05 | 8.36397 | | 100.28 |
| Relative humidity fraction 11 | [-] | | 0.976 | | |
| Moisture content 11 | [kg/m³] | | 9.63558 | | |
| Relative humidity fraction 12 | [-] | | 0.977 | | |
| Moisture content 12 | [kg/m³] | | 9.81468 | | |
| **SUCTION** | | | | | |
| Number of suction points | | 13 | 4 | 9 | 5 |
| Moisture content 1 | [kg/m³] | 0 | 0.03 | 0 | 0 |
| Liquid transport coefficient 1 | [m²/s] | 0.000000018 | 0.0000000056 | 0 | 0 |
| Moisture content 2 | [kg/m³] | 2 | 0.04 | 60 | 72 |
| Liquid transport coefficient 2 | [m²/s] | 0.00000001864115 | 0.0000000089 | 0.000000003 | 0.0000000000741 |
| Moisture content 3 | [kg/m³] | 4 | 0.05 | 100 | 85 |
| Liquid transport coefficient 3 | [m²/s] | 0.00000001930515 | 0.000000014 | 0.0000001 | 0.000000000253 |
| Moisture content 4 | [kg/m³] | 6 | 0.06 | 160 | 100 |
| Liquid transport coefficient 4 | [m²/s] | 0.00000001999279 | 0.00000002 | 0.0000001 | 0.00000000101 |
| Moisture content 5 | [kg/m³] | 7 | | 240 | 118 |
| Liquid transport coefficient 5 | [m²/s] | 0.00000002034574 | | 0.00000012 | 0.00000000128 |
| Moisture content 6 | [kg/m³] | 8 | | 320 | |
| Liquid transport coefficient 6 | [m²/s] | 0.00000002070493 | | 0.00000022 | |
| Moisture content 7 | [kg/m³] | 9 | | 360 | |
| Liquid transport coefficient 7 | [m²/s] | 0.00000002107045 | | 0.0000006 | |
| Moisture content 8 | [kg/m³] | 10 | | 380 | |
| Liquid transport coefficient 8 | [m²/s] | 0.00000002144243 | | 0.0000009 | |
| Moisture content 9 | [kg/m³] | 50 | | 400 | |
| Liquid transport coefficient 9 | [m²/s] | 0.00000004317976 | | 0.00000045 | |
| Moisture content 10 | [kg/m³] | 100 | | | |
| Liquid transport coefficient 10 | [m²/s] | 0.0000001035828 | | | |
| Moisture content 11 | [kg/m³] | 200 | | | |
| Liquid transport coefficient 11 | [m²/s] | 0.0000005960781 | | | |
| Moisture content 12 | [kg/m³] | 300 | | | |
| Liquid transport coefficient 12 | [m²/s] | 0.000003430193 | | | |
| Moisture content 13 | [kg/m³] | 400 | | | |
| Liquid transport coefficient 13 | [m²/s] | 0.00004735235 | | | |

| FIELD | UNIT | CLAY[1] | MORTAR[1] | GROUT[2] | CONCRETE[2] |
|---|---|---|---|---|---|
| | | **REDISTRIBUTION** | | | |
| Number of redistribution points | | 13 | 4 | 9 | 5 |
| Moisture content 1 | [kg/m³] | 0 | 0.03 | 0 | 0 |
| Liquid transport coefficient 1 | [m²/s] | 0.000000018 | 0.0000000056 | 0 | 0 |
| Moisture content 2 | [kg/m³] | 2 | 0.04 | 60 | 72 |
| Liquid transport coefficient 2 | [m²/s] | 0.00000001864115 | 0.0000000089 | 0.000000003 | 0.00000000000741 |
| Moisture content 3 | [kg/m³] | 4 | 0.05 | 100 | 85 |
| Liquid transport coefficient 3 | [m²/s] | 0.00000001930515 | 0.000000014 | 0.000000008 | 0.0000000000253 |
| Moisture content 4 | [kg/m³] | 6 | 0.06 | 160 | 100 |
| Liquid transport coefficient 4 | [m²/s] | 0.00000001999279 | 0.00000002 | 0.000000008 | 0.000000000101 |
| Moisture content 5 | [kg/m³] | 7 | | 240 | 118 |
| Liquid transport coefficient 5 | [m²/s] | 0.00000002034574 | | 0.000000013 | 0.000000000128 |
| Moisture content 6 | [kg/m³] | 8 | | 320 | |
| Liquid transport coefficient 6 | [m²/s] | 0.00000002070493 | | 0.0000001 | |
| Moisture content 7 | [kg/m³] | 9 | | 360 | |
| Liquid transport coefficient 7 | [m²/s] | 0.00000002107045 | | 0.0000003 | |
| Moisture content 8 | [kg/m³] | 10 | | 380 | |
| Liquid transport coefficient 8 | [m²/s] | 0.00000002144243 | | 0.0000007 | |
| Moisture content 9 | [kg/m³] | 50 | | 400 | |
| Liquid transport coefficient 9 | [m²/s] | 0.00000004317976 | | 0.000001 | |
| Moisture content 10 | [kg/m³] | 100 | | | |
| Liquid transport coefficient 10 | [m²/s] | 0.0000001035828 | | | |
| Moisture content 11 | [kg/m³] | 200 | | | |
| Liquid transport coefficient 11 | [m²/s] | 0.0000005960781 | | | |
| Moisture content 12 | [kg/m³] | 300 | | | |
| Liquid transport coefficient 12 | [m²/s] | 0.000003430193 | | | |
| Moisture content 13 | [kg/m³] | 450 | | | |
| Liquid transport coefficient 13 | [m²/s] | 0.00004735235 | | | |
| | | **DIFFUSION** | | | |
| Number of data pairs | | 11 | 10 | 1 | 1 |
| Relative humidity fraction 1 | [-] | 0 | 0 | 0 | 0 |
| Water Vapor Diffusion Resistance Factor 1 | [-] | 16.4177354 | 8.97 | 8.3 | 180 |
| Relative humidity fraction 2 | [-] | 0.1 | 0.1 | | |
| Water Vapor Diffusion Resistance Factor 2 | [-] | 16.2019745 | 4.95 | | |
| Relative humidity fraction 3 | [-] | 0.2 | 0.2 | | |
| Water Vapor Diffusion Resistance Factor 3 | [-] | 15.93170247 | 2.77 | | |
| Relative humidity fraction 4 | [-] | 0.3 | 0.3 | | |
| Water Vapor Diffusion Resistance Factor 4 | [-] | 15.58873705 | 2.73 | | |
| Relative humidity fraction 5 | [-] | 0.4 | 0.4 | | |
| Water Vapor Diffusion Resistance Factor 5 | [-] | 15.12736018 | 3.42 | | |
| Relative humidity fraction 6 | [-] | 0.5 | 0.5 | | |
| Water Vapor Diffusion Resistance Factor 6 | [-] | 14.44876038 | 9.52 | | |
| Relative humidity fraction 7 | [-] | 0.6 | 0.6 | | |
| Water Vapor Diffusion Resistance Factor 7 | [-] | 13.39871602 | 13.57 | | |
| Relative humidity fraction 8 | [-] | 0.7 | 0.7 | | |
| Water Vapor Diffusion Resistance Factor 8 | [-] | 11.85632115 | 16.67 | | |
| Relative humidity fraction 9 | [-] | 0.8 | 0.8 | | |
| Water Vapor Diffusion Resistance Factor 9 | [-] | 9.91228559 | 54.67 | | |
| Relative humidity fraction 10 | [-] | 0.9 | 0.9 | | |
| Water Vapor Diffusion Resistance Factor 10 | [-] | 7.895481779 | 79.5 | | |
| Relative humidity fraction 11 | [-] | 1 | | | |
| Water Vapor Diffusion Resistance Factor 11 | [-] | 6.121554296 | | | |

| FIELD | UNIT | CLAY[1] | MORTAR[1] | GROUT[2] | CONCRETE[2] |
|---|---|---|---|---|---|
| | | **THERMAL CONDUCTIVITY** | | | |
| Number of thermal coordinates | | 5 | 8 | 2 | 2 |
| Moisture content 1 | [kg/m³] | 0 | 0 | 0 | 0 |
| Thermal conductivity 1 | [W/m·K] | 2.1875 | 1.722 | 0.2 | 1.6 |
| Moisture content 2 | [kg/m³] | 36 | 17.91 | 650 | 180 |
| Thermal conductivity 2 | [W/m·K] | 2.6469 | 1.942 | 1.424 | 2.602 |
| Moisture content 3 | [kg/m³] | 72 | 35.82 | | |
| Thermal conductivity 3 | [W/m·K] | 3.1063 | 2.092 | | |
| Moisture content 4 | [kg/m³] | 126 | 53.73 | | |
| Thermal conductivity 4 | [W/m·K] | 3.3906 | 2.172 | | |
| Moisture content 5 | [kg/m³] | 216 | 71.64 | | |
| Thermal conductivity 5 | [W/m·K] | 4.375 | 2.232 | | |
| Moisture content 6 | [kg/m³] | | 89.55 | | |
| Thermal conductivity 6 | [W/m·K] | | 2.282 | | |
| Moisture content 7 | [kg/m³] | | 107.46 | | |
| Thermal conductivity 7 | [W/m·K] | | 2.322 | | |
| Moisture content 8 | [kg/m³] | | 125.37 | | |
| Thermal conductivity 8 | [W/m·K] | | 2.372 | | |

Source: [1]Annex 24 (KUMARAN, 1996); [2]EnergyPlus moisture materials library